Composition, properties, origin and evolutionary pathways of solid bitumens from SE Turkey- Improved process understanding through advanced geochemical characterization

vorgelegt von

M.Sc. Erdölgeologie

Seyed Hossein Hosseini Baghsangani

geb. in Torbatejam, Iran

von der Fakultät VI - Planen Bauen Umwelt
der Technischen Universität Berlin
zur Erlangung des akademischen Grades

Doktor der Naturwissenschaften
Dr. rer. nat.

genehmigte Dissertation

Promotionsausschuss:

Vorsitzender: Prof. Dr. Tomás Manuel Fernandez-Steeger
Gutachter: Prof. Dr. Heinz Wilkes
Gutachter: Prof. Dr. Wilhelm Dominik

Tag der wissenschaftlichen Aussprache: 22. Februar 2018

Berlin 2018

For Kiana & Baran

ACKNOWLEDGEMENTS

Firstly, I would like to express my deepest gratitude to my supervisors Prof. Brian Horsfield and Prof. Heinz Wilkes, for their continuous support and also for sharing their profound knowledge and experience. This research would not have been possible without their endless support, guidance and insight. Besides my supervisors, I would like to thank the rest of my thesis committee: Prof. Wilhelm Dominik and Prof. Tomás Manuel Fernandez-Steeger, for their insightful comments and encouragement. Dr. Stefanie Pötz and Dr. Andrea Vieth-Hillebrand is greatly acknowledged for scientific contribution and sharing their immense knowledge. I am also grateful to Dr. Orhan Kavak and Prof. M. Namık Yalçın, for providing a very nice sample set for this research and also for their comments and suggestions that improved the quality of this work. The group leader of organic geochemistry section at the GFZ, Dr. Kai Mangelsdorf, is also thanked for the financial support during last months of my study.

My sincere gratitude goes to Claudia Engelhardt, who helped me a lot in overcoming numerous obstacles I have been facing through my study. I can't imagine the organic geochemistry section without her. I also would like to thank Cornelia Karger, Anke Kaminsky, Ferdinand Perssen, Kristin Günther, Doreen Noack and Mirco Rahn, for their technical assistance and analytical services which were conducted into this study.

Over these nearly five years, I had the opportunity to make friends with so many people from different countries and cultures. My special thanks goes to my dear friends Nina, Shengyu, Volker, Sascha, Mehrdad, Faezeh, Nick and Mareike for their constant support and truthful friendship throughout these years, and for the good laughs and unforgettable moments that we have had together.

Last but not the least, I would like to express my special gratitude to my family, my wife, Kiana, and my lovely daughter, Baran, for their continued love and encouragement without which I most certainly could not have completed this endeavor. This dissertation is dedicated to Kiana and Baran.

LIST OF PUBLICATIONS

As part of this thesis the following articles and conference contributions were published:

Articles

- **Hosseini, S. H.,** B. Horsfield, S. Poetz, H. Wilkes, M. N. Yalçın, and O. Kavak, (2017). Role of maturity in controlling the composition of solid bitumens in veins and vugs from SE Turkey as revealed by conventional and advanced geochemical tools: *Energy & Fuels*, v. 31, p. 2398-2413.
  DOI: 10.1021/acs.energyfuels.6b01903

- **Hosseini, S. H.,** B. Horsfield, H. Wilkes, A. Vieth-Hillebrand, M. N. Yalçın, and O. Kavak, (2018). Comprehensive geochemical correlation between surface and subsurface hydrocarbon occurrences in the Batman-Mardin-Şırnak area (SE Turkey): *Marine and Petroleum Geology,* v. 93, p. 95-112.
  https://doi.org/10.1016/j.marpetgeo.2018.02.035

- **Hosseini, S. H.,** S. Poetz, B. Horsfield, H. Wilkes, M. N. Yalçın, and O. Kavak (2018). The incorporation mechanism and thermal evolution of aromatic organosulphur compounds in heavy oils and solid bitumens from SE Turkey as revealed by ultra-high resolution APPI (+) FT-ICR MS. (final draft ready for submission).

Conference contributions

- **Hosseini, S. H.,** H. Wilkes, B. Horsfield, S. Poetz, O. Kavak, M. N. Yalçın (2015). Maturity influence on sulphur compounds and condensed aromatic hydrocarbons in asphaltites from SE Turkey as revealed by ultrahigh resolution mass spectrometry. *27th IMOG*, Prague, Czech Republic.

ABSTRACT

The south-eastern region of Turkey is the most petroliferous region of the country and there are many surface and subsurface hydrocarbon occurrences. In particular, this region is noted for the widespread occurrence of solid bitumen veins and vugs, ostensibly generated from the same source but showing different physicochemical characteristics depending upon their geographic location. Although they have been the subject of various geochemical studies, yet the origin, and formation mechanism(s) remain inconclusive and the high molecular weight constituents has not been ultimately elucidated mostly due to limitations of the employed geochemical tools. This dissertation addresses some of the ambiguous geochemical characteristics of the Turkish solid bitumens using an interdisciplinary approach from pyrolysis techniques to high resolution mass spectrometry.

Firstly, the thermal maturity was assessed in solid bitumens as it plays the major role in transforming solid bitumens. According to various maturity-related parameters, a clear maturity trend was observed across the region increasing from west to east which is strongly related to regional tectonic history as compressional pressure did not occur with the same intensity across the region and increases towards the east. Also, thermal alteration processes were found to be the main mechanism by which solid bitumens have been formed. Furthermore, special efforts were made for speciation and characterization of polar compounds containing nitrogen, sulphur and oxygen (NSO) of high molecular weight making use of fourier transform ion cyclotron resonance mass spectrometry combined with electrospray ionization in the negative ion mode (ESI FT-ICR MS). The influence of thermal stress on heteroatomic compounds was investigated as well. The acidic fractions appear to be enriched in fully aromatic compounds containing 1 to 2 pyrrolic nitrogen atoms and 0 to 2 thiophenic sulphur atoms and their alkyl-substituted homologues. Double bond equivalent and carbon number distributions revealed that with increasing maturity condensation, aromatisation and side-chain cracking reactions take place. At highest

maturation levels, side-chain cracking has proceeded so far that further condensation and aromatisation processes are not possible.

In the next step, by including oil seepage as well as heavy oil samples from nearby seeps and oilfields, a correlation study was successfully conducted to determine whether a genetic relationship exists between the surface and subsurface petroleum occurrences in the region. A strong genetic affinity was observed, as revealed by various source-sensitive molecular parameters. A marine carbonate unit was inferred to be the common source for all petroleum occurrences, with two exceptions: the Dadaş and İşkar seeps appear to be derived from marine shale and the Silvanka Sinan oil seems to have originated from a younger source. Thereafter, the influence of "phase effect" on chemical composition of different petroleum types was highlighted using additional parameters on low-thermally degraded bitumens, low-biodegraded seeps as well as heavy oils. The relative abundances of homohopanes revealed that in solid bitumens the intensity of lower homologs (C_{31}-) is much higher compared to the liquid occurrences and it is reversed at higher homologs (C_{33}- to C_{35}-), possibly because of thermal cracking of high molecular weight homologues during and/or after solidification. Similarly, variations of the $\delta^{13}C$ values of individual *n*-alkanes (*n*-C_{14} to *n*-C_{34}) for solid bitumens of different degradation levels and heavy oils indicate that solid bitumens (from -27 to -21‰) are more enriched in ^{13}C than the heavy oils (from -31 to -27‰). The observed difference can mainly be attributed to the "phase effect" as other effective parameters are known to be the same i.e. source unit and its depositional setting.

Finally, since the investigated petroleum occurrences are sulphur-rich, a special focus was laid on the organic sulphur compounds (OSC), unravelling the incorporation mechanism(s) as well as thermal evolutionary pathways using positive-ion atmospheric pressure photoionization (APPI) coupled with FT-ICR MS. According to various bulk and molecular-level data e.g. low-temperature reservoirs, the presence of non-biodegraded extra-heavy oils, variations of sulphur with ongoing maturation etc., it is clear that sulphur has been introduced into the source kerogen through bacterial sulphate reduction (BSR) mechanism at early diagenesis.

Variations of OSCs in the genetically-related petroleum occurrences of different phases are of geochemically interest. It appears that thermal evolutionary pathways in both, heavy oils and solid bitumens, are similar as the observed distribution patterns for OSCs is exactly the same in both low API gravity oils and crude extracts from least mature solid bitumens, with $S_1 > S_2 > S_3 > S_1O_1 > S_2O_1 > N_1S_1 > N_1S_2 > S_4$. Moreover, with advancing maturation the observed variations in the relative abundances of OSCs are comparable in both. Interestingly, in the high-thermally degraded bitumens (T_{max} > 470 ºC) an inversion was observed in the relative abundances of nearly all major OSCs which is attributed to the extremely hydrogen deficiency and the presence of highly active thermally-released sulphur elements at the elevated maturation levels. The evolutionary pathways of OSCs were demonstrated using the Van Krevelen plots and Venn Diagrams as well.

It can be concluded that Turkish solid bitumens have been formed due to the thermal alteration of the parent oils. The precursor oil was either the subsurface heavy oils or both have been generated from a common source. They have different characteristics depending upon the degree of thermal degradation progressing in gradual stages from asphaltites to pyrobitumens. The geological setting, tectonic history, non to low biodegradation rates, different petroleum systems and so on, suggest this part of southeastern Turkey as a unique natural laboratory, suitable for geochemical and geological studies.

KURZFASSUNG

Die südöstliche Türkei ist die ölreichste Region des Landes, in der sich viele Erdölvorkommen im Oberflächenaufschluss sowie im Untergrund befinden. Insbesondere ist diese Region für ihre weitverbreiteten Vorkommen von Asphaltgängen und asphaltgefüllten Gesteinshohlräumen bekannt, die anscheinend vom gleichen Muttergestein gespeist wurden, aber unterschiedliche physikochemische Eigenschaften, je nach geographischer Lage, besitzen. Obwohl sie bereits oft Gegenstand geochemischer Studien waren, blieben ihr Ursprung und ihre Bildungsmechanismen schleierhaft. Besonders die hochmolekularen Bestandteile gaben aufgrund unzureichender geochemischer Untersuchungsmethoden Rätsel auf. Diese Dissertation befasst sich mit der Zwiespältigkeit bzw. den unbekannten geochemischen Eigenschaften der türkischen Asphaltvorkommen und benutzt einen interdisziplinären Ansatz, der Pyrolyse-Techniken bis zu hochauflösender Massenspektroskopie einschließt.

Zuerst wurde die thermische Reife der Asphalte bewertet, die, eine entscheidende Rolle bei der Umwandlung von Asphalten spielt. Mehrere Reifeparameter zeigen einen deutlichen, regional ansteigenden Trend von Westen nach Osten, der stark mit der regionalen strukturgeologischen Entwicklung zusammenhängt, da Kompressionsspannungen nicht mit der gleichen Intensität auftreten und nach Osten zunehmen. Der thermische Alterierungsprozess ist der Hauptmechanismus, welcher die Asphalte generiert. Weiterhin wurden hochmolekulare, polare Heterokomponenten, die aus Stickstoff, Sauerstoff und Schwefel (NSO) bestehen, mittels Fourier Transform Ion Cyclotron-Massenspektroskopie gekoppelt mit negativer Elektrospray-Ionisierung (ESI negative FT-ICR-MS) spezifiziert, charakterisiert und auf den Einfluss von thermischen Stress untersucht. Die azidische Fraktion scheint mit vollaromatischen Komponenten angereichert zu sein, die 1 bis 2 pyrrolische Stickstoffatome und 0 bis 2 thiophenische Schwefelatome sowie deren alkyl-substituierte Homologe enthalten. Double bond equivalents (DBE) und Kettenlängenverteilungen zeigen, dass mit zunehmenden thermischen Stress

Kondensierungs-, Aromatisierungsreaktionen und Seitenkettenaufspaltung einhergehen. Im höchsten Reifelevel sind Seitenkettenspaltungen soweit fortgeschritten, dass keine weitere Kondensierung und Aromatisierung möglich sind.

Im nächsten Schritt wurden regionale Schwerölproben aus Ölfeldern und natürlich austretenden Ölausbissen erfolgreich korreliert, um einen genetischen Zusammenhang von Ölvorkommen an der Erdoberfläche und im Untergrund zu untersuchen. Fazies-bestimmende Parameter zeigen eine starke genetische Affinität und eine marine Karbonatschicht wird als gemeinsames Muttergestein für alle Ölvorkommen angenommen; mit zwei Ausnahmen: die Dadaş- und İşkar-Ausbisse scheinen von marinen Schiefern gespeist zu sein und die Silvanka-Sinan-Öle aus einem jüngeren Gestein. Danach wurde der Einfluss von „Phaseneffekten“ auf die chemische Zusammensetzung verschiedener Öltypen beleuchtet, indem zusätzliche Parameter benutzt wurden, die spezifisch für niedrige thermische und biogene Alterierung sind. Die relative Verteilung von Homohopanen zeigt, dass die Intensität der leichten Homologe (C_{31-}) in den Asphalten wesentlich höher ist als in Ölen, und dass diese Beobachtung für schwerere Homologe (C_{33-35}) umgekehrt ist; wahrscheinlich wegen thermischer Spaltung der hochmolekularen Homologe während und/oder nach der Verfestigung. Ähnlich zeigen Variationen in $\delta^{13}C$-Werten der einzelnen *n*-Alkane (*n*-C_{14} bis *n*-C_{34}) in Asphalten verschiedener Reife und Schwerölen, dass Asphalte (-27 bis -31 ‰) gegenüber Schwerölen (-31 bis -27 ‰) in ^{13}C angereichert sind. Die beobachteten Unterschiede werden hauptsächlich „Phaseneffekten“ zugeschrieben, da andere effektive Parameter gleich sind, z. B. Muttergesteinsfazies und –ablagerungsmilieu.

Schlussendlich wurde der Fokus auf organische Schwefelkomponenten (OSC) gelegt, da die untersuchten Ölvorkommen als schwefelreich bekannt sind. Einbaumechanismen und thermische Reifepfade wurden mittels FT-ICR MS gekoppelt mit positiver-ion atmospheric pressure photoionization (APPI) entschlüsselt. Durch Kombination verschiedener Daten von großer bis auf molekulare Ebene, wie z. B. niedrige Reservoirtemperatur, das Vorkommen von nicht-biodegradierten, extrem schweren Ölen, Variationen im Schwefelgehalt mit

zunehmender Reife etc., wird klar, dass Schwefel in das originäre Kerogen des Muttergesteins durch bakterielle Schwefelreduktion (BSR) während der frühen Diagenese eingebaut wurde.

OSC-Variationen in genetisch verwandten Ölen verschiedener Phasen sind von geochemischem Interesse. Es scheint, als wären thermische Entwicklungspfade in Schwerölen und Asphalten gleich, da die Verteilungsmuster von OSCs in schweren Ölen und niedrig-reifen Asphalt-Extrakten gleich sind und sich in folgender Reihenfolge ändern: $S_1 > S_2 > S_3 > S_1O_1 > S_2O_1 > N_1S_1 > N_1S_2 > S_4$. Zudem sind die beobachteten Variationen in den relativen Häufigkeiten der OSCs mit zunehmender Reifung in beiden vergleichbar. Interessanterweise ist in den thermisch hochdegradierten Asphalten (T_{max} > 470 °C) eine Inversion der relativen Mengen aller hauptsächlich vorkommenden OSCs zu beobachten, was der extremen Wasserstoffarmut sowie dem Auftreten von hochaktivem Schwefel zugerechnet werden kann, der während der thermischen Degradation in diesen Reifestadien gebildet wurde. Die Entwicklungspfade der OSCs sind in van-Krevelen-Diagrammen und Venn-Diagrammen illustriert.

Zusammenfassend ist zu sagen, dass türkische Asphalt-Vorkommen aufgrund thermischer Reifung der Ausgangsöle gebildet wurden. Diese Vorgängeröle sind entweder Schweröle im Untergrund oder wurden beide von einer gemeinsamen Quelle gespeist. Sie haben verschiedene Charakteristika, die von dem Grad der thermischen Reife abhängen, und sich graduell von Asphaltiten zu Pyrobitumen entwickeln. Die geologischen Bedingungen, tektonische Geschichte, mangelnde bis niedrige Biodegradationsraten, verschiedene Erdölsysteme, usw. empfehlen diese Region im Südwesten der Türkei als einzigartiges natürliches Laboratorium für geochemische und geologische Studien.

CONTENTS

ACKNOWLEDGEMENTS _____ *I*

LIST OF PUBLICATIONS _____ *III*

ABSTRACT _____ *V*

KURZFASSUNG _____ *VIII*

CONTENTS _____ *XII*

LIST OF FIGURES _____ *XV*

LIST OF TABLES _____ *XIX*

LIST OF ABBREVIATIONS _____ *XX*

1. INTRODUCTION _____ ***1***

1.1. Solid Bitumen Occurrences in the World _____ 1

1.2. Components of Solid Bitumen _____ 3

1.3. Classification Systems _____ 5

1.4. Formation Mechanisms _____ 8

1.4.1. Depositional environment and petroleum composition _____ 9

1.4.2. Thermal alteration _____ 11

1.4.3. Fluid expulsion and bitumen segregation _____ 13

1.4.4. Biodegradation _____ 14

1.5. Research Perspectives and Objectives _____ 16

1.6. Structure of the Dissertation _____ 19

2. ROLE OF MATURITY IN CONTROLLING THE COMPOSITION OF SOLID BITUMENS 21

2.1. Abstract _____ 21

2.2. Introduction _____ 22

2.3. Geological Setting and Possible Formation Mechanism of Veins _____ 26

2.4. Description of Samples _____ 27

2.5. Analytical Methods _____ 28

2.6. Results and Discussion _____ 30

2.6.1. Bulk organic matter content and type _____ 30

2.6.2. Macromolecular building blocks _____ 33

2.6.3. Extractable organic matter _____ 34

2.6.4. Biomarker analysis _____ 37

2.6.5. FT-ICR MS analysis _____ 40

2.6.5.1. Broadband spectra and elemental class composition _____ 41

2.6.5.2. Compound classes _____ 43

2.6.5.3. Double bond equivalent distributions _____ 44

2.6.5.4. Carbon number distributions _____ 48

2.7. Conclusions _____ 51

2.8. Acknowledgment _____ 52

3. COMPREHENSIVE GEOCHEMICAL CORRELATION BETWEEN SURFACE AND SUBSURFACE PETROLEUM OCCURRENCES OF SE-TURKEY _____ 54

3.1. Abstract _____ 54
3.2. Introduction _____ 55
3.3. Geological Setting and Sample Set _____ 58
3.4. Analytical Methods _____ 61
3.4.1. Rock-Eval pyrolysis & TOC analysis _____ 61
3.4.2. Thermovaporisation- and pyrolysis-gas chromatography _____ 61
3.4.3. Solvent extraction & hydrocarbon fractionation _____ 62
3.4.4. Gas chromatography _____ 62
3.4.5. Gas chromatography-mass spectrometry _____ 63
3.4.6. Gas chromatography-isotope ratio mass spectrometry _____ 63
3.5. Results and Discussion _____ 64
3.5.1. Heavy oils _____ 64
3.5.2. Oil seepages _____ 71
3.5.3. Solid bitumens _____ 75
3.5.4. Correlation criteria _____ 77
3.5.4.1. Homohopane distribution _____ 77
3.5.4.2. Aromatic hydrocarbon distributions _____ 78
3.5.4.3. Compound-specific stable C isotope signatures of *n*-alkanes _____ 83
3.6. Conclusions _____ 85
3.7. Acknowledgement _____ 86

4. ORGANIC SULPHUR COMPOUNDS – INSIGHTS INTO THEIR FORMATION USING ULTRA-HIGH RESOLUTION MASS SPECTROMETRY _____ 88

4.1. Abstract _____ 88
4.2. Introduction _____ 89
4.3. Study Area and Sample Set _____ 92
4.4. Analytical Program _____ 93
4.4.1. APPI (+)-FT-ICR MS _____ 93
4.5. Results and Discussion _____ 94
4.5.1. Elemental class distributions _____ 94
4.5.2. Sulphur-containing compound classes _____ 97
4.5.3. Incorporation mechanism of organic sulphur _____ 99
4.5.4. Evolution of organic sulphur compounds _____ 103
4.5.4.1. Sulphur-containing compound classes _____ 103
4.5.4.2. Aromaticity of sulphur-containing compounds _____ 104
4.5.4.3. Modified van Krevelen diagrams _____ 104
4.5.4.4. Alkylation degree _____ 107
4.5.4.5. Venn Diagram analysis _____ 108
4.6. Conclusions _____ 112

5. SUMMARY AND OUTLOOK _____ 114

5.1. Summary _____ 114
5.2. Outlook _____ 118

REFERENCES _____ *121*

LIST OF FIGURES

Fig. 1. 1. Natural bitumen quantities and geographical distribution; TONBIP: total original natural bitumen in place; ONBIP: original natural bitumen in place (Meyer *et al*., 2007). ……**3**

Fig. 1. 2. Solvent fractionation scheme of solid bitumens (modified from Wen *et al*., 1978)…….……**4**

Fig. 1. 3. A generic classification of solid bitumens based on solubility, fusibility and H/C ratio. Modified from Hunt, 1979; Cornelius, 1987……**6**

Fig. 1. 4. A genetic classification of solid bitumens proposed by Curiale (1986)……..…….**7**

Fig. 2. 1. a) Geographic location of the studied solid bitumen's veins as well as some oil seepages and heavy oilfields in SE Turkey. The vein's names are given in Table 1. **b)** Left: The dyke-shape Harbul vein in the Gerçüş Formation as host rock; Right: Some of studied solid bitumens in hand specimen to show their different appearance. **c)** The stratigraphic column of SE Turkey and occurrence of solid bitumens in different sedimentary units - modified after Kavak *et al*. (2010) and Lebküchner *et al*. (1972)...**27**

Fig. 2. 2. The variation of **a)** Hydrogen Index; **b)** extractable organic matter yields (/TOC) and **c)** "Oil Saturation Index" (S1/TOC) as a function of maturity in studied solid bitumens from SE Turkey. d) Tmax contour map shows a maturity trend from west to east across the study area. The vein's names are given in Table 2.1……..……..**32**

Fig. 2. 3. Open system pyrolysis gas chromatograms for selected solid bitumens from SE Turkey with different maturation levels……..……...**34**

Fig. 2. 4. a) The chain length distribution of total C_1-C_5 resolved pyrolysate, C_6-C_{14} n-alkenes plus *n*-alkanes and C_{15+} *n*-alkenes plus *n*-alkanes showing composition changes with ongoing maturation in studied solid bitumens (after Horsfield, 1989). Please note that the Petroleum Type Organofacies fields are based on kerogen pyrolysates, and are shown here simply for reference. **b)** Differentiation of pyrolysate composition using relative proportions of non-1-ene plus pentacos-1-ene, toluene and 2,5-dimethylthiophene (after di Primio and Horsfield, 1996)……..……**35**

Fig. 2. 5. Thermovaporization gas chromatograms of solid bitumens show different patterns at different locations equatable with different thermal maturity levels across the investigated area……..……...……...**36**

Fig. 2. 6. Correlation of maturity parameters based on aromatic hydrocarbons versus T_{max} values for the studied solid bitumens; **a)** methyldibenzothiophene ratio. **b)** methylphenanthrene index 1 and **c)** trimethylnaphthalene ratio……..…...……**39**

Fig. 2. 7. Distributions of dibenzothiophene and alkylated dibenzothiophenes for selected solid bitumens with different maturity from SE Turkey illustrating changes in abundances and patterns……..…….……..**40**

Fig. 2. 8. Broadband negative ion ESI FT-ICR mass spectra of solid bitumens of increasing maturity (as indicated by T_{max} values). The pie charts show the elemental class distribution. N_1 compounds are depicted with triangles, N_1S_1 compounds with circles and O_2 compounds with squares…….....……..**42**

Fig. 2. 9. Compound class distribution of different compound classes in solid bitumens from SE Turkey……..…….……**43**

Fig. 2. 10. DBE distribution of the N_1, N_1S_1, N_1S_2 and O_2 compound classes in solid bitumens from SE Turkey. T_{max} (ºC) values are given in the legend and plausible core structures for the most abundant DBE classes are provided……..……**45**

Fig. 2. 11. Maturity controlled variations in the relative abundance of selected DBE classes for the N_1 (a, b) and N_1S_1 (c) compound classes…….....……**47**

Fig. 2. 12. Carbon number distribution of the N_1 12, 15 and 18 DBE classes as well as the N_1S_1 14, 17 and 20 DBE classes in solid bitumens from SE Turkey. T_{max} (°C) values are given in the legend and the chemical structures depict the respective core structures……...**49**

Fig. 2. 13. Colour coded DBE versus carbon number diagrams of the N_1, N_1S_1 and O_2 compound classes for selected samples with different maturation levels……....……..**50**

Fig. 2. 14. Maturity-controlled carbon number distribution of aliphatic side chains of the DBE 9 N_1 compound class (likely carbazoles) for solid bitumens from SE Turkey (after Mahlstedt *et al*. (2016)……..……...…….**51**

Fig. 3. 1. a) Geographic location of solid bitumen's veins as well as oil seepages and heavy oilfields in the study area. The related names are given in Table 3.1. **b)** Left: The dyke-shape Harbul vein in the Gerçüş Formation as host rock; Right: Some of solid bitumens in hand specimen to show their different appearance (Hosseini *et al*., 2017a). **c)** The stratigraphic column of SE Turkey displaying the reservoir formations for studied oils as well as host rocks for solid bitumen veins……..……..……**59**

Fig. 3. 2. a) The bulk composition of different petroleum types from SE Turkey using relative abundances of SARA fractions; T_{max} ranges of solid bitumens as well as API gravities for some of oils are shown. **b)** Source identification using regular sterane distributions (C_{27}-C_{28}-C_{29})……..……..……..**65**

Fig. 3. 3. Open system pyrolysis-GC of different sample types from SE Turkey…….**65**

Fig. 3. 4. a) Distribution patterns of total C_1-C_5 resolved pyrolysate, C_6-C_{14} *n*-alkenes plus *n*-alkanes and C_{15+} *n*-alkenes plus *n*-alkanes in different sample types from SE Turkey (after Horsfield, 1989); b) Differentiation of pyrolysate composition using relative

proportions of non-1-ene plus pentacos-1-ene, toluene and 2,5-dimethylthiophene (after di Primio and Horsfield, 1996)……..……..…….**66**

Fig. 3. 5. The n-alkane, isoprenoid, hopane and sterane distributions in selected samples from surface and subsurface petroleum occurrences in SE Turkey……..……**67**

Fig. 3. 6. Characterization of depositional environment and lithology of the source unit(s) using saturated and aromatic parameters in different petroleum occurrences from SE Turkey: **a)** Pr/Ph versus C_{29}/C_{27} (20*R*) sterane ratios; **b)** DBT/P versus Pr/Ph ratios; **c)** the C_{35} homohopane index versus C_{30} sterane index, and **d)** the C_{27} Dia/(Dia+Reg) sterane versus $T_s/(T_s+T_m)$ ratios……...……**69**

Fig. 3. 7. Correlation of maturity parameters based on aromatic hydrocarbons versus: **a)** API gravities for the studied heavy oils; **b)** T_{max} values for the studied solid bitumens…....**73**

Fig. 3. 8. Homohopane distributions for different petroleum occurrences from SE Turkey…….**78**

Fig. 3. 9. The relative abundances of aromatic hydrocarbon compounds in selected samples from each sample type of SE Turkey; **a)** All investigated aromatic compounds; **b)** Dibenzothiophenes; **c)** Naphthalenes; **d)** Phenanthrenes; **e)** Aromatic steroids; **f)** Fluorenes……..…..……**81**

Fig. 3. 10. Compound-specific $\delta^{13}C$ values of n-alkanes in heavy oils and solid bitumens of SE Turkey……..…….……**84**

Fig. 3. 11. Variation of average $\delta^{13}C$ values with maturation levels in Turkish solid bitumen…**85**

Fig. 4. 1. Broadband positive-ion APPI FT-ICR mass spectra of selected samples of different maturation levels from heavy oils and solid bitumens as indicated by API gravities and T_{max} values, respectively. The embedded pie diagrams display the elemental class distribution……..…….……**95**

Fig. 4. 2. Distribution of the major S-containing compound classes normalized to the sum of all S-containing compounds and their variations as a function of maturity in heavy oils and solid bitumens from SE Turkey……..…….……**98**

Fig. 4. 3. Distribution of carbon number against DBE for the S_1, S_2 and S_3 compound classes measured by APPI(+)-FT-ICR MS. These plots are colour coded by their relative abundance normalized to the highest abundance measured for each sample. There is a scale change in the DBE axis for each compound class. Value in upper right corner of plots is the relative intensity of each compound class relative to total monoisotopic ion abundances (Tab. 4.2). Plausible core structures for selected DBE classes are provided as well……..……...……..**102**

Fig. 4. 4. DBE distribution of the S_1, S_2, S_3, S_1O_1 and N_1S_1 compound classes in heavy oils and solid bitumens from SE Turkey……..……...……..**105**

Fig. 4. 5. The 3D Van-Krevelen plots for elemental data obtained from the positive-ion APPI FT-ICR MS for the major S-containing compounds of heavy oils and solid bitumens from SE Turkey……...…….……**106**

Fig. 4. 6. Carbon number distribution at the low as well as high DBEs of the S_1 compound class in selected samples of both petroleum types. The chemical structures depict the respective possible core structures……..……..……..**109**

Fig. 4. 7. Variations of elemental compositions, irrespective of their intensity values, in both heavy oils and solid bitumens as a function of maturity using two-set Venn Diagrams. Sample A in both sample types is used as low-maturity reference. The elemental class distributions of unique elements in each union as well as compound class distributions of only S-containing components are illustrated by pie charts……**111**

LIST OF TABLES

Table 2. 1. Data for Rock-Eval pyrolysis, solvent extraction and liquid chromatographic fractionation of solid bitumens from SE Turkey……**31**

Table 2. 2. Indicators of thermal maturity for solid bitumens from SE Turkey using GC and GC-MS data……..…….**38**

Table 3. 1. Bulk parameters of different sample types from SE Turkey. Estimated biodegradation levels are given as well……...……**60**

Table 3. 2. Source-related biomarkers obtained from GC and GC-MS data of different sample types in SE Turkey……...……...**68**

Table 3. 3. Thermal maturity indicators calculated based on saturate and aromatic fractions in all investigated samples from SE Turkey……**72**

Table 3. 4. Relative abundances of the major series of aromatic hydrocarbon compounds and their alkylated counterparts in different sample types of SE Turkey…….……**80**

Table 4. 1. Elemental composition and ratios of whole oils and crude extracts of solid bitumens, obtained from APPI (+) and ESI (-) FT-ICR MS……..…….**96**

Table 4. 2. Total monoisotopic ion abundances of the major chemical species in heavy oils and solid bitumens of SE Turkey, detected by APPI-(+) FT-ICR MS…….…….**98**

LIST OF ABBREVIATIONS

AOP	Asphaltene onset pressure
API	American Petroleum Institute
APPI	Atmospheric pressure photoionization
BSR	Bacterial sulphate reduction
BTEX	Benzene, toluene, ethylbenzene and xylenes
CPI	Carbon Preference Index
CS_2	Carbon disulphide
DCM	Dichloromethane
DBE	Double bond equivalent
EOM	Extractable organic matter
ESI	Electrospray ionization
FID	Flame Ionization Detector
FT-ICR MS	Fourier transform-ion cyclotron resonance mass spectrometry
GC	Gas chromatography
GC-MS	Gas chromatography-mass spectrometry
GC-IRMS	Gas chromatography-isotope ratio mass spectrometry
GOR	Gas to oil ratio
HC	Hydrocarbon
HI	Hydrogen Index
HMWH	High molecular weight hydrocarbon
LMWH	Low molecular weight hydrocarbon
MeOH	Methanol
MPa	Megapascal
MPLC	Medium pressure liquid chromatography
m/z	Mass to charge ratio
N_1 class	Nitrogen-containing compounds with one N atom
NSO	Polar compounds containing nitrogen, sulphur and oxygen
OI	Oxygen Index

ONBIP	Original natural bitumen in place
OSC	Organic sulphur compound
OWC	Oil-water contact
PAH	Polycyclic aromatic hydrocarbon
PDB	Pee Dee Belemnite
PI	Production Index
PNA	Polynuclear aromatic
P-N-A	Paraffinic-Naphthenic-Aromatic
Py	Pyrolysis
Pr/Ph	Pristane/ Phytane
S_1	Sulphur-containing compounds with one S atom
SARA	Saturate, aromatic, resin, asphaltene
S/N	Signal-to-noise ratio
T_{max}	Temperature of maximum pyrolysis yield
TCA	Thermal chemical alteration
TMIA	Total monoisotopic ion abundance
TOC	Total organic carbon
TONBIP	Total original natural bitumen in place
TSR	Thermochemical sulphate reduction
Tvap	Thermovaporisation gas chromatography
R_c	Calculated vitrinite reflectance
R_o	Vitrinite reflectance
UCM	Unresolved complex mixture (also hump)

1. INTRODUCTION

1.1. Solid Bitumen Occurrences in the World

Solid bitumen occurs in veins and vugs in a wide variety of geological settings around the world. It may be brown, black, yellow or orange in colour, and may be brittle with a conchoidal fracture, or soft, elastic and malleable. These vugs and veins are particularly abundant in petroleum provinces (Curiale, 1986). A widely accepted definition, proposed by Abraham (1960), is that bitumens in general are fusible substances, semi-solid or solid, which can be extracted using organic solvents. The term "solid bitumen", also called "natural bitumen" or "native bitumen" is not very well defined in the literature and due to the limited knowledge of the chemical structure, its definition and classification is mainly based on empirical parameters. They can be defined as allochthonous organic materials that migrated from their source rocks and are now solids or semisolids at surface or subsurface conditions (e.g. Curiale, 1986). They have been known since antiquity and have been put to use for various purposes. For instance, the Greeks employed it in warfare, as the "Greek Fire", Babylonians used it for mortar between bricks and stones in the construction of buildings and Egyptians used bitumen in the construction of boats made of reeds. In more recent times, particularly during the early days of petroleum exploration, surficial bitumen occurrences were employed in searching out subsurface accumulations of hydrocarbons (Mossman and Nagy, 1996). Nowadays, they have various applications in our daily life e.g. road construction, dark-colored printing inks, paints, oil well drilling muds and cements, foundry sand additives and a wide variety of chemical products, though their nature is still poorly understood and there is no general agreement yet as to what exactly constitutes bitumen. This is understandable because bitumens are complex organic substances containing hydrocarbons and high concentrations of covalently bonded nitrogen, oxygen, sulphur, and may be associated with the presence of trace and heavy metals such as iron, titanium, molybdenum, vanadium, nickel and uranium in different proportions in "random polymer-like" molecular structures (e.g. Mossman and Nagy, 1996; Attanasi and Meyer, 2010). As regards commercial utilization, these characteristics result in higher costs for

extraction, transportation, and refining than are incurred with conventional oil. Despite their cost and technical challenges, major international oil companies have found it desirable to acquire, develop, and produce these resources in increasing volumes. They can make an important contribution to future oil supply if they can be extracted and transformed into usable refinery feedstock at sufficiently high rates and at costs that are competitive with alternative sources (Attanasi and Meyer, 2010).

Natural bitumen occurrences are globally widespread. For example, they are found in the Cretaceous Athabasca tar sands of Alberta, western Canada (Nagy and Gagnon, 1961); in the Eocene Green River Formation of the Uinta Basin, Utah, USA (Hunt, 1963; Verbeek and Grout, 1992); in Triassic sandstones of the Karoo System in the Malagasy Republic (Cornelius, 1984); in Cretaceous- Eocene sandstones in southwestern Iran (Goodarzi and Williams, 1986); in vein type deposits of asphaltic substances in southeastern Turkey (Orhun, 1969); in the Miocene Monterey Formation of California (Curiale, 1986); in the Permian Lucaogou Formation of the Junggar Basin, north-west China (Monson and Parnell, 1992); in Cretaceous limestones of Argentina (Abraham, 1960) and so on.

Meyer *et al*. (2007) and then Attanasi and Meyer (2010) have reported natural bitumen quantities based upon a detailed review of the literature in conjunction with available databases. According to these authors, natural bitumen is reported in 598 deposits in 23 countries, occurs both in clastic and carbonate reservoir rocks and commonly in small deposits at, or near, the earth's surface. Outside Canada, 367 natural bitumen deposits are reported in 22 other countries. The total natural bitumen resource in known accumulations amounts to 5,505 billion barrels of oil originally in place, which includes 993 billion barrels as prospective additional oil. This resource is distributed in 192 basins containing heavy oil and 89 basins with natural bitumen (Meyer *et al*., 2007; Attanasi and Meyer, 2010) (Fig.1.1).

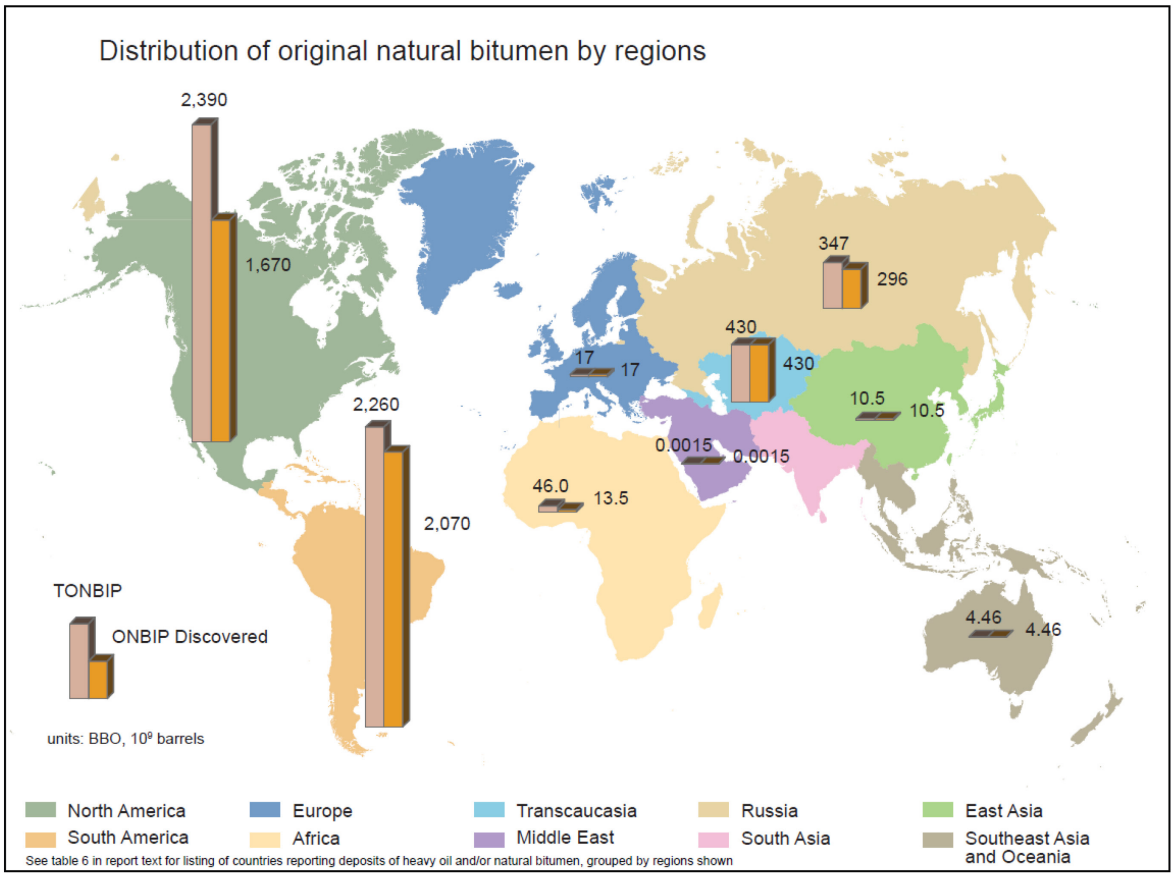

Fig 1.1. Natural bitumen quantities and geographical distribution; TONBIP: total original natural bitumen in place; ONBIP: original natural bitumen in place (Meyer *et al*., 2007).

1.2. Components of Solid Bitumen

The structure of bitumens is usually investigated using fractionation on the basis of solubility in various organic solvents (Fig. 1.2). The differences between these fractions are highly dependent on the method used (Hellmuth, 1989). The main components are hydrocarbons (paraffinic, naphthenic, and aromatic) but also include various amounts of non-hydrocarbon heterocyclic compounds i.e. resins, asphaltenes and pre-asphaltenes that constitute the heavy (high molecular weight) constituents of solid bitumens and are referred to as asphaltics (Meyer and De Witt, 1990). Pre-asphaltenes (carbenes and carboids) are present in very small amounts, usually less than 2 percent, are insoluble in

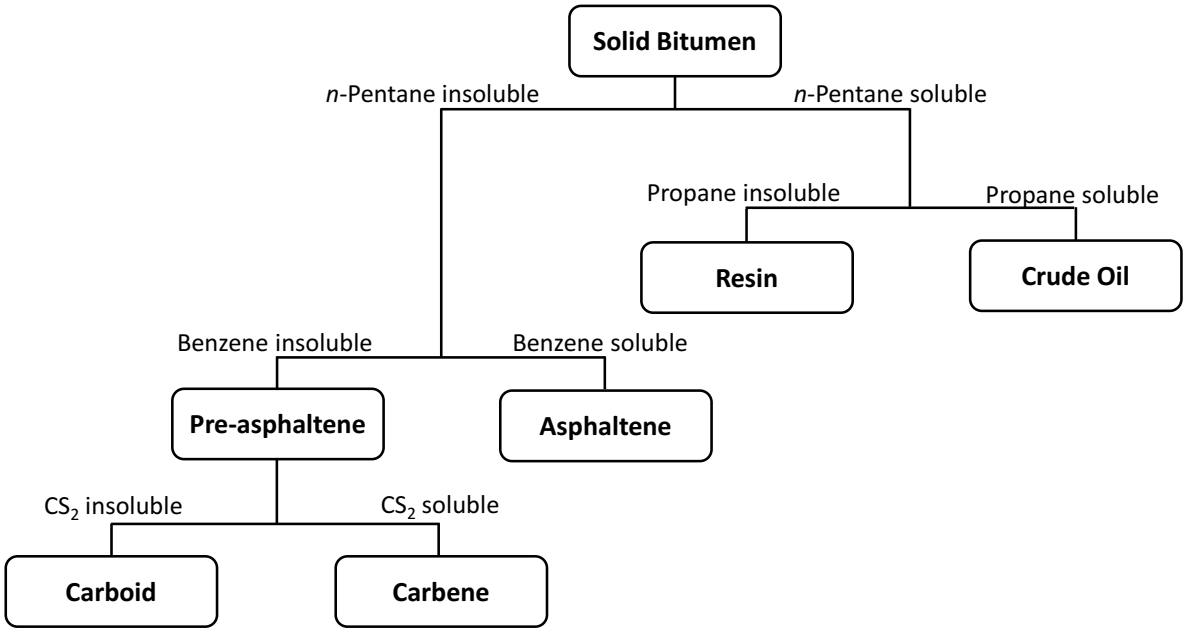

Fig. 1.2. Solvent fractionation scheme of solid bitumens (modified from Wen *et al*., 1978).

n-pentane, and are commonly disregarded (Yen and Chilingarian, 2000). Asphaltenes are very large molecules, most often incorporating heteroatoms and trace metals, and are soluble in carbon disulphide but insoluble in *n*-pentane. Nitrogen, sulphur, and oxygen combine with aliphatic, alicyclic and aromatic hydrocarbon skeletons to form heterocyclic compounds, termed NSO compounds, which are strongly polar. Resins are also large molecules that are strongly polar; they are soluble in both carbon disulphide and *n*-pentane (Meyer and De Witt, 1990). The sequential progression from crude oils to resins to asphaltenes to carbenes is associated with an increase in molecular size. The molecular weights of various fractions in bitumen vary from about 300 to 1500 for oily fraction and resins, from about 600 to 10000 for asphaltenes, and probably to higher values for carbenes (e.g. Wen *et al*., 1978).

An alternative approach has been proposed by Larter (1984), using isothermal or programmed temperature pyrolysis of the bitumen, to fractionate the pyrolysate into three boiling range cuts of *n*-alkanes i.e. C_1-C_8, C_9-C_{15} and C_{16}-C_{35}. In addition, using these

pyrolysate cuts in a ternary diagram, a simple and rapid screen characterization of bitumens is possible. For instance, aliphatic materials such as Ozocerite plot near the high boiling pyrolysate axis (> nC$_{15}$), whereas involatile aromatic bitumens such as Anthraxolite producing pyrolysates which are dominated by low boiling compounds (<nC$_8$) (Larter, 1984).

1.3. Classification Systems

During the last six decades, various attempts were made to introduce a chemically-based classification system for bituminous substances, though there is no general agreement yet. The most important nomenclature and classification for bitumens is that of Abraham (1960) and almost all later classifications are based on that. The traditional classifications are based on physicochemical properties such as solubility, fusibility, elemental analysis (H, C, O, N, S, Ash), hardness, and color, together with viscosity, density and optical reflectivity (e.g. Abraham, 1960; Hunt, 1979; Cornelius, 1987; Jacob, 1989; Jacob, 1993). Based upon these physicochemical properties, bitumens have been subdivided into several classes (see Fig. 1.3). Accordingly, solid bitumens may be divided into two main groups on the basis of their solubility in carbon disulphide (CS_2). The pyrobitumens are dark colored, hard, and insoluble in CS_2 and are divided into two subgroups based upon the H/C ratios. The Impsonite, Anthraxolite and Shungite subgroup is essentially metamorphosed and has atomic H/C ratios between 0.1 and 0.8. The Elaterite, Ingramite, Wurtzilite as well as Albertite subgroup is characterized by atomic H/C ratios as high as 1.6. Elaterite and Wurtzilite contain 3 to 4 weight percent sulphur and have undergone various degrees of vulcanization. Albertite and Ingramite are low in sulphur, have H/C only slightly greater than unity, and appear to be more highly indurated forms of natural asphalt (Hunt, 1979; Meyer and De Witt, 1990). The soluble bitumens in CS_2 form the other group; they generally contain various amounts of admixed mineral matter from their host rocks and fall into three subgroups based upon their relative fusibility: Mineral Waxes, Natural Asphalts, and Asphaltites. The mineral waxes are similar to the pyrobitumens in that they have atomic H/C greater than unity.

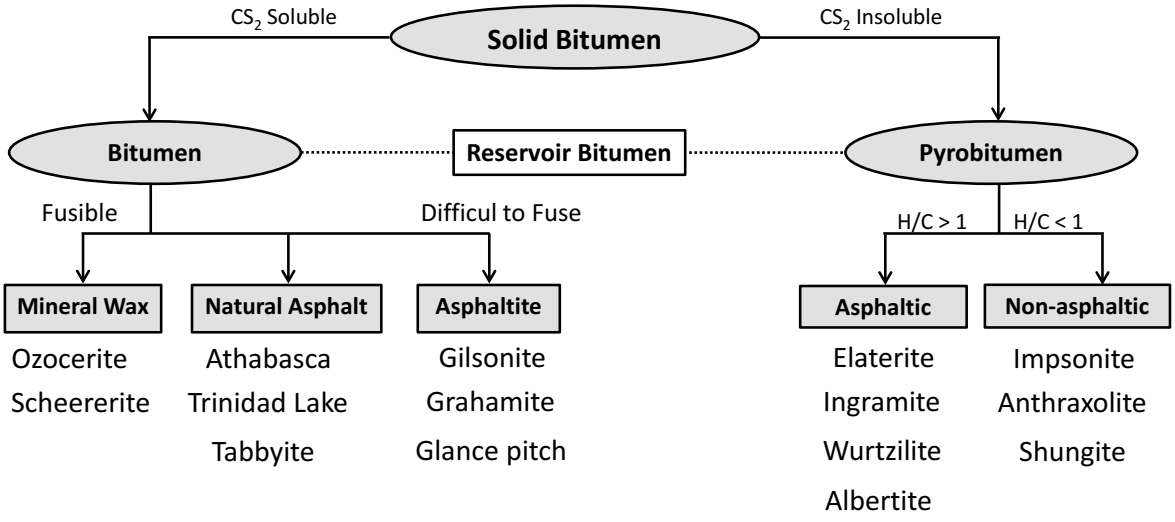

Fig. 1.3. A generic classification of solid bitumens based on solubility, fusibility and H/C ratio. Modified from Hunt, 1979; Cornelius, 1987.

However, they differ from the pyrobitumens and from the other soluble natural bitumens chemically because the waxes are mostly normal paraffins, whereas pyrobitumens consist substantially of asphaltics, and the other natural bitumens are composed almost entirely of aromatic hydrocarbons and asphaltics, to the virtual exclusion of paraffins. Ozocerite, the most common mineral wax, is easily fusible, has an atomic H/C ratio of about 1.5, and is made up almost entirely of paraffins. The natural asphalts are black, easily soluble, fuse at 50-160 °F, frequently contain admixed mineral matter, and are usually composed in part of NSO-compounds and trace metals. Because only natural asphalt is of quantitative importance or of economic significance, the general term natural bitumen is frequently, although incorrectly, used as a synonym for natural asphalt. The Asphaltites are very dark colored solids that will fuse, but only at temperatures above about 230 °F, and are almost completely soluble (Meyer and De Witt, 1990).

Solid reservoir bitumens are black, solid, graphitic or asphaltic particles or coatings within the pores of oil- or gas-bearing reservoir rocks, having been derived from the

petroleum contained therein. Their formation has been mainly attributed to natural processes including deasphalting, thermal alteration, and biodegradation, leading to variations in solubility in CS_2 (Rogers *et al*., 1974; Curiale, 1986; Stasiuk, 1997). The insoluble reservoir bitumens mostly have atomic H/C ratios of less than 1 and densities of about 1.15 to 1.40, whereas the soluble forms have H/C of about 1.2 to 1.5 and densities of 1.02 to 1.14 (Meyer and De Witt, 1990).

Curiale (1986) stated that the traditional classification scheme for solid bitumens is entirely generic and that the different names for different kinds of solid bitumens contain little genetic information content. He therefore proposed a genetic classification scheme whereby source rock-derived solid bitumens are assigned a position on a continuum between early-generation products of rich source rocks (pre-oil) and products of the alteration of once-liquid petroleum which was generated in and migrated from a mature oil source rock and was subsequently degraded (post-oil) (Fig. 1.4). Once formed, all solid bitumens may be subject to the same modification processes (Curiale, 1986). However, it should be kept in mind that solid bitumens are in a state of transition. Even the composition of solid bitumen from a single deposit will often vary, depending upon the degree of exposure and the extent of metamorphosis.

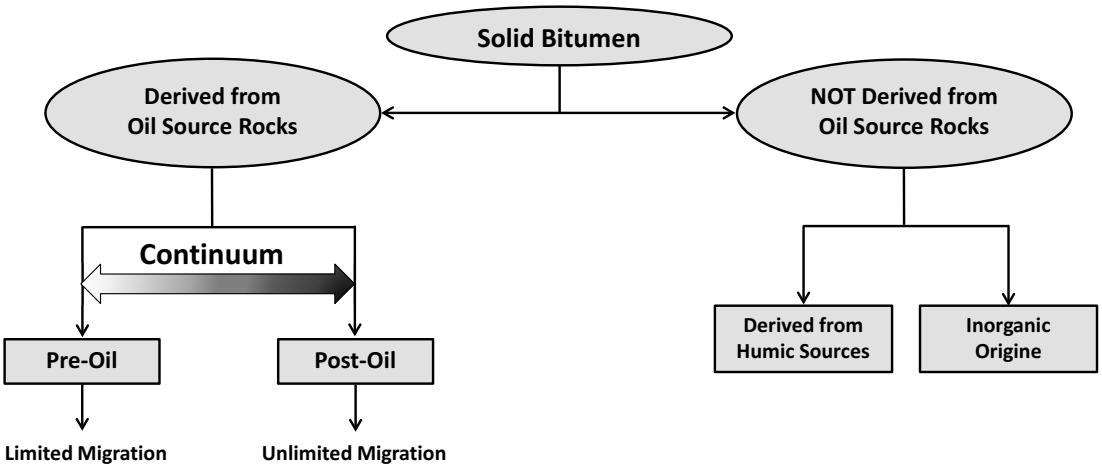

Fig. 1.4. A genetic classification of solid bitumens proposed by Curiale (1986).

1.4. Formation Mechanisms

According to the both generic and genetic classifications discussed above, solid bitumen is alteration product of organic matter, which can be either associated with mineral deposits e.g. Elaterite, Wurtzilite, Albertite, etc., or derived from petroleum source rocks i.e. pre-oils and post-oils (Curiale, 1986; Parnell *et al*., 1993; Rigali and Nagy, 1997; Parnell, 2004). The thrust in the current dissertation is on petroleum-related solid bitumens. As alteration products of conventional oils, they are often enriched in polar constituents such as asphaltenes. Deasphalting occurs as a result of disturbance in the thermodynamic equilibrium state of crude oils via various processes e.g. gas or light hydrocarbon injection during enhanced oil recovery operations (Dahl and Speers, 1986; Monger and Fu, 1987); depressurization of the reservoir during production operations; in-reservoir oil mixing (Larter *et al*., 1990); adsorption of asphaltenes onto clay minerals (Sachsenhofer *et al*., 2006); gravity segregation in the oil column (Schulte, 1980) and reservoir uplift (Hirschberg *et al*., 1984). Furthermore, the petroleum fluid's asphaltene concentration is shown to be controlled by its viscosity (Werner et al., 1996). Werner et al. (1998) have demonstrated in an investigation on synthetic crude oils that viscosity of petroleum fluids depends on the gas content, temperature, pressure and composition of the oils. At selected experimental conditions (35 MPa, 100ºC) they identified an elevated risk of asphaltenes precipitation for petroleum fluids when the gas concentration is larger than the critical gas content (~ 28 wt.%) and when the aromatics content remains below 25 wt.% (Werner et al., 1996; Werner et al., 1998). Moreover, asphaltene precipitation within a reservoir or migration pathway may be the result of biodegradation, fluid mixing and/or pressure drop below the asphaltene onset pressure (AOP) (Mahon *et al*., 2009). For example, the migration of early-charged oil into a horizon containing "fizz gas" may result in a higher gas-oil-ratio (GOR) fluid mixture and a shift to higher AOP as compared to the migrated oil. Another example is charging an existing accumulation of unstable oil with a high maturity, high GOR fluid resulting in higher AOP for the fluid accumulation. These two end-members increase the probability of asphaltene flocculation within the oil and precipitation of an intergranular tar at the point of mixing (Mahon *et al*., 2009).

A bitumen formed by asphaltene precipitation is a soluble residue (Levandowski *et al*., 1973) composed predominantly of asphaltenes, polar compounds and aromatic hydrocarbons, which would have a lower H/C atomic ratio but a similar carbon isotopic ratio compared with the precursor oil (Rogers *et al*., 1974; George *et al*., 1994).

Several major natural processes, acting alone or in tandem, may control the deposition and formation of solid bitumens, including: **a**) deposition environment, b) thermal alteration, c) fluid expulsion and bitumen segregation and **d**) biodegradation (e.g. Evans *et al*., 1971; Rogers *et al*., 1974; Curiale, 1986; George *et al*., 1994; Stasiuk, 1997; Hwang *et al*., 1998).

1.4.1. Depositional environment and petroleum composition

Although it is widely accepted that solid bitumen is the alteration products of once liquid petroleum fluids through at least one of the aforementioned secondary alteration processes, depositional conditions can play a key role.

Organic matter input and depositional conditions of the sediments that become source rocks exert primary control on the petroleum compositions. Accordingly, Tissot and Welte (1984) have been classified crude oils based primarily on the content of the various structural types of hydrocarbons to the *paraffinic*, *paraffinic-naphthenic*, *naphthenic*, *aromatic-intermediate*, *aromatic-naphthenic* and *aromatic-asphaltic* oils (Tissot and Welte, 1984). In this regard, the quality of kerogen within the organic matter plays a key role. The chemical structure of a shallow immature kerogen varies with the original mixture of organisms and with the physical, chemical and biochemical conditions of deposition. They are classified based on elemental analysis ratios as Type I, II, III and IV which are defined at low maturation levels by their atomic H/C and O/C ratios (Tissot and Welte, 1984; Scott, 1989). Mixing of various components during organic matter deposition may lead to intermediate kerogen types such as Type I/II or Type II/III. For instance, Type I kerogen is derived substantially from algae in lacustrine setting that can mainly generate high-wax *paraffinic* oils, but depending upon its thermal

maturation can also generate gas. An example of Type I kerogen is found in the Green River Formation of Uinta Basin. Also, the source material of Type II kerogen is mainly plankton with some contribution from algae in reducing marine environments that can generate various types of petroleum from *paraffinic-naphthenic* to *aromatic-intermediate,* depending upon the organofacies as well as lithology of the source rock i.e. clastic vs. non-clastic. Although oil-prone source rocks, whether shales or carbonates commonly show similar characteristics including lamination, high TOC and hydrogen-rich organic matter, the generated oils from carbonate rocks are typically richer in cyclic hydrocarbons and sulphur compared with those from shales (e.g. Peters *et al*., 2005; McCarthy *et al*., 2011).

Furthermore, the depositional conditions have an important influence on the petroleum composition. The Uinta Basin has long been noted for its remarkable vein deposits of several types of solid hydrocarbons. However, Hunt (1963) stated that salinity is the most important single factor governing the composition of the different types of solid bitumens in the Uinta Basin. The major changes in the composition of the bitumens correlate stratigraphically with the changes in mineralogy and fossil type. In general, the dominant molecular structure of the bitumens changes from paraffin chains to aromatic rings, and to chain and ring compounds high in sulphur and nitrogen, the most important representatives being Ozocerite, Albertite, Gilsonite, and Wurtzilite, respectively (Hunt, 1963). Although the original waters were oxidizing (brakish water to highly saline), they later became strongly reducing, and the toxic hydrogen sulphide in the bottom layers resulted in a tremendous accumulation of organic matter. This resulted in the deposition of several thousand feet of bituminous sediments; by far the most important of them is Gilsonite (Hunt *et al*., 1954; Hunt, 1963; Verbeek and Grout, 1992; Nciri *et al*., 2014). The formation mechanisms of the vein deposits in the Uinta Basin are of interest and have been long debated. According to Hunt *et al*. (1954), the area later became uplifted. Then the cracks were opened slowly as uplift progressed and were simultaneously filled with the bituminous material that would later, upon increasing polymerization, harden into the solids we now see. The changes in the types of bitumens originating in successively younger beds coincide with changes in the minerals and the

fossils. Apparently they all are a reflection of changes in depositional environment (Hunt, 1963; Verbeek and Grout, 1992).

1.4.2. Thermal alteration

According to Curiale (1986), solid bitumens can be differentiated by the thermal conditions in their source at the time of expulsion. Organic-rich source rocks may generate thermally immature bitumen that migrates short distances and solidifies in voids and fractures. Alternatively, petroleum expelled from mature source rocks can migrate considerable distances and accumulate in reservoir units where secondary processes, such as biodegradation, thermochemical sulphate reduction (TSR), or thermal chemical alteration (TCA), may form solid bitumens. Both TCA and TSR solid bitumens formed via post-accumulation reservoir processes are largely condensed structures having atomic H/C < 1 and more than 35% of the carbon in aromatic rings (^{13}C NMR fa > 0.35); also both can give rise to highly aromatic, insoluble residues (pyrobitumens) (Kelemen *et al*., 2008; Kelemen *et al*., 2010).

TCA-solid bitumen forms when large polynuclear aromatic (PNA) and NSO compounds thermally crack, resulting in alkyl side-chain cleavage, heteroatom elimination, and condensation reactions. TCA-solid bitumen can occur disseminated throughout the reservoir pore space or can be concentrated in fractures and voids, in specific stratigraphic units, or in production zones within the same reservoir unit as exemplified by Tengiz Field, Kazahkstan (Hwang *et al*., 1998; Walters *et al*., 2006). Also the black residue (pyrobitumen) and natural gas in the Jurassic Smackover Formation is formed by thermal alteration of petroleum by late Cretaceous igneous intrusions (Parker, 1974) by hydrogen disproportionation. In the Aquitaine Basin (France), natural asphalt has been found in a borehole at depths between 1.9 and 4.2 km (Connan and Van Der Weide, 1978). Deep burial of a reservoired oil is expected to have the same effect (George *et al*., 1994). TCA may follow non-thermal processes, such as gravity segregation, biodegradation and asphaltene precipitation (Kelemen *et al*., 2010). One of the most prominent features of this type of solid bitumen is the presence of lighter *n*-

alkanes, which are absent in degraded surficial bitumens. The limited liberation of saturated hydrocarbons during thermal alteration is accompanied by the condensation of hydrogen donors to polyaromatic high-molecular structures, as exemplified by asphaltenes and pyrobitumen. Thus the bitumen becomes increasingly insoluble and infusable (Hellmuth, 1989). During progressively thermal cracking, isotopically light methane is cracked off hydrocarbons whose isotopic compositions become heavier (George *et al*., 1994; Wilhelms and Larter, 1994).

In contrast, TSR is a redox reaction where petroleum is oxidized to CO_2 and inorganic sulphate is reduced to H_2S (Orr, 1974; Orr, 1978; Aizenshtat *et al*., 1995; Kelemen *et al*., 2010). TSR can form bitumens enriched in sulphur and occurs in relatively hot (> 100 ºC) carbonate-evaporite reservoirs (e.g. Walters *et al*., 2015). Whereas TCA mostly shifts the hydrocarbon product distribution toward lighter hydrocarbons with a smaller fraction (of hydrocarbon product) converting to pyrobitumen, TSR can result in the almost complete destruction of hydrocarbons and the formation of large quantities of H_2S (Kelemen *et al*., 2010). It appears that solid bitumen is common to all reservoirs where petroleum has been altered by TSR (Machel *et al*., 1995). TSR-bitumens are largely insoluble, exhibit high reflectivity (>1.5% R_o), produce negligible pyrolysate yields (HI ~ 0-80 mg/g TOC), and are associated with elemental sulphur (Sassen, 1988; Machel *et al*., 1995). High concentrations of sulphur (>10 wt%) with enriched $\delta^{34}S$ values relative to the parent petroleum fluid are considered to be characteristic of TSR-bitumens (Powell and Maqueen, 1984; Sassen, 1988; Machel *et al*., 1995; Kelemen *et al*., 2010). Solid bitumens originating from TSR may petrographically resemble highly mature TCA solids and appear to be associated with or incorporate sulphur (Sassen, 1988; Stasiuk, 1997; Kelemen *et al*., 2008). Walters and co-workers using atmospheric pressure photoionization (APPI) combined with FT-ICR MS, analyzed genetically related unaltered and TSR-altered oils from the Upper Jurassic (Oxfordian) Smackover Formation. They found that TSR altered oils and condensates contain highly condensed polynuclear aromatic and naphthenoaromatic species with 0-3 sulphur atoms, which are not present in petroleum fluids of equivalent maturity that have not experienced TSR. Also they called these species "*proto-solid bitumen*" as they represent the type of organic

compounds that could easily precipitate from the TSR altered oils with slight chemical alteration or changes in reservoir conditions (Walters *et al*., 2011).

1.4.3. Fluid expulsion and bitumen segregation

The formation of stable oil-water emulsions with alkaline solutions is a common practice in enhanced oil recovery methods (Ruble *et al*., 1994). The alkaline solutions react with acidic components present in the crude oils to produce petroleum soaps, which are generally sodium salts of carboxylic acids (Taylor and Hawkins, 1992). The petroleum soaps are capable of adsorbing at the oil-water interface and lowering interfacial tension to a degree that emulsification may occur (Taylor and Hawkins, 1992).

Periodically a thick, viscous, liquid hydrocarbon termed "gilsonite tar" can be found oozing from the wall rock in certain exhumed areas of the mines in the Uinta Basin of northeastern Utah. It is proposed that a similar situation may have occurred in the formation of “gilsonite tar”, which could have been facilitated by the presence of the alkaline ground waters.

Recent structural investigations (Verbeek and Grout, 1992; Verbeek and Grout, 1993) indicate that the gilsonite veins originated as large hydraulic extension fractures whose formation was prompted, in part, by high pore-fluid pressures in the source beds. The fracturing initiated the escape of large amounts of Formation water, followed by the forceful injection of the viscous precursor to gilsonite (Verbeek and Grout, 1992; Verbeek and Grout, 1993). This Formation water has a very high alkalinity (pH > 9) which is presumably provided by sodium carbonate minerals found in the upper Green River Formation (Bradley, 1931). Microscopic examination of the “gilsonite tar” by Ruble *et al*. (1994) revealed the presence of a large proportion of clear circular droplets encased in a light brown hydrocarbon matrix which in fresh samples made up approximately 40% of the overall composition of the “gilsonite tar”. Such an emulsion could then provide a means for previous and continued migration of “gilsonite tar” into the veins from source beds in deeper portions of the basin. Upon emplacement into the

veins the eventual de-emulsification of the bitumen component, possibly combined with other alteration processes such as hydrocarbon devolitalization, polymerization, and/or oxidation (Bell and Hunt, 1963), resulted in the eventual solidification of the gilsonite tar into gilsonite (Ruble *et al*., 1994).

1.4.4. Biodegradation

Biodegradation of crude oil involves the progressive utilization of certain types of hydrocarbons by microorganisms. This process can occur at the surface (when the oil has been exposed as in a seep), in the reservoir and during migration (Cassani and Eglinton, 1991). Based on observations on compositional changes in crude oils, classification systems describing the extent of biodegradation have been suggested (e.g. Volkman *et al*., 1984; Peters and Moldowan, 1993; Fisher *et al*., 1998). According to these systems, different types of oil constituents are degraded sequentially (*n*-alkanes > mono-cyclic alkanes > alkylbenzenes > isoprenoid alkanes > alkylnaphthalenes > bicyclic alkanes > steranes > hopanes) (Milner *et al*., 1977; Alexander *et al*., 1983; Cassani and Eglinton, 1991; Wilkes *et al*., 2000). Oxidation of oil during biodegradation leads to a systematic decrease in paraffin content with increasing degradation and an increase in oil density, sulphur content, acidity, and viscosity (Connan, 1984), resulting in some cases in extra-heavy oil accumulations, such as the Orinoco Tar Belt in Venezuela and the Athabasca Tar Sands in Alberta, Canada (Demaison, 1977; Connan *et al*., 1980). Biodegradation accompanied with water washing may play a major role in the formation of some solid bitumens due to selective and successive removal of light liquid hydrocarbons (e.g. Williams and Goodarzi, 1981; Connan, 1984; Huc *et al*., 2000). Until about two decades ago it was generally accepted that these effects are mainly caused by aerobic bacteria (e.g. Palmer, 1993). Sufficient oxygen and nutrient supply for the action of aerobic bacteria in undeveloped reservoirs was assumed to be provided by meteoric waters (Wilkes *et al*., 2000). However, biodegradation of crude oil is also observed in reservoirs where oxygen is not available but anoxic conditions prevail (Connan *et al*., 1995).

Anaerobic biodegradation of hydrocarbons is now widely accepted as a significant process in natural environments (e.g. Widdel and Rabus, 2001; Wilkes *et al*., 2003; Larter *et al*., 2006; Vieth and Wilkes, 2006). Petroleum biodegradation proceeds under anaerobic conditions in any reservoir that has a water leg and has not been heated to temperatures more than 80 ºC (Larter *et al*., 2006). Many compositional changes seen in shallow petroleum reservoirs, such as sequential and systematic removal of various hydrocarbons, selective degradation of specific isomeric compounds in individual petroleum compound classes, and the production of carboxylic acids as byproducts, closely mimic changes seen in field and laboratory biodegradation settings (Larter *et al*., 2006). This alteration differs from that caused by physical processes such as phase fractionation or water washing, and it is consistent with the compositional changes being related to the extensive biological metabolism of oils in the reservoir (e.g. Connan, 1984; Volkman *et al*., 1984; Rowland *et al*., 1986; Wenger *et al*., 2001; Peters and Fowler, 2002; Head *et al.*, 2003; Larter *et al*., 2006). There is still some debate on the exact order in which different compounds are removed from crude oil during anaerobic biodegradation, but the strongest deterioration of petroleum quality occurs from slight to moderate biodegradation (Wenger *et al*., 2001) or between biodegradation levels 1 and 4 (Peters *et al*., 2005). While the aerobic organisms employ molecular oxygen as a highly reactive cosubstrate during degradation of hydrocarbons, under anoxic conditions, the reactions of hydrocarbon degradation have to proceed via oxygen-independent steps (Wilkes *et al*., 2000). In most reservoirs with low concentrations of aqueous sulphate, methanogenic degradation is a primary mechanism of petroleum degradation, whereas in waters containing abundant sulphate, sulphate reduction and sulphide production may dominate (Larter *et al*., 2006).

Within reservoirs, field observations typically record at oil-water contacts (OWCs) a coincidence of the lowest oil quality and the strongest biological and molecular evidence for hydrocarbon degradation, suggesting that most petroleum degradation occurs at this interface (Larter *et al*., 2003). This conclusion is sensible because at the OWC, organisms can live in free water necessary for life and find food (oil) and reactants (water, oxidants) to generate energy and biomass (Head *et al*., 2003; Larter *et al*., 2006).

Finally, it should be kept in mind that various combinations of the aforementioned formation mechanisms are also possible.

1.5. Research Perspectives and Objectives

Recent years have seen an increased interest in studying the composition, properties, and ways of processing of solid and viscous liquid natural bitumen (e.g. Walters *et al*., 2006; Kelemen *et al*., 2008; Kelemen *et al*., 2010; Kavak *et al*., 2010;Walters *et al*., 2011; Helms *et al*., 2012; Shalaby *et al*., 2012; Connan *et al*., 2013; Kara-Gülbay and Korkmaz, 2013; Cobbold *et al*., 2014). Southeastern Turkey is the main oil-producing region in the country and there are various surface and subsurface petroleum occurrences i.e. solid bitumen veins and vugs, oil seeps as well as crude oils. Since 1960s, they have been the focus of numerous studies (e.g. Orhun, 1969; Lebküchner, 1969; Lebküchner *et al*., 1972; M. A. Ala, 1979; Mueller *et al*., 1995; Yalçin Erik *et al*., 2005; Yalçın Erik and Özcelik, 2007; Kavak *et al*., 2010). The main focus has been on the physicochemical properties of petroleum occurrences, their geological outline as well as geochemical characteristics. There are still some fundamentally important questions to be answered about the solid bitumen veins and their relationship to the conventional petroleum system in the region, and these form the basis of the current research project:

1) Literature review reveals that solid bitumen veins are showing different physicochemical characteristics depending upon their geographic locations (e.g. Lebküchner *et al*., 1972). Also they are thought to have originated from the same source (Kavak *et al*., 2010). So, the first question is why do they display a wide variety in physicochemical properties? Are they genetically related, and if so, how have they evolved over geological time?

2) As discussed above, various factors acting alone or together can result in solid bitumen formation, globally. So, by which mechanism(s) have the Turkish solid bitumens been formed?

3) Despite the fact that a few correlation studies have been conducted to compare surface and subsurface petroleum occurrences in the region, a clear genetic relationship between them has remained elusive; therefore in the frame of this project a correlation study was included.
4) literature review reveals that petroleum occurrences in the investigated area are sulphur-rich (e.g. Mueller *et al*., 1995; Nairn and Alsharhan, 1997; Kavak, 2011). To the best of my knowledge no attempt has been made to characterize the S-containing compounds in detail, mostly due to analytical deficiencies and difficulties. Since organosulphur compounds are mainly present in medium and complex macromolecules (Sinninghe Damste and De Leeuw, 1990), it is of interest to find out how advanced geochemical tools can be used to characterize such polar components in the investigated petroleum system.

In this cumulative dissertation, the above mentioned questions are addressed using an array of advanced organic geochemical methods that includes total organic carbon (TOC), Rock-Eval pyrolysis, Soxhlet extraction, medium pressure liquid chromatography (MPLC), gas chromatography (GC), thermovaporization- and pyrolysis-gas chromatography (PY-GC), gas chromatography-mass spectrometry (GC-MS), gas chromatography-isotope ratio mass spectrometry (GC-IRMS) and ultra-high resolution fourier transform-ion cyclotron resonance-mass spectrometry (FT-ICR MS) in its different ionization modes.

The logistics of the work programme was as follows. The main initial focus, presented in **Chapter 2**, was laid on solid bitumen veins, their geochemical characteristics and possible formation mechanisms, applying various conventional and advanced geochemical tools. To achieve that, twenty-two solid bitumen samples from seventeen different veins and vugs, all from Şırnak province in SE Turkey, were gathered. Evaluation and interpretation of the obtained bulk and molecular data is provided new insights into the putative solid bitumen formation mechanisms and contribute to an improved understanding of their physical and chemical properties.

In the next phase of this project, presented in **Chapter 3**, a comprehensive geochemical correlation study was conducted for on surficial petroleum occurrences i.e. solid bitumen veins and seep oils, and subsurface crude oils from proximal oilfields to determine whether a genetic relationship exist between them. For this, thirty solid bitumens along with ten heavy oils and thirteen oil seeps are investigated mainly using the obtained data from source-sensitive biomarkers as well as compound-specific stable carbon isotopes of *n*-alkanes. Unfortunately, no samples from potential source rocks were available for inclusion in the work, though it is possible to infer their geochemical characteristics using source-sensitive biomarkers in the investigated samples. Literature review reveals that in southeastern Turkey four different oil families (1-4) have been distinguished by employing biomarker and carbon isotope ratios (Zumberge *et al*., 1992; Connan *et al*., 2006). Some previous correlation studies on Turkish solid bitumens and proximal oils are indicated that the adjacent crude oils belong to the Family 2 which is ostensibly generated from the Upper Jurassic/Lower Cretaceous carbonate units (Erdem-Senatalar *et al*., 1991; Kavak, 2011). Furthermore, they have been compared with solid bitumen occurrences and some close similarities in terms of chemical composition have been found, suggesting a same origin for both. On the other hand, using the same approach, a correlation study has been conducted between solid bitumens (from Seridahli vein) and neighbor heavy oils that found no genetic relationship (Mueller *et al*., 1995). Therefore, a comprehensive geochemical approach was needed in order to investigate possible genetic affinities between the two.

One of the raised questions during this study was related to the sulphur-containing compounds. Although according to literature the investigated petroleum occurrences are known to be sulphur-rich, their concentrations in all petroleum types were low, as revealed by PY-GC results in chapter 3, indicating that they occur in condensed ring structures. Therefore, as summarized in **Chapter 4**, we then focused on geochemical characteristics of organosulphur compounds using ultra-high resolution mass spectrometry to determine how sulphur was introduced into the organic matter and through which mechanism(s). According to the results from the correlation study in Chapter 3 there is a strong genetic relationship between solid bitumen veins and

subsurface heavy oils. Therefore, this region serves as a natural laboratory for investigating the compositional evolutionary pathways of sulphur components in different phases i.e. liquid and solid as well as in a wide variety of maturation levels.

1.6. Structure of the Dissertation

Chapter 2 reveals how different kinds of chemical compounds in solid bitumens are influenced by alteration processes particularly thermal maturity variations. Their possible formation mechanism is also discussed. Chapter 2 has already been published:

Chapter 3 shows how various geochemical parameters are used to compare surface and subsurface petroleum occurrences from southeastern Turkey. Chapter 3 has already been published:

Chapter 4 describes how sulphur introduced into the investigated petroleum fluids. The geochemical evolution pathway(s) of S-containing compounds are also investigated. Chapter 4 is a draft manuscript which is currently under review by co-authors prior to submission.

In **Chapter 5** "summary and outlook" is provided.

2. ROLE OF MATURITY IN CONTROLLING THE COMPOSITION OF SOLID BITUMENS

This chapter reproduced with permission from ***Hosseini, S. H.,*** *B. Horsfield, S. Poetz, H. Wilkes, M. N. Yalçın, and O. Kavak., (2017). Role of maturity in controlling the composition of solid bitumens in veins and vugs from SE Turkey as revealed by conventional and advanced geochemical tools:* Energy and Fuels*, v. 31, p. 2398-2413 (postprint),* DOI: 10.1021/acs.energyfuels.6b01903. Copyright (2017) American Chemical Society.

2.1. Abstract

Solid bitumens found in veins and cracks may have formed from once liquid petroleum by thermal chemical alteration like maturation or by oxidative processes associated with thermochemical sulphate reduction (TSR), biodegradation or weathering. In this study, we investigated 22 solid bitumen samples from 17 different veins in the Şırnak Province in southeast Turkey using conventional and advanced geochemical tools with respect to their formation. Southeast Turkey is located in an active collision zone from the Alpine orogeny and compressional pressure occurred with different intensity across the region generating an overall increase in maturation from west to east. A special focus was laid on the characterization of polar compounds containing nitrogen, sulphur and oxygen (NSO) of high molecular weight using Fourier transform ion cyclotron resonance mass spectrometry with electrospray ionization in negative ion mode (ESI-FT-ICR-MS). The results indicate that, among possible secondary processes, thermal stress plays the major role in transforming solid bitumen compositions across the

region after their initial emplacement in subsurface veins and vugs. Hydrogen Index and amount of extractable organic matter correlate well with T_{max}. A progressive shortening of *n*-alkyl chains and increasing proportions of aromatic hydrocarbons are observed by pyrolysis-GC. While common maturity ratios based on saturated biomarkers are at equilibrium or saturated biomarkers are below detection limit for samples with T_{max} >450 ºC, those based on aromatic hydrocarbons like phenanthrenes or alkyldibenzothiophenes are useful to describe the whole range of thermal chemical alteration. ESI-FT-ICR-MS results reveal a dominance of nitrogen and sulphur compounds (N_yS_z) with 1 - 2 pyrrolic nitrogen atoms and 0 - 2 thiophenic sulphur atoms and nitrogen only (N_y) compounds with 1 - 2 pyrrolic nitrogen atoms. Condensation, aromatization and side-chain cracking reactions of NSO compounds take place with ongoing maturation as indicated by double bond equivalent and carbon number distributions. At highest maturation levels, side-chain cracking has proceeded so far that further condensation and aromatization processes are not possible which can be interpreted as an indication that solid bitumens have formed from migrated, reservoired petroleum and not from source rock kerogen. An increase in oxygen containing compounds indicates oxidation processes which most likely occurred after emplacement.

2.2. Introduction

Veins and vugs of what we here term solid bitumen have been reported from a wide variety of localities and geological settings around the world. Their colour usually ranges between shades of brown to black (Abraham, 1960), though yellow and orange varieties are known (Volk *et al*., 2000). They may be brittle, in which case they display conchoidal fracture, or they may be soft, elastic and malleable. Any given bitumen may appear homogeneous in hand specimen, or contain fragments of the current host rock or the rock from which it originated (Cobbold *et al*., 1999). While vugs and veins containing bitumen occur in coal-bearing or mineralized strata (Gu *et al*., 2012; Stevenson *et al*., 1990), they are particularly abundant in petroleum provinces (Curiale, 1986). The largest veins in the Neuquén Basin of Argentina, for instance, are meters

wide, kilometers to tens of kilometers in length and extend to great depth; they are often steeply-dipping and show intrusive relationships with their wall rocks, and may be orientated perpendicular to where major intrusives have pierced organic-rich marine shales (Cobbold *et al*., 1999; Cobbold *et al*., 2014). The orientations of the veins may also be in accordance with the direction of oblique convergence between tectonic plates (Cobbold *et al*., 1999). The veins of the Uinta Basin, associated with extremely organic-rich lacustrine shales, are similarly extensive (Hunt, 1963). High heating and cooling rates may have brought about the formation of fractures due to tensile failure, and caused generation of the fluids whose residues now constitute the bitumen itself.

The classification of solid bitumen was for many years based on physicochemical properties such as solubility in carbon disulphide, fusibility, H/C and O/C atomic ratios, viscosity and optical reflectivity (Abraham, 1960; Hunt *et al*., 1954; Cornelius, 1987; Jacob, 1989). Based on these operational classifications natural bitumen types have been defined using a nomenclature based on a mixture of type locality and assumed mode of origin, including ozocerite, asphaltite as well as impsonite, and their sub-divisions. For example asphaltite's sub-divisions are gilsonite, glance pitch and grahamite, based on their volatile matter content and reflectivity (Cornelius, 1987). Curiale proposed that these names be succeeded by a genetic classification scheme. His reference was a continuum between early-generation products of rich source rocks (pre-oil) and products of the alteration of once-liquid petroleum which had been generated in and migrated from a mature oil source rock and was subsequently degraded (post-oil) (Curiale, 1986). Of course, solid bitumens may display chemical and physical properties related to their degree of organic metamorphism attained after emplacement, as exemplified by occurrences in southeast Turkey (Lebküchner, 1969; Orhun, 1969). In that regard, pyrobitumen forms at extremely high levels of thermal stress (Stasiuk *et al*., 1999). Needless to say, oxidation processes come into play at or near outcrops and subcrops where molecular oxygen and/or anaerobic electron acceptors are available, causing an increase in molecular weight and decrease in H/C ratio (Bartle *et al*., 1981).

Here we focus on the solid bitumen veins of southeast Turkey, and in particular on their poorly characterized polar compounds. The study area is the most petroliferous

region in Turkey and there are many oil fields, oil seepages and solid bitumen veins occurring in close proximity. Although this region belongs to the Persian Gulf Basin, where many of the world's largest structurally-controlled oilfields occur, the accumulations are small by Middle Eastern standards (Ala and Moss, 1979). According to Lebküchner *et al*. solid bitumen veins form the main part of the surficial petroleum occurrences in SE Turkey (Lebküchner *et al*., 1972), amounting to about 82 million tons (Kar, 2006).

Various geological and geochemical studies have been conducted on the Turkish solid bitumens in order to determine their origin, formation mechanisms as well as geochemical characteristics. Lebküchner and Orhun studied their distinctive characteristic properties, compared them with asphaltic substances from around the world and, based on their solubility in carbon disulphide, classified them as asphaltic pyrobitumens and substances with compositions falling between asphaltite and asphaltic pyrobitumens (Lebküchner, 1969; Orhun, 1969). According to these authors, Turkish solid bitumens display a wide variety in character depending upon geographic location, geological origins and the degrees of progress in metamorphism related to tectonic events. The elemental composition of solid bitumens revealed that they are sulphur-rich, and the amounts of associated mineral matter are quite high (22 to 64%) which is rather unusual for bitumens in general (Orhun, 1969).

Kavak correlated solid bitumens from 12 different veins in the Şırnak area with two oil samples from the Raman and Dinçer oil fields using screening and molecular parameters and concluded that they have the same or similar origin (Kavak, 2011). Some authors, using the same approach, confirmed that a genetic relationship exists between the oils and solid bitumens, and suggested the Upper Jurassic/Lower Cretaceous carbonates of the Cudi Group to be a common source (Kara-Gülbay and Korkmaz, 2012; Yalçın, 2012). However, others have reported that the hydrocarbon potential of this unit as being low (Yalçın Erik and Özcelik, 2007). Mueller *et al*. studied solid bitumens from the Seridahli vein and five oils from different oilfields and on the basis of biomarker distributions concluded that there is no genetic relationship between the studied oils and solid bitumens (Mueller *et al*., 1995). A relatively recent report suggested a Middle

Jurassic source rock (Yolaçan Fm.) as the origin of the heavy oils and solid bitumens (Çorbacıoğlu, 2015). Thus, while the origin of solid bitumens is still under debate, there is general agreement that they were once either liquid or semi-liquid petroleum, and that their placement age is Miocene or younger (Lebküchner *et al*., 1972; Ala and Moss, 1979; Bartle *et al*., 1981; Erdem-Senatalar *et al*., 1991; Hiçyılmaz and Altun, 2006; Kavak *et al*., 2010). The aforementioned studies employed various geochemical analytical methods including Rock-Eval pyrolysis, determination of total organic carbon (TOC) content, biomarker as well as isotope analyses, but had limitations regarding their ability to fully unravel the compositional complexity. The analytical window mainly covered the hydrocarbons with molecular masses up to approximately 500 Dalton. The polar compounds, which make up a large proportion of the overall compositional signature, have remained unexplored, but thanks to FT-ICR MS technology new insights are possible.

Electrospray ionization combined with Fourier transform Ion Cyclotron Resonance mass spectrometry (ESI FT-ICR MS) is a relatively recently developed analytical tool that has been proven to be well suited for characterising polar components in petroleum and source rocks (Hughey *et al*., 2007; Hur *et al*., 2010; Helms *et al*., 2012; Liao *et al*., 2012), including those of high molecular weight (HMW). It has been used to investigate specific molecular structural changes in bitumen and oils related to thermal maturation(Hughey *et al*., 2004; Oldenburg *et al*., 2014; Poetz *et al*., 2014; Mahlstedt *et al*., 2016) and other alteration processes like biodegradation, thermogenic sulphate reduction (TSR) or oxidation e.g. weathering (Kim *et al*., 2005; Li *et al*., 2010; Walters *et al*., 2015; Chen *et al*., 2016). In this contribution, polar compounds in solid bitumens from veins and vugs in SE Turkey are investigated using FT-ICR MS, in combination with pyrolysis and other geochemical methods, thereby contributing new information on their mode of formation.

2.3. Geological Setting and Possible Formation Mechanism of Veins

The tectonic history of SE Turkey has been documented in detail (Ala and Moss, 1979; Şengör and Yilmaz, 1981; Hempton, 1985; Yilmaz *et al*., 1993; Gorur and Tuysuz, 2001; Okay, 2008). The most important period of folding and thrusting in this region spanned the Upper Cretaceous-early Pliocene interval (Ala and Moss, 1979). During this period of time the region underwent two major episodes of Alpine deformation which occurred in the Late Cretaceous and Middle Eocene-Miocene. The first episode was caused by the subduction of the Arabian Plate beneath the Anatolian Plate along the Bitlis-Zagros Suture Zone (Şengör and Yilmaz, 1981) and created the structural traps and fractures (Cater and Gillcrist, 1994). The latter episode occurred as a result of the progressive elimination and complete closure of the ocean(s) which led to the collision between Eurasia and the Arabian Plate (Yilmaz, 1993). Due to this main phase of the Alpine orogeny compressional folds developed; all the hydrocarbon accumulations so far discovered in SE Turkey are held in anticline traps formed during this last phase of the Alpine movements (Ala and Moss, 1979). All explored hydrocarbon traps are located in the central and western part of the northern margin of the Arabian platform, while solid bitumen veins are mainly present in the eastern part (Fig. 2.1.a). The main reason for this distribution is most likely attributed to regional tectonics, as compressional pressure did not occur with the same intensity across the region and increases towards the east (Egeran, 1951).

According to various studies hydrocarbon generation and expulsion in SE Turkey occurred during Middle Eocene-Upper Miocene (Lebküchner *et al*., 1972; Ala and Moss, 1979; Bartle *et al*., 1981; Erdem-Senatalar *et al*., 1991; Demirel *et al*., 2001; Hiçyılmaz and Altun, 2006; Kavak *et al*., 2010). It appears that the compressional forces resulted from the main phase of Alpine orogeny in Miocene led to the formation of deep, open tensional cracks above and below thrust faults and in faulted anticlines (Nairn and Alsharhan, 1997). It seems due to these superimposed structural deformations that the cap rock units are breached and the already trapped heavy oils may have been squeezed toward the surface (Nairn and Alsharhan, 1997) and distributed in the around faults and cracks.

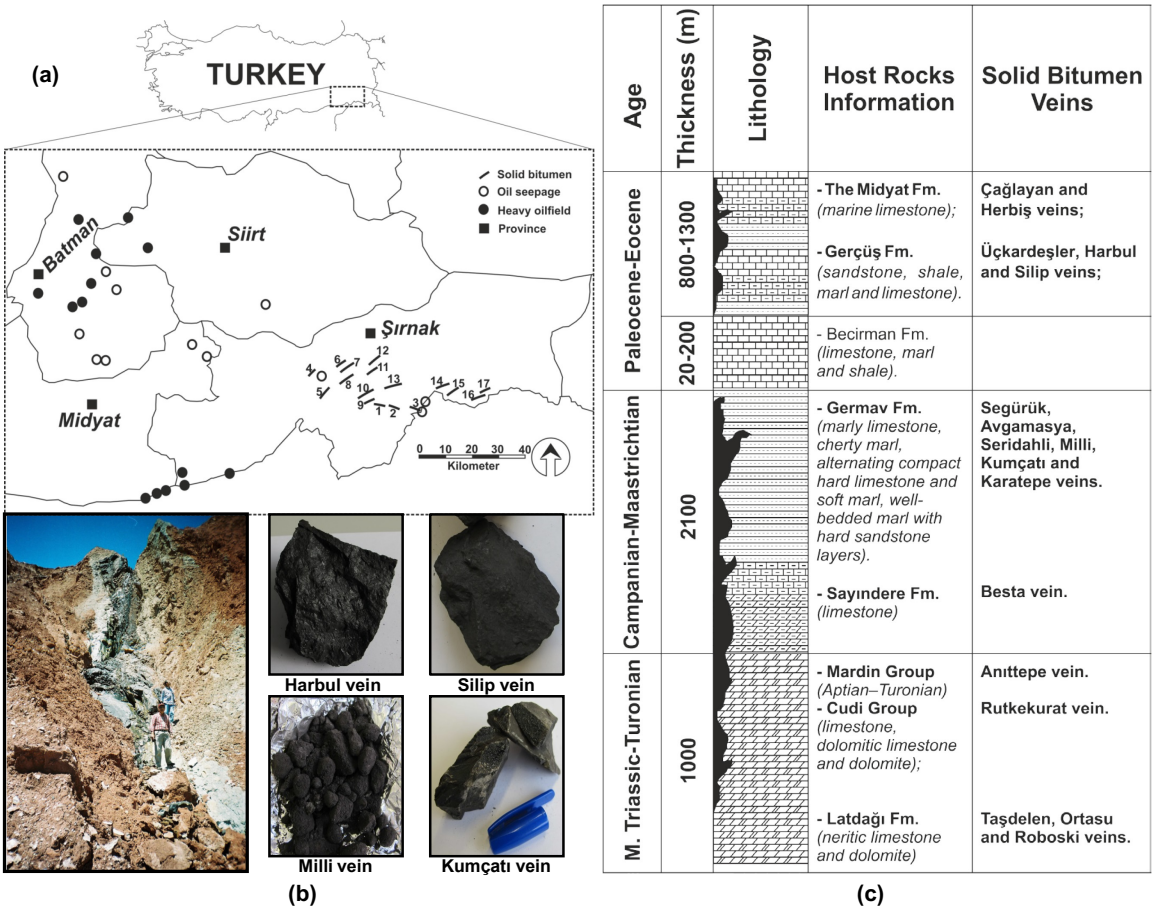

Fig. 2.1. a) Geographic location of the studied solid bitumen's veins as well as some oil seepages and heavy oilfields in SE Turkey. The vein's names are given in Table 1. **b)** Left: The dyke-shape Harbul vein in the Gerçüş Formation as host rock; Right: Some of studied solid bitumens in hand specimen to show their different appearance. **c)** The stratigraphic column of SE Turkey and occurrence of solid bitumens in different sedimentary units - modified after Kavak *et al*. (2010) and Lebküchner *et al*. (1972).

2.4. Description of Samples

Twenty-two solid bitumen samples from seventeen different veins were selected. All these samples are collected from surface outcrops of veins and vugs, which may have a thickness up to 100 meters. The lateral continuity is in general up to kilometers (e.g.

3500 m for the Avgamasya vein). In Figure 2.2.b one of these veins (Harbul) is shown, along with some pictures from different veins in hand specimen. All these veins are located in the Şırnak province of SE Turkey and found as fault and crack fills in NE-SW and NW-SE trending veins and fractures (Fig. 2.1.a) (Kavak *et al*., 2010). These different trends for vein orientation are attributed to tectonic events. Lebküchner classified the Turkish solid bitumen veins in two major groups based on their positions related to the Cudi overthrust with more than 60 km long (Lebküchner, 1969). Among the studied solid bitumen in the present work, the Üçkardeşler, Harbul and Silip veins are occurrences originated in and below overthrust and others are in the hanging part of the Cudi overthrust. Solid bitumen occurrences are distributed in sedimentary units of different ages (Fig. 2.1.c). They are observed in the Cudi group (Jurassic-Cretaceous), Germav (Upper Cretaceous-Paleocene) and Gerçüş (Eocene) Formations as well as in the Midyat Group (Eocene). The distribution of solid bitumens in these host rocks is complicated. For example Harbul and Silip veins (Gerçüş Fm.) or Milli and Kumçatı veins (Germav Fm.) have a same host rock but they are different in appearance and transformation level (Fig. 2.1.b). It appears that there is no regularity in occurrence and form of the bitumens as a function of stratigraphy, a point made by Lebküchner almost fifty years ago (Lebküchner, 1969).

2.5. Analytical Methods

The finely ground solid bitumens were analyzed using a Rock-Eval 6 instrument (Behar *et al*., 2001), starting isothermally at 300°C for 3 minutes and subsequently heating to 650°C at 25°C/min. A standard sample was run as every tenth sample and checked against the acceptable range. Total organic carbon (TOC) values were determined using a Leco SC-632 instrument. Prior to analysis, diluted HCl was added to the finely crushed samples to remove carbonate.

Thermovaporisation- and pyrolysis-gas chromatography (Tvap & PY-GC) analyses were conducted on all finely crushed solid bitumens. For Tvap-GC analysis, between 1

and 30 mg of sample, depending on Rock-Eval results (TOC and S2), were placed in a glass capillary tube (30 mm long; internal diameter ~1.5 mm) with pre-cleaned quartz wool (600°C in air for >1h) and then sealed. The glass tubes were cracked at 300°C and free hydrocarbons were collected at -196°C in a cryogenic trap, from which they were liberated by ballistic heating into a HP-Ultra 1 fused silica capillary column (50 m length, 0.32 mm internal diameter and 0.52 μm film thickness) mounted in an Agilent Technology (AT) 6890A gas chromatograph equipped with a flame ionization detector (FID). The GC oven temperature was programmed from 40°C to 300°C at 5°C/min and helium was used as carrier gas (30 ml/min). For PY-GC analysis samples were placed in a glass capillary tube with both ends open and inserted in the sample holder. The sample was extracted thermally at a temperature of 300°C for 5 min to release and vent the volatile constituents. Then pyrolysis was carried out by heating from 300 to 600°C at 50°C/min and holding for 2 min. The products were focused in a cryogenic trap from which they were later injected on to the capillary column by ballistic heating. For both methods, Tvap- and PY-GC, hydrocarbon peaks were identified by comparison with reference chromatograms and quantification was performed using n-butane as an external standard.

A Soxhlet apparatus was used to extract bitumens using dichloromethane:methanol 99:1 (v:v). After asphaltene removal using n-hexane, the maltenes were fractionated using medium pressure liquid chromatography (MPLC) to obtain aliphatic hydrocarbon, aromatic hydrocarbon and resin fractions. Aliphatic hydrocarbon fractions were analyzed by gas chromatography (AT 6890A); the GC oven was programmed from 40°C (2 min isothermal) to a final temperature of 300°C (65 min isothermal) at a heating rate of 5°C/min with a constant carrier gas flow rate (1ml/min). The aliphatic and aromatic hydrocarbon fractions were analyzed using gas chromatography-mass spectrometry (GC-MS). Compound separation was performed using an AT 6890A GC equipped with a PTV injection system and a fused silica capillary column (BPX5; 50 m × 0.22 mm i. d., f. t. = 0.25 μm). Helium was used as carrier gas, and the temperature of the GC oven was programmed from 50°C (1 min) to 310°C at a rate of 3°C/min, followed by an isothermal phase of 10 minutes. For compound identification, the GC instrument was linked to a

Finnigan MAT 95 XL mass spectrometer operating in the electron impact mode (70 eV). 5α-Androstane and 1-ethylpyrene were used as internal standards for aliphatic and aromatic hydrocarbon fractions, respectively.

Total extracts were analysed using ultrahigh resolution FT-ICR MS combined with ESI in the negative ion mode, enabling acidic compounds like carboxylic acids, phenols and carbazoles to be ionized. The ultrahigh resolution achieved by a high magnetic field strength enables the simultaneous detection of several thousand NSO compounds to be made in one single measurement. The instrument was a 12 Tesla FT-ICR mass spectrometer equipped with an Apollo II ESI ion source, both from Bruker Daltonik GmbH. Before injection, samples were diluted with methanol:toluene 1:1 (v:v), and ammonia (NH_3) was then added to facilitate deprotonation of acidic constituents during analysis. Compound classes comprising pyrrolic nitrogen, phenolic and carboxylic acids, alone (N_y, O_x) or in combination (N_yS_z, O_xN_y, O_xS_z, $O_xN_yS_z$) were identified. Detailed descriptions of the method as well as the mass calibration and data analysis procedures have been published by Poetz *et al*. (2014) and Noah *et al*. (2015).

2.6. Results and Discussion

2.6.1. Bulk organic matter content and type

Rock-Eval parameters and TOC contents are given in Table 2.1. The TOC values show a wide range (between 2 to 54 %) without any obvious relation to the vein's locations. Clearly, there is a variable admixture of mineral matter and organic carbon in the vein bitumens.

The organic carbon in the bitumen varies in its proportion of "live" versus "dead" components. In Figure 2.2.a the "live" component, Hydrogen Index (HI), is shown to decrease with increasing T_{max} values. The curve resembles classical curves for the thermal evolution of Type II kerogen, but the S2 signal is here directly related to the abundance of pyrolysable macromolecular moieties in the bitumen (Tab. 2.1).

Table 2.1. Data for Rock-Eval pyrolysis, solvent extraction and liquid chromatographic fractionation of solid bitumens from SE Turkey.

	Name of Vein	Rock Eval Pyrolysis							Solvent Extraction (DCM + 1% MeOH)					
		TOC (wt.%)	S2*	HI*	OI*	PI	Tmax (°C)	S1/TOC*	EOM*	Sat. (%)	Aro. (%)	NSO-(%)	Asph. (%)	Sat./Aro.
1	**Üçkardeşler**	50.5	287	569	0	0.06	433	38.2	888	6.1	15.9	37.7	40.3	0.4
2	**Harbul-1**	51.0	316	619	0	0.06	434	40.1	578	3.3	13.7	45.2	37.7	0.2
	Harbul-2	54.3	297	546	9	0.06	435	34.5	895	7.3	12.1	39.7	40.9	0.6
3	**Silip**	42.2	12	28	0	0.04	487	1.3	289	n.d.	n.d.	n.d.	17.3	n.d.
4	**Kumçatı**	2.4	8	324	8	0.10	443	35.1	309	12.6	20.4	45.7	21.3	0.6
5	**Çağlayan**	53.0	100	189	1	0.12	456	25.6	79	22.7	38.7	29.8	8.8	0.6
6	**Segürük-1**	39.3	230	586	0	0.06	437	36.1	381	3.2	13.5	40.4	43.0	0.2
	Segürük-2	42.0	204	485	8	0.06	437	28.5	556	7.2	13.1	32.7	47.0	0.6
7	**Avgamasya-1**	38.5	183	474	0	0.06	440	32.1	255	5.0	21.0	46.7	27.3	0.2
	Avgamasya-2	37.3	90	241	1	0.09	450	22.5	112	13.3	35.6	33.4	17.7	0.4
8	**Seridahli-1**	20.1	27	133	23	0.08	464	12.0	36	25.0	46.9	21.8	6.3	0.5
	Seridahli-2	41.8	59	140	1	0.10	465	16.0	66	23.0	29.8	16.0	31.2	0.8
9	**Rutkekurat**	22.2	13	57	1	0.05	487	2.9	26	15.6	44.0	15.6	24.8	0.4
10	**Karatepe-1**	37.7	10	25	1	0.01	550	0.2	11	10.2	41.9	13.8	34.1	0.2
	Karatepe-2	46.3	35	76	1	0.09	480	7.6	29	27.6	47.8	14.5	10.1	0.6
11	**Milli**	10.0	1	14	76	0.11	451	1.7	77	9.4	20.2	37.0	33.4	0.5
12	**Herbiş**	30.5	1	3	21	0.16	550	0.6	2	20.1	11.7	36.6	31.5	1.7
13	**Besta**	13.3	2	18	5	0.08	597	1.5	8	20.1	51.7	18.0	10.3	0.4
14	**Anıttepe**	32.3	5	15	2	0.05	588	0.8	4	24.1	53.4	14.8	7.7	0.5
15	**Taşdelen**	38.5	13	33	2	0.03	517	1.2	7	15.2	65.0	13.4	6.3	0.2
16	**Ortasu**	36.0	3	9	41	0.01	550	0.1	4	11.3	33.8	24.9	30.0	0.3
17	**Roboski**	12.2	3	21	4	0.09	562	2.0	6	13.9	62.8	20.2	3.0	0.2

*** Units: S2** = mg HC/g Solid Bitumen; **HI** = mg HC/g TOC; **OI** = mg CO_2/g TOC; **S1/TOC** = mg HC/g TOC; **EOM** = mg/g TOC.

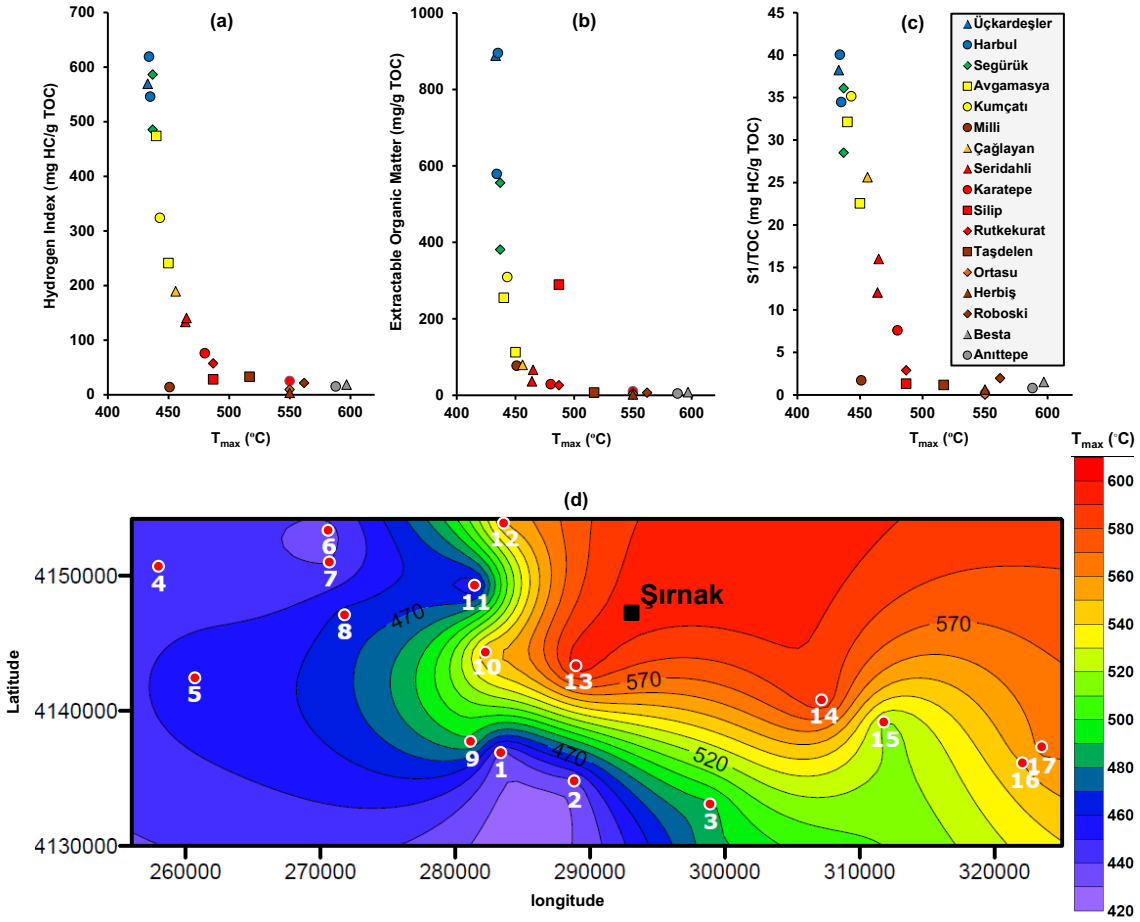

Fig. 2.2. The variation of **a)** Hydrogen Index; **b)** extractable organic matter yields (/TOC) and **c)** "Oil Saturation Index" (S1/TOC) as a function of maturity in studied solid bitumens from SE Turkey. **d)** T_{max} contour map shows a maturity trend from west to east across the study area. The vein's names are given in Table 2.1.

The diagram reveals that with increasing maturity there is a drop in the proportion of organic carbon that is volatilisable, equating to an increase in dead carbon, caused by a combination of live to dead carbon conversion or live carbon depletion. This is in good agreement with the results of elemental analysis whereby the hydrogen content of asphaltic substances in SE Turkey decreases as organic metamorphism proceeds (Orhun, 1969). As shown by the T_{max} contour map (Fig. 2.2.d), there is a clear maturity trend which increases from west to east across the region in the direction of the tectonically

active zone. The same maturity trend has also been reported for indigenous organic matter in different sedimentary units (Harput *et al*., 1992). It should be noted that T_{max} at very high maturity levels displays increased scatter due to the flat profile of the S2 peak, but the overall T_{max} profile remains as shown. Oxygen Index (OI) values are generally low (0 – 10 mg CO_2/g TOC); higher values (21 – 76 mg CO_2/g TOC) measured on four samples in the east might reflect enhanced levels of weathering (Lo and Cardott, 1995; Kavak *et al*., 2010).

2.6.2. Macromolecular building blocks

Open system PY-GC is a powerful tool for characterising the macromolecular components in source rock and reservoir bitumens (Horsfield *et al*., 1991; Muscio *et al*., 1991). The pyrograms for selected samples of different thermal transformation levels indicate that the distribution of structural moieties is strongly influenced by thermal maturity (Fig. 2.3). The less mature samples are dominated by *n*-alk-1-ene/*n*-alkane doublets, with simple aromatic compounds such as BTEX (benzene, toluene, ethylbenzene and xylenes) in low abundance. As maturation proceeds, a progressive shortening of *n*-alkyl chains takes place due to thermal cracking. This is readily discernible in the ternary plot depicting chain length distribution (Horsfield, 1989), with the proportion of gaseous pyrolysate progressively increasing, particularly for mature and overmature samples (Fig. 2.4.a). The Petroleum Type Organofacies which generated the bitumen is inferred to be Low Wax Paraffinic-Naphthenic-Aromatic (Horsfield, 1989).

The shortening in *n*-alkyl chain length is accompanied by increasing proportions of aromatic moieties (Fig. 2.4.b). Interestingly, the amounts of sulphur compounds produced by pyrolysis are low, falling in the Intermediate category (di Primio and Horsfield, 1996). With regard to the latter, sulphur-rich asphaltenes from low maturity source rocks generate copious quantities of alkylthiophenes from the moieties bound by sulphur-sulphur and carbon-sulphur bridges (Kohnen *et al*., 1991).

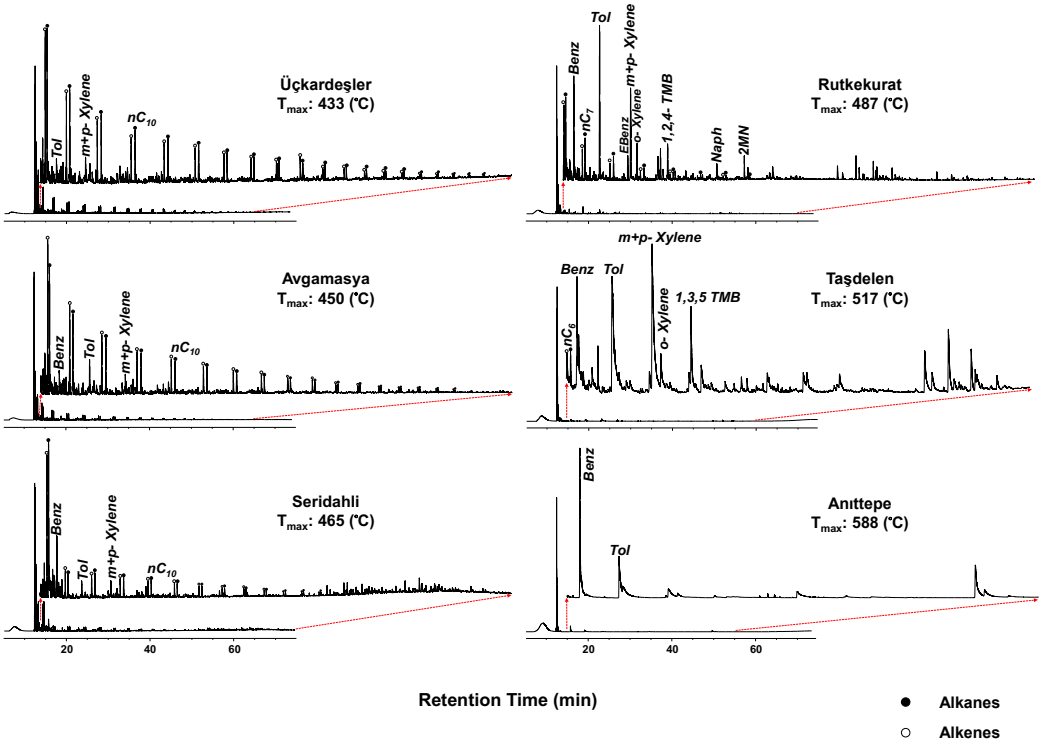

Fig. 2.3. Open system pyrolysis gas chromatograms for selected solid bitumens from SE Turkey with different maturation levels.

The low abundance of sulphur detected by Py-GC points to the bulk of sulphur in the bitumens being in refractory structures, such as condensed ring systems, and not in a form that is labile and degradable by pyrolysis.

2.6.3. Extractable organic matter

Changes in HI are correlated with the extractability (mg/g TOC) of the vein bitumens in dichloromethane. The yield of extractable organic matter (EOM) is strongly related to thermal transformation level (see Tab. 2.1; Fig. 2.2.b), as revealed when extractability is plotted versus T_{max} values. In most published studies Turkish solid bitumens are considered as asphaltite. However, based on solvent extractabilities, the current sample

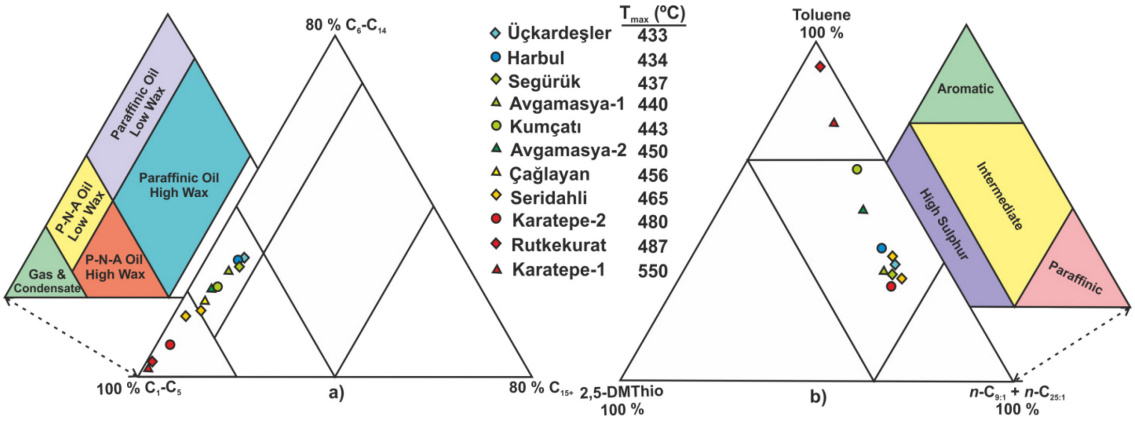

Fig. 2.4. a) The chain length distribution of total C_1-C_5 resolved pyrolysate, C_6-C_{14} *n*-alkenes plus *n*-alkanes and C_{15+} *n*-alkenes plus *n*-alkanes showing composition changes with ongoing maturation in studied solid bitumens (after Horsfield, 1989). Please note that the Petroleum Type Organofacies fields are based on kerogen pyrolysates, and are shown here simply for reference. **b)** Differentiation of pyrolysate composition using relative proportions of non-1-ene plus pentacos-1-ene, toluene and 2,5-dimethylthiophene (after di Primio and Horsfield, 1996).

series is classified as mainly spanning asphaltite to asphaltic pyrobitumen, and even asphaltic pyrobitumen in the middle and eastern parts of the investigated area (Orhun, 1969). S1/TOC values show a progressive decrease with increasing T_{max} (Fig. 2.2.c), entirely consistent with the progressive changes in extractability noted above.

As far as source rocks in general concerned, Production Index (PI) increases then decreases as catagenesis proceeds and is then succeeded by metagenesis (Espitalie *et al*., 1977). In reservoir rocks of a given maturity level, PI is correlated with the ratio of hydrocarbons to non-hydrocarbons (Horsfield *et al*., 1991). For the vein bitumens in the current study PI is low (<0.16) throughout the entire suite (Tab. 2.1), pointing to relatively high proportions of non-hydrocarbons being present at all maturity stages. Values increase then decrease as T_{max} increases, the inversion occurring at around 470°C. At the very highest levels of maturity PI is extremely variable, in part because of

extremely low S1 and S2 signals. Saturate/aromatic ratios are low throughout the entire series (Tab. 2.1).

The Tvap gas chromatograms shown in Figure 2.5 display the compositional changes occurring in thermally extractable organic matter as a function of T_{max}, with maturity increasing in an easterly direction. The free hydrocarbons in the low maturity vein bitumens (left-hand side of Fig. 2.5) are largely in the form of unresolved complex mixtures. Resolved absorbed gas, saturated and aromatic hydrocarbons are observed too. Normal alkanes present up to C_{31} and dibenzothiophenes are the most abundant aliphatic and aromatic compounds, respectively. Also triterpanes are detectable only in this part of study area.

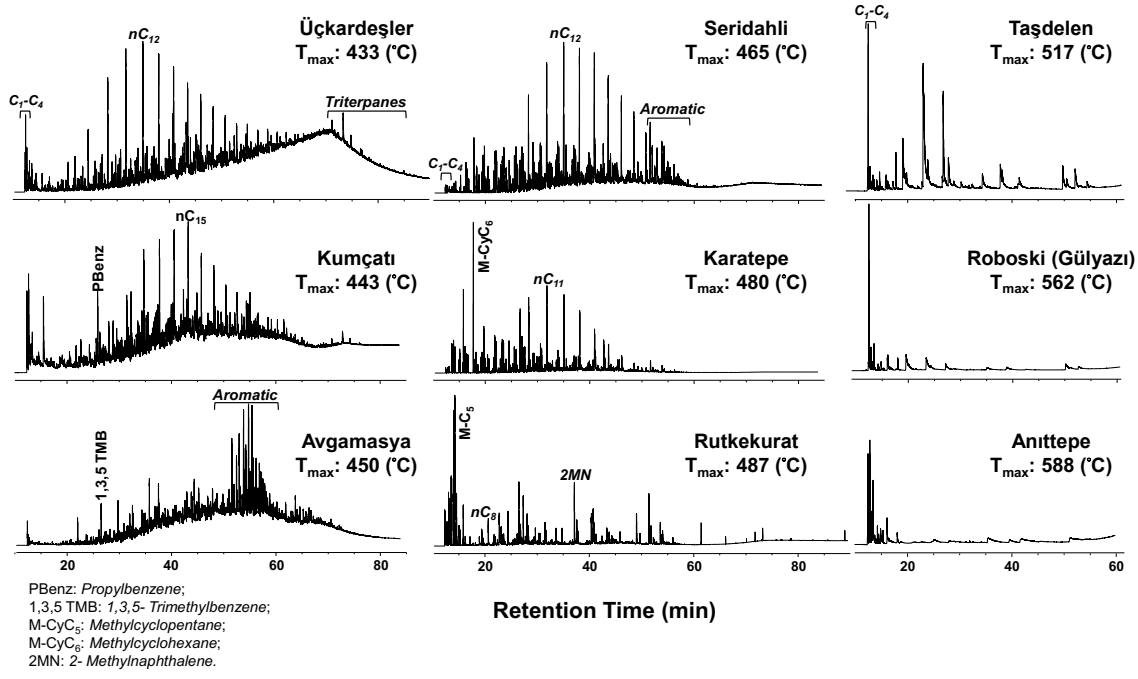

Fig. 2.5. Thermovaporization gas chromatograms of solid bitumens show different patterns at different locations equatable with different thermal maturity levels across the investigated area.

The middle column in Figure 2.5 is representative for highly mature vein bitumens located in the central part of the study area (T_{max} range 460 to 500°C). They show no hump but only resolved hydrocarbons including normal alkanes up to C_{21} as well as aromatic hydrocarbons. Finally, chromatograms in the right column in Figure 2.5 represent highly overmature solid bitumens that are found in the eastern part of investigated area (T_{max} > 500°C). In these samples there are only some absorbed gas and very little amounts of resolved hydrocarbons which are mainly simple aromatic compounds. The overall change in fingerprints is in agreement with the maturity zonation already established.

2.6.4. Biomarker analysis

Some widely-used maturity sensitive molecular parameters determined from GC and GC-MS data of saturated and aromatic fractions of solid bitumens from SE Turkey are given in Table 2.2. Unsurprisingly, abundances of saturated biomarkers, e. g. hopanes and steranes, clearly decrease with increasing maturity. Selected maturity sensitive parameters from saturated biomarkers in Table 2.2 are at epimerisation and isomerisation equilibrium or close to it, except for the T_s/T_m ratios, and can provide no further information in particular for high and overmature solid bitumens. T_s/T_m ratios (Tab. 2.2) are not measurable for all highly mature solid bitumens but in the western part of study area they reflect increasing maturity towards the east.

Aromatic hydrocarbons are more thermally resistant than saturated biomarkers and their distributions change in a regular fashion with increasing maturity up to high levels (Radke, 1987). Selected maturity-sensitive parameters for aromatic compounds are given in Table 2.2. In Figure 2.6 some of these parameters are correlated with T_{max} values which confirmed the geographical maturity trend suggested for the study area. The methyldibenzothiophene as well as trimethylnaphthalene ratios are correlated well with T_{max} values (Fig. 2.6.a and 2.6.c). The methylphenanthrene index increases with increasing T_{max} values then decreases at higher maturation levels (Fig. 2.6.b).

Table 2.2. Indicators of thermal maturity for solid bitumens from SE Turkey using GC and GC-MS data.

	Name of Vein	Saturates				Aromatics					
		CPI	ββ-C_{29}	20*S* C_{29}	T_s/T_m	TMNR	TeMNR	MPI 1	MPI 2	MDBT Ratio 2	MDR
1	**Üçkardeşler**	0.98	0.55	0.52	0.04	0.77	0.90	0.88	1.01	2.07	3.62
2	**Harbul-1**	1.05	0.60	0.46	0.05	0.36	0.52	0.77	0.89	0.86	0.81
	Harbul-2	0.95	0.60	0.42	0.04	0.60	0.76	0.72	1.14	0.98	0.98
3	**Silip**	0.89	0.62	0.52	n.d.	0.62	0.77	0.71	0.80	1.48	1.92
4	**Kumçatı**	1.06	0.64	0.45	0.27	0.49	0.76	0.56	0.62	1.42	1.74
5	**Çağlayan**	1.18	0.60	0.48	n.d.	0.55	0.86	0.82	0.97	1.46	2.03
6	**Segürük-1**	1.08	0.62	0.45	0.05	0.37	0.61	0.64	0.77	0.93	0.90
	Segürük-2	1.03	0.62	0.41	0.10	0.39	0.64	0.72	0.82	0.87	0.81
7	**Avgamasya-1**	0.95	0.60	0.47	0.10	0.50	0.69	0.59	0.65	1.21	1.36
	Avgamasya-2	1.18	0.59	0.51	1.11	0.66	0.86	0.57	0.63	1.47	1.92
8	**Seridahli-1**	1.04	n.d.	n.d.	1.76	0.76	0.88	1.06	1.32	2.13	8.80
	Seridahli-2	1.02	n.d.	n.d.	n.d.	0.80	0.90	1.16	1.39	1.71	4.24
9	**Rutkekurat**	1.09	n.d.	n.d.	n.d.	0.95	0.98	1.60	1.81	1.73	12.04
10	**Karatepe-1**	1.25	n.d.	0.53	n.d.	0.96	0.98	1.48	1.66	1.59	12.54
	Karatepe-2	1.02	n.d.	n.d.	n.d.	0.93	0.96	1.32	1.44	1.84	28.26
11	**Milli**	1.04	0.63	0.49	n.d.	0.74	0.82	0.90	1.03	1.93	6.43
12	**Herbiş**	0.81	n.d.	n.d.	n.d.	n.d.	n.d.	0.25	0.36	4.39	13.98
13	**Besta**	1.00	0.53	0.47	n.d.	n.d.	n.d.	0.93	1.22	2.50	42.67
14	**Anıttepe**	n.d.	n.d.	n.d.	n.d.	n.d.	n.d.	0.68	0.77	2.25	31.77
15	**Taşdelen**	1.02	n.d.	n.d.	n.d.	0.93	1.00	1.63	2.01	2.13	38.18
16	**Ortasu**	0.90	n.d.	n.d.	n.d.	0.94	0.97	0.98	1.25	1.67	7.31
17	**Roboski**	1.12	n.d.	n.d.	n.d.	0.89	n.d.	1.31	1.59	2.27	36.12

CPI = $[(C_{23}+C_{25}+C_{27})+(C_{25}+C_{27}+C_{29})]/2(C_{24}+C_{26}+C_{28})$;	Kotarba *et al*. (2007)
ββ-C_{29} = 14β(H),17β(H)/(14β(H),17β(H) + 14α(H),17α(H))-C_{29} steranes (20*R* + 20*S*);	van Graas (1990)
20*S* C_{29} = 20*S*/(20*S* + 20*R*)-14α(H),17α(H)-C_{29} steranes;	
T_s/T_m = 18α(H)-22,29,30 –trisnorneohopane (T_s)/ 22,29,30 –trisnorhopane (T_m);	
TeMNR = 1,3,6,7-TeMN/(1,3,6,7 + 1,2,5,6+1,2,3,5-TeMN);	van Aarssen *et al*. (1999)
TMNR = 1,3,7-TMN/(1,3,7 + 1,2,5-TMN);	
MPI 1 = 1.5(2-MP+3-MP)/(P+1-MP+9-MP);	Radke *et al*. (1986); Radke (1988)
MPI 2 = 3×2-MP/(P+1-MP+9-MP);	
MDBT Ratio 2 = (2-MDBT + 3-MDBT + 4-MDBT)/(1-MDBT + 2-MDBT + 3 MDBT);	
MDR = 4-MDBT/1-MDBT.	

The observed trend resembles that seen for a maturity series of shales and coals containing type III organic matter (Radke and Welte, 1981). It should be noted that some anomalies are observed in maturation assessment using aromatic hydrocarbons in particular for the Üçkardeşler and Ortasu veins. This indicates that factors other than simply thermal stress may have been at work (Sivan *et al*., 2008).

The most abundant compounds in the aromatic fractions of the studied solid bitumens are alkyldibenzothiophenes. The relative concentrations of homologues of methyl-, dimethyl- and trimethyldibenzothiophenes (MDBT, DMDBT and TMDBT, respectively) are sensitive to maturity, i.e. DMDBTs and TMDBTs compared to MDBTs show a tendency to decrease at advanced levels of thermal transformation (Chakhmakhchev *et*

al., 1997). The relative concentration of these sulphur-containing aromatic species is not the same across the investigated area. In the western and central parts with mature and highly mature samples abundances change in the order DMDBTs > TMDBTs > MDBTs > DBT, whereas in the eastern part with overmature samples the order is MDBTs > DMDBTs > DBT > TMDBTs. Increasing maturity generally tends to increase the ratio of the thermodynamically more stable β- to the less stable α-substituted isomers of certain aromatic compounds in bitumens (Radke, 1987); based thereon several maturity parameters have been introduced (Radke *et al*., 1986; Radke, 1988; Chakhmakhchev and Suzuki, 1995; Chakhmakhchev *et al*., 1997; Santamarıa-Orozco *et al*., 1998). In Figure 2.7 distributions of dibenzothiophene and alkylated dibenzothiophenes for some of the solid bitumens with different maturation level are shown. 1-MDBT with lower stability decreases relative to 3-MDBT as well as 4-MDBT with increasing maturity. Furthermore, DBT concentration increases with ongoing maturation. MDR ratios show relatively little increase with maturity in the samples taken from the western part and rise quickly at advanced levels of maturity (Tab. 2.2). A similar trend has been reported in previous studies on aromatic sulphur compounds (Schou and Myhr, 1988; Dzou *et al*., 1995; Chakhmakhchev *et al*., 1997).

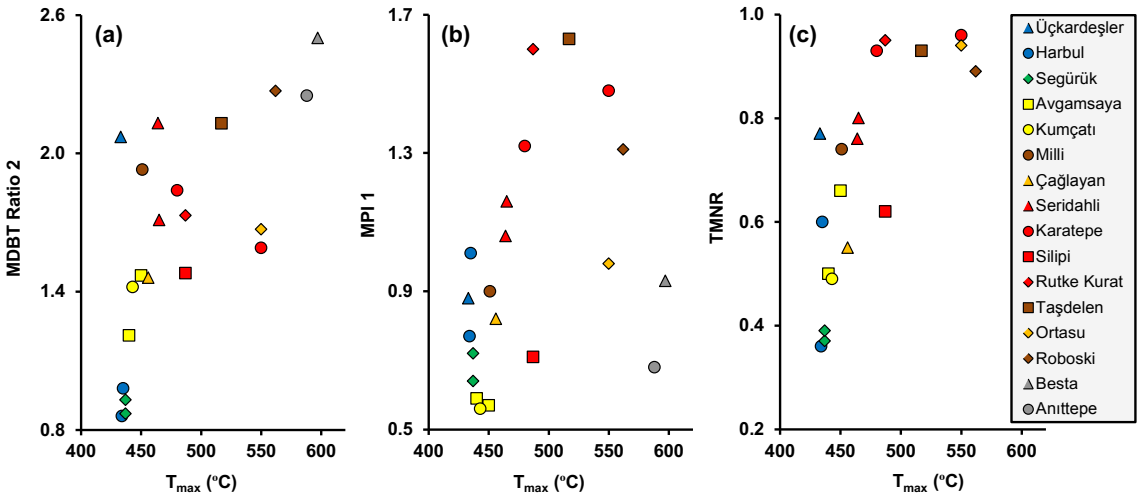

Fig. 2.6: Correlation of maturity parameters based on aromatic hydrocarbons versus T_{max} values for the studied solid bitumens; **a)** methyldibenzothiophene ratio. **b)** methylphenanthrene index 1 and **c)** trimethylnaphthalene ratio.

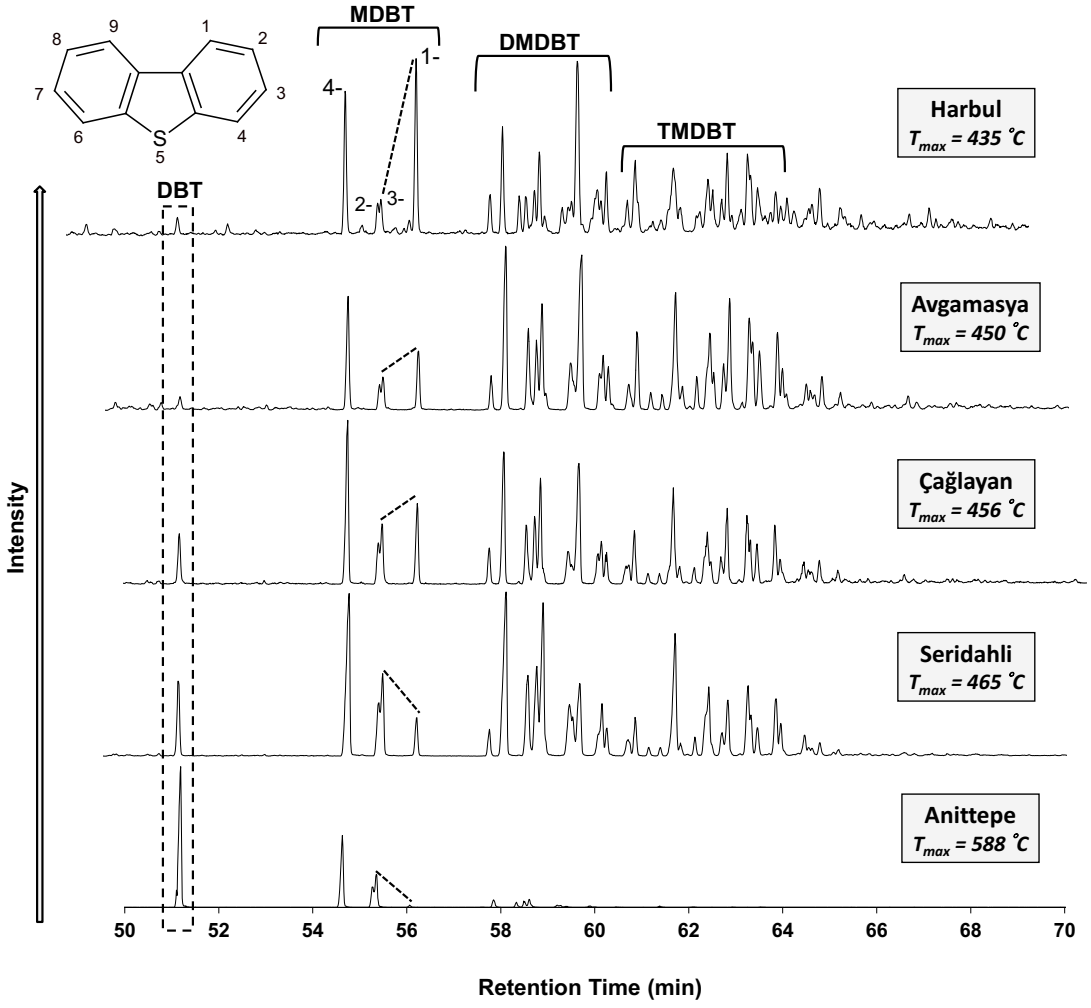

Fig. 2.7. Distributions of dibenzothiophene and alkylated dibenzothiophenes for selected solid bitumens with different maturity from SE Turkey illustrating changes in abundances and patterns.

2.6.5. FT-ICR MS analysis

The soluble organic matter in ten selected solid bitumen samples covering the whole study area as well as the range of maturity were analysed using FT-ICR MS analysis in the negative ion mode upon electrospray ionisation. The composition of the acidic constituents in the bitumens in general and the compositional changes with maturation

and with respect to possible other alteration processes like TSR or biodegradation are described here in detail.

2.6.5.1. Broadband spectra and elemental class composition

The (-)-ESI broadband mass spectra in Figure 2.8 show at first sight a strong alteration of the signal pattern and distribution with ongoing maturation. While the number of (assigned) monoisotopic peaks shows no systematic variation, the weight-average (M_w) and number-average (M_n) molecular weights decrease. It appears that this decrease is caused by a depletion of compounds with *m/z* values greater than ~ 300.

The elemental class composition (illustrated with pie charts in Figure 2.8) reveals a predominance of nitrogen and sulphur (N_yS_z) and nitrogen only (N_y) compounds containing pyrrolic nitrogen alone or combined with thiophenic sulphur (possible molecular structures are shown in Figure 2.10). High amounts of sulphur incorporated in the organic matter of Turkish solid bitumen have been reported previously (Kar, 2006; Kavak *et al*., 2010; Sert *et al*., 2011). Since (-)-ESI ionization is insensitive to thiophenic sulphur compounds, sulphur compounds are only observed in combination with pyrrolic nitrogen. To our knowledge comparably high amounts of (-)-ESI-FT-ICR-MS-detectable acidic N_yS_z compounds have not been reported for any type of petroleum sample up to now, not even for other types of solid bitumen. For comparison, the heavily biodegraded Canadian tar sands as an example of dispersed solid bitumen contain a large fraction of one to four ring carboxylic acids dominating the (-)-ESI spectra while the (-)-ESI accessible fraction of the Gilsonite bitumen from the Uinta Basin in north-eastern Utah reveals an immature signature of saturated fatty acids (Smith *et al*., 2008; Helms *et al*., 2012). In contrast, the abundance of sulphur-containing species within the elemental class distribution of the acidic bitumen constituents is relatively low for both the tar sands (4.9%) and Gilsonite (<3%) (Jacob, 1989; Smith *et al*., 2008).

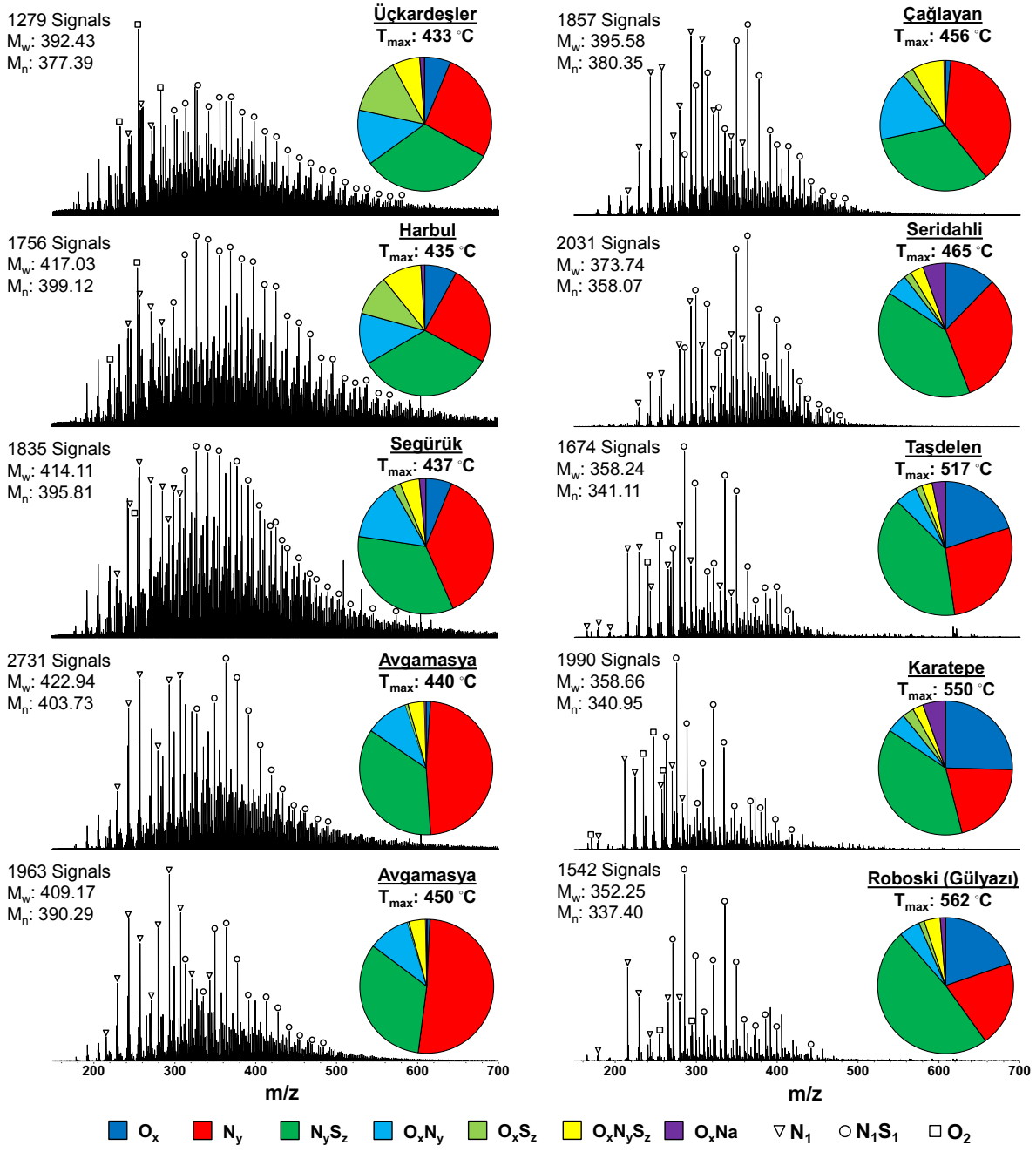

Fig. 2.8. Broadband negative ion ESI FT-ICR mass spectra of solid bitumens of increasing maturity (as indicated by T_{max} values). The pie charts show the elemental class distribution. N_1 compounds are depicted with triangles, N_1S_1 compounds with circles and O_2 compounds with squares.

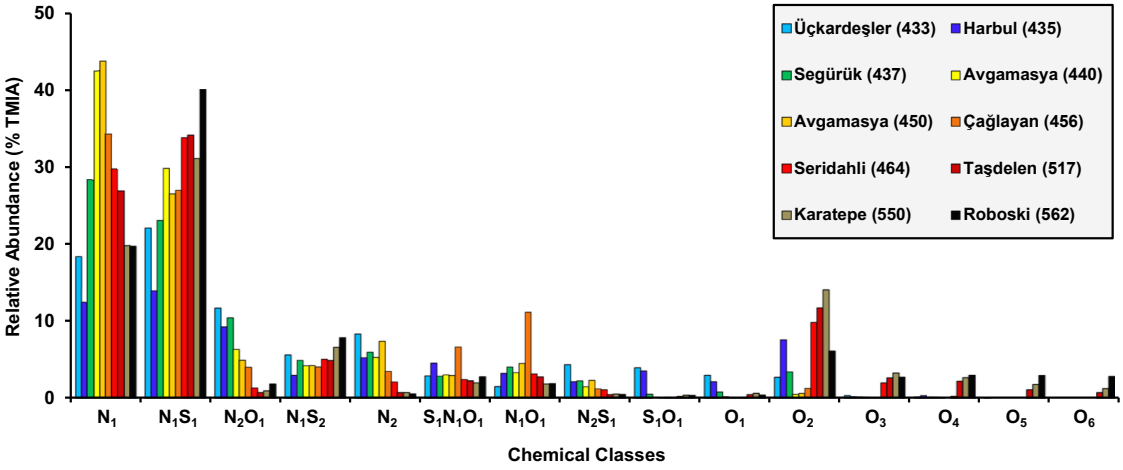

Fig. 2.9. Compound class distribution of different compound classes in solid bitumens from SE Turkey.

Among the Turkish sample set, the samples of early maturity (Üçkardeşler, Harbul) are dominated by N_yS_z compounds (~30% of total monoisotopic ion abundance, TMIA) and N_y compounds in slightly lesser amounts. O_xS_z and N_yO_x compounds each make up 10 – 15% TMIA while the O_x and $O_xN_yS_z$ class intensities are ~10% TMIA. The intensity of the N_yS_z class remains constant within the peak mature window but again increases for late mature samples (to 49% TMIA), while the N_y class is enriched first (increase from 25 to 38%) but again decreases in late mature samples (from 38 to 22%). The O_x class decreases in samples with early to intermediate maturity but becomes again prominent in the late mature samples. The abundance of all other classes decreases gradually from early to late maturity.

2.6.5.2. Compound classes

Figure 2.9 shows the distribution of the most abundant compound classes in the solid bitumens. The N_1S_1 and N_1 classes are most prominent in all samples. The N_1 class consisting of carbazole-type compounds rises from 12% for the low maturity Harbul vein

to 43% in the Avgamasya vein and then decreases to 20% TMIA for the overmature Roboski vein. It has previously been reported for other petroleum sample types like crude oils and source rock bitumen that neutral nitrogen compounds show increasing abundances with ongoing maturation up to vitrinite reflectances of 1.45% (Hughey *et al*., 2004; Oldenburg *et al*., 2014; Poetz *et al*., 2014). The observed decrease of the N_1 class abundance at maturation levels (T_{max}> 450) here is probably attributed to the neoformation of N_1S_1 and N_1S_2 compounds at high maturation levels: their relative abundance increases from 14% to 40% and 3% to 8% TMIA, respectively. The absolute intensities of the N_1 class indeed decrease for the late mature samples Taşdelen, Karatepe and Roboski suggesting that parts of the N_1S_1 compounds are formed via sulphur incorporation into N_1 compounds. The relative ion abundances of other compound classes show clear maturity related trends as well. The N_2O_1, N_2, N_2S_1 and O_1 compound classes decrease with increasing maturity while the O_2 compound class goes through a minimum at intermediate maturities. The oxygen classes with 3 to 6 oxygen atoms are almost entirely absent at early to medium maturity and but increasingly present at high maturation levels. This might be an indication for oxidation processes having occurred, most likely after emplacement. The $S_1N_1O_1$ and N_1O_1 classes seem to be constant at ~3% TMIA except for the Çağlayan sample which shows higher abundances. In the following part, we will concentrate on the N_y, N_yS_z, and O_x compounds.

2.6.5.3. Double bond equivalent distributions

The double bond equivalent (DBE) as a measure for aromaticity describes the number of double bonds and rings in a molecule. The DBE distributions of four selected compound classes (N_1, N_1S_1, N_1S_2 and O_2) of the solid bitumens are illustrated in Figure 2.10. The total DBE value range is enlarged by (N_1, N_1S_2) or shifted to (N_1S_1) higher DBEs with advancing maturation. The N_1 class of the early mature samples from Üçkardeşler and Harbul shows a DBE range from 9 to 18. A preferential enrichment of DBE classes representing fully aromatized compounds like carbazoles (DBE 9), phenylindoles (DBE 10) and benzocarbazoles (DBE 12) is observed.

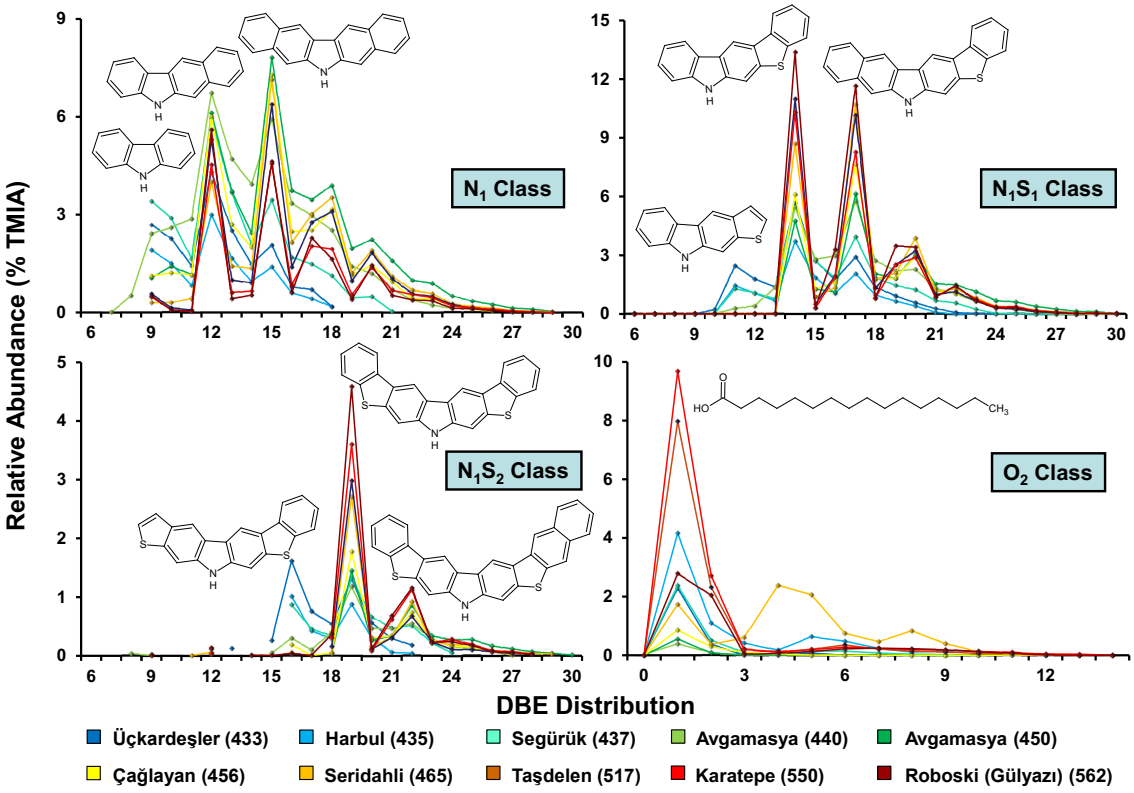

Fig. 2.10. DBE distribution of the N_1, N_1S_1, N_1S_2 and O_2 compound classes in solid bitumens from SE Turkey. T_{max} (ºC) values are given in the legend and plausible core structures for the most abundant DBE classes are provided.

Both range and distribution pattern strongly resembles those found in reservoired crude oils in the North Sea (Oldenburg *et al*., 2014; Mahlstedt *et al*., 2016). A vitrinite reflectance of approximately 0.8% R_o is inferred for the early mature bitumen veins based on a comparison with those North Sea oil data, and this is in broad accordance with the aromatic maturity parameters presented earlier in this contribution. There are lesser similarities to the N_1 DBE class distribution of source rocks of comparable maturity (Poetz *et al*., 2014). The late mature samples exhibit a DBE value range from 9 to 27 with local maxima for benzocarbazoles (DBE 12), dibenzocarbazoles (DBE 15), pyrenobenzoindoles (DBE17), naphthobenzocarbazoles (DBE 18) and benzopyrenocarbazoles (DBE 20). DBE classes 12, 15 and 18 represent expanded

members of *ortho*-fused benzo-annelated carbazoles, while DBE classes 17 and 20 contain o*rtho*- and *peri*-fused benzo-annelated carbazoles. One example per DBE for a nonalkylated core structure is given in Figure 2.10. In general, the shift to higher DBE values is indicative for an increased degree of condensation and aromatization of the organic compounds. DBE range and distribution pattern of the higher maturity samples are very similar to those found in source rock extracts of the Posidonia Shale from northwest Germany (Poetz *et al*., 2014).

The DBE distribution of the N_1S_1 class appears to be very similar to that of the N_1 class. The overall DBE range is from 11 to 21 in the less mature samples and from 14 to 26 in the late mature samples. Maxima occur at DBE 11, 14 and 17 (less mature) and DBE 14, 17, 19, 20 and 22 (more mature samples). By analogy with the N_1 compound structures these DBE distributions provide strong evidence that the sulphur atom, like the nitrogen atom, is bound in aromatic five-membered rings (thiophenic sulphur). Mostly *ortho*-fused N_1S_1 compounds are present (DBE 11, 14, 17 and 20, exemplary structures of potential core structures are depicted in Figure 2.10).

In the N_1S_2 class, the DBE distribution maxima are at DBE 16, 19 and 22 since here 3 heteroatoms are now in five-membered aromatic rings which are again *ortho*-fused with benzene rings. However, there is one major difference to the N_1 and N_1S_1 classes: lower DBE classes show relatively large intensities in the early mature samples but are somehow removed with ongoing maturation (DBE 9 - 12 for N_2 and DBE 15 – 17 for N_1S_2).

The DBE distribution of the O_2 class looks quite different from that of the other classes. Most samples covering the whole maturation range contain exclusively compounds with 1 DBE (fatty acids) and 2 DBE (fatty acids with one unsaturation or ring). An enrichment of naphthenic acids (indicative for biodegradation) is only observed for sample Seridahli. This might show that this sample experienced mild biodegradation at some point in its history. In contrast, however, the thermovaporization gas chromatogram of Seridahli sample shows an *n*-alkane distribution, arguing against biodegradation.

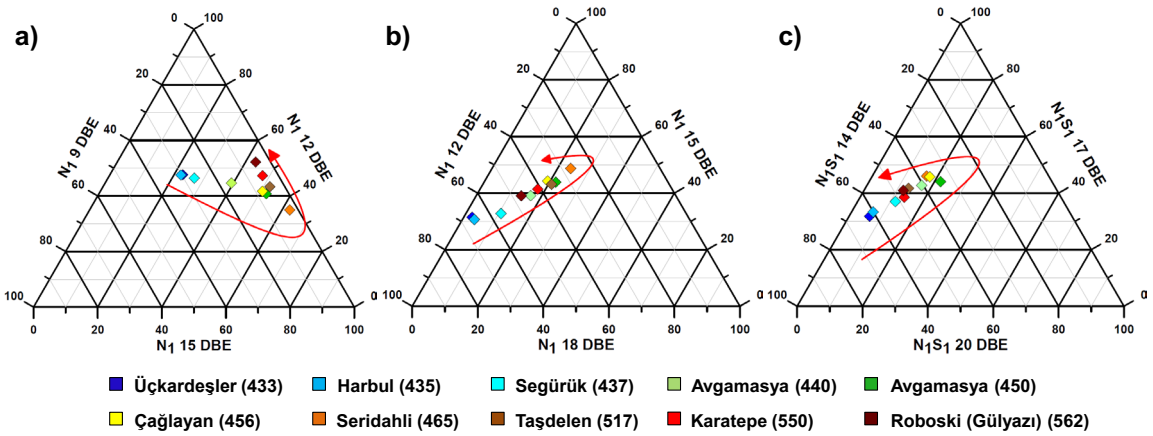

Fig. 2.11. Maturity controlled variations in the relative abundance of selected DBE classes for the N_1 (a, b) and N_1S_1 (c) compound classes.

Ternary diagrams displaying the relative changes of three of the most abundant DBE classes of the N_1 class are a promising tool for maturation assessment in crude oils and extracted bitumens from hydrocarbon source rocks (Oldenburg *et al*., 2014; Poetz *et al*., 2014). The triangular plot based on the N_1 9, 12 and 15 DBE classes used for crude oils nicely displays the maturity driven enrichment of DBE 15 compounds for samples up to a T_{max} value of 465 (Figure 2.11.a) as observed before for bitumen samples from source rocks (Poetz *et al*., 2014). Surprisingly, for overmature samples (T_{max} >500 °C) which mainly belong to the eastern part of the study area, the relative intensity of carbazoles remains constant while benzocarbazoles increase and dibenzocarbazoles decrease. This reversal can be observed as well in the N_1 12, 15 and 18 DBE ternary diagram (Figure 2.11.b). The ternary diagram for N_1S_1 14, 17 and 20 DBE reveals similar maturity-controlled changes including the inversion for samples with T_{max} >500 °C (Fig. 2.11.c).

Since no (-)-ESI-FT-ICR MS data have been published on bitumen samples of this elevated maturity up to now, we have to speculate if this inversion is a general phenomenon or is specific for the solid bitumens analysed here. If there is no additional source for molecules than the bitumen (e.g. kerogen) the formation of the next higher member of the series of *ortho*-annelated pyrrolic nitrogen compounds would require

compounds with a minimum number of 4 carbon atoms in alkyl chains attached to two adjacent carbon atoms of the core structure. Otherwise, no cyclization and aromatization is possible and thermal cracking will occur solely which would not change the relative abundance of the individual DBE classes significantly (cracking in the side chain leaves a compound in the DBE class in which it was before cracking). We would then expect that the more mature samples plot in the same region in the ternary diagram as their less mature counterparts, which is not observed. Therefore, other mechanisms and reactions may play a role for samples in this maturity window. For example, compounds of other classes containing additional heteroatoms with comparable DBE could lose a heteroatom and then contribute to the 12 DBE N_1 (N_2 class) or 14 DBE N_1S_1 (N_1S_2 class) compounds.

2.6.5.4. Carbon number distributions

Thermal maturation has a significant influence on the carbon number distributions in a homologous series (Hughey *et al*., 2004). The carbon number distribution of selected DBE classes of the N_1 and N_1S_1 compound classes are shown in Figure 2.12, while Figure 2.13 displays colour coded DBE versus carbon number plots for the N_1, N_1S_1 and O_2 classes. The carbon number distributions of the N_1 class as well as the N_1S_1 class clearly indicate maturity driven differences among the solid bitumen samples. The carbon number ranges and the mean carbon numbers are reduced with ongoing maturation due to advanced side chain cracking reactions (Fig. 2.12). A similar pattern has been reported for N_1, N_1O_1 and N_1S_1 compounds in Posidonia Shale samples of different maturity (Poetz *et al*., 2014). The three least mature samples (Üçkardeşler, Harbul and Segürük) show a broad distribution of carbon numbers representing compounds with 0 to 20 carbon atoms in the alkyl side chains while in the overmature samples Taşdelen, Karatepe and Roboski only compounds with 0 to 4 carbon atoms in the alkyl side chains are left. The N_1 12 DBE class even contains three members only with 0, 1 and 2 carbon atoms in alkyl side chains. These findings supports the inversion found for the overmature samples in the DBE ternary diagram, since these N_1 compounds

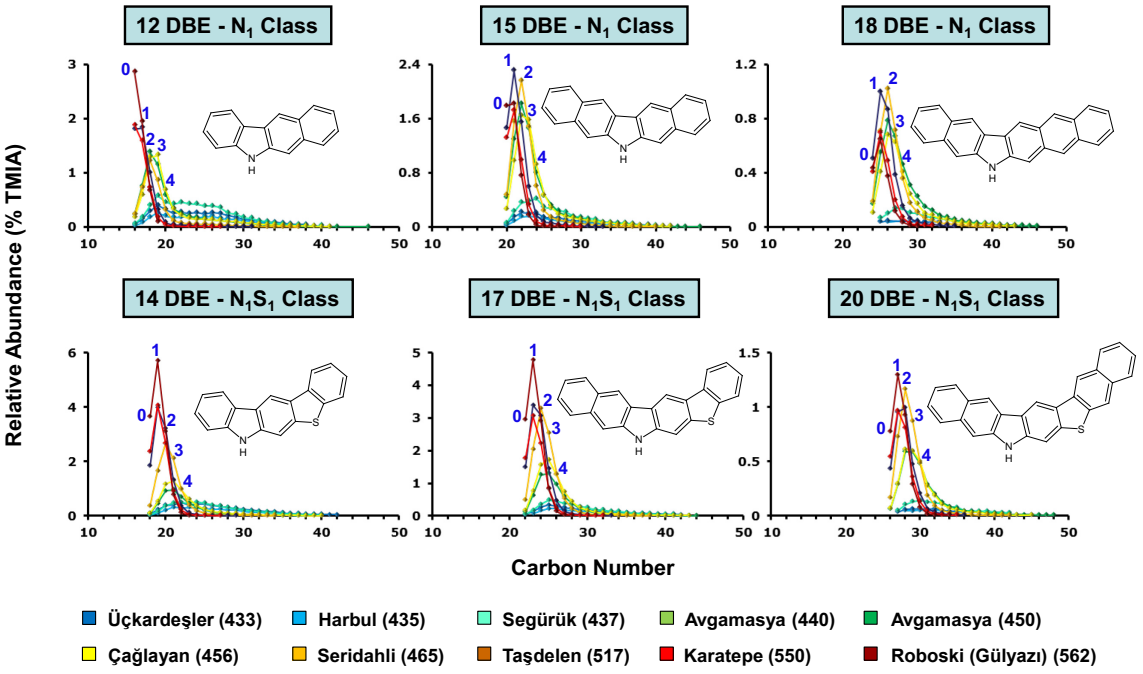

Fig. 2.12. Carbon number distribution of the N_1 12, 15 and 18 DBE classes as well as the N_1S_1 14, 17 and 20 DBE classes in solid bitumens from SE Turkey. T_{max} (°C) values are given in the legend and the chemical structures depict the respective core structures.

are not able to form 15 DBE compounds via cyclization and aromatization due to a too small number of alkyl carbon atoms. Additionally, this is a strong indication that the solid bitumens have been formed from migrated and reservoired petroleum solely and not within a source rock, where cracking of abundant kerogen matter could be an additional source for fresh bitumen compounds of longer and more alkyl chains.

In contrast, the compounds in the O_2 class do not show this concentration of highly condensed aromatic compounds with low alkylation level. The low maturity samples are dominated by the C_{16} and C_{18} fatty acids which are ubiquitous in geological samples and may be a contamination or an indication for the input of fresh organic matter from microorganisms at outcrop. The samples of high maturity contain additional O_2 compounds with DBE values up to 14 (Seridahli) and 12 (Roboski) and carbon numbers between 10 and 25. Compounds of similar DBE and carbon number range are found in

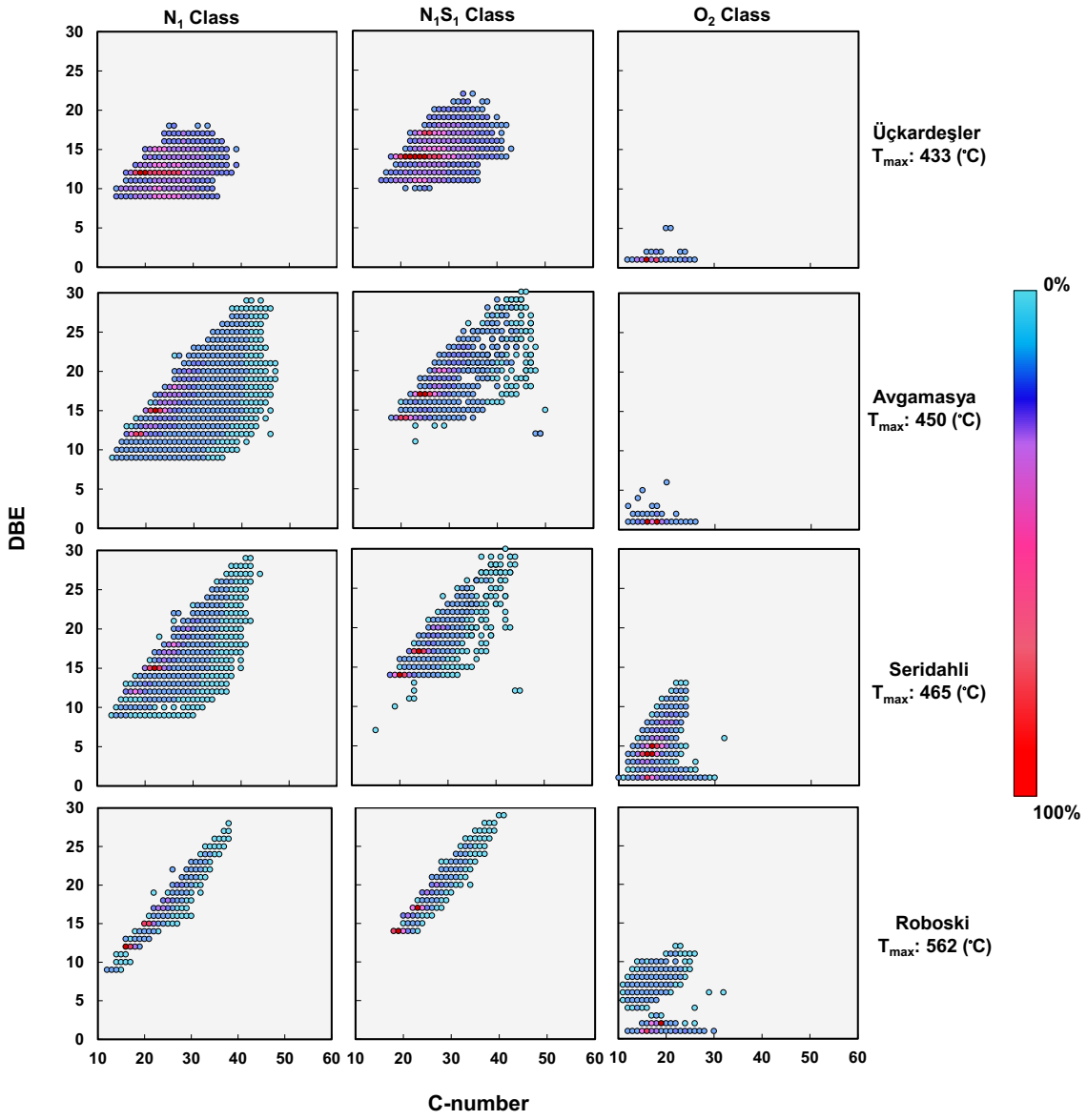

Fig. 2.13. Colour coded DBE versus carbon number diagrams of the N_1, N_1S_1 and O_2 compound classes for selected samples with different maturation levels.

the $O_{3\text{-}6}$ classes of the same samples. Following the observations of Walters *et al*. (2015), we can interpret these compounds as oxidation products formed by TSR. However, other oxidation processes such as weathering might be responsible as well. Other complementary investigations are needed to finally answer this question.

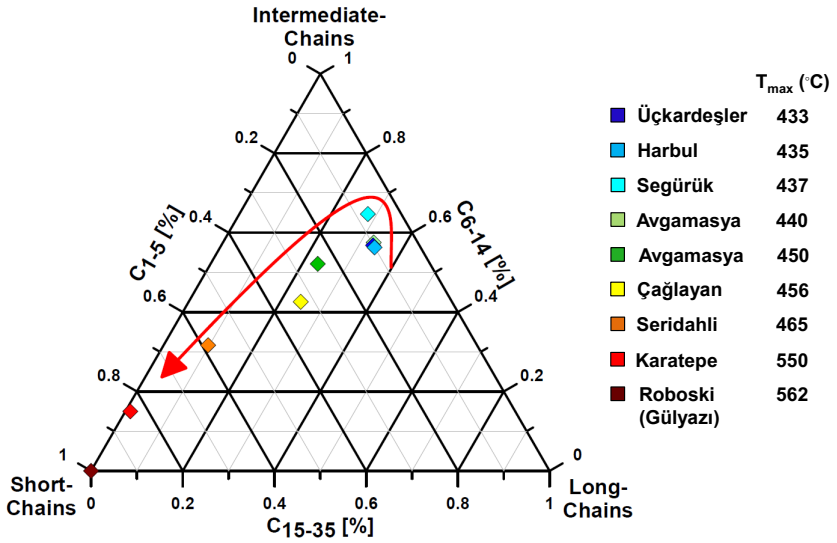

Fig. 2.14. Maturity-controlled carbon number distribution of aliphatic side chains of the DBE 9 N_1 compound class (likely carbazoles) for solid bitumens from SE Turkey (after Mahlstedt *et al*. (2016).

A ternary diagram displaying the relative distribution of carbon in the alkyl side chains can be used to monitor the impact of thermal cracking at different stages of maturity (Fig. 2.14) (Mahlstedt *et al*., 2016). This plot clearly reveals that with increasing maturity the relative ion abundances of structures with side chains containing a lower number of carbon atoms significantly increases which furthermore is well correlated with the chain-length distribution as revealed by PY-GC results (see also Fig. 2.4.a).

2.7. Conclusions

Multiple conventional and advanced geochemical methods have been used to study the wide range of chemical characteristics of Turkish solid bitumens. Results indicate that post-emplacement thermal stress is the main factor controlling the chemical composition of solid bitumens, with the degree of thermal alteration being strongly related to regional tectonic history. There is a clear maturity trend across the region from

west to east. T_{max} values rise from 433 to 588 °C and the contents of volatile and extractable organic matter decrease significantly. Saturated biomarkers such as hopanes and steranes are absent at high maturation levels but aromatic fractions and in particular alkylated dibenzothiophenes are still there. Maturity assessment using these sulphur-containing aromatic species authenticate the observed maturity trend and concentration of high molecular weight compounds decrease with increasing maturity due to thermal cracking. Moreover, the chemical composition of NSO-compounds is controlled mainly by thermal stress, as documented by progressive aromatization, condensation and side chain cracking. At highly advanced maturation, pyrrolic compounds are not able to form higher DBE compounds via cyclization and aromatization. Thermochemical sulphate reduction may have contributed to oxygen incorporation.

2.8. Acknowledgment

We would like to thank the TKI Şırnak, especially A. Tunç, M. Aydin and S. Yardimci for providing samples and C. Karger, A. Kaminsky, F. Perssen and K. Günther for laboratory analyses at the GFZ. We also would like to thank P. Craddock and the anonymous reviewer for their valuable comments and suggestions to improve the quality of the manuscript.

3. COMPREHENSIVE GEOCHEMICAL CORRELATION BETWEEN SURFACE AND SUBSURFACE PETROLEUM OCCURRENCES OF SE-TURKEY

This chapter reprinted with permission from ***Hosseini, S. H.,*** *B. Horsfield, H. Wilkes, A. Vieth-Hillebrand, M. N. Yalçın, and O. Kavak, (2018). Comprehensive geochemical correlation between surface and subsurface hydrocarbon occurrences in the Batman-Mardin-Şırnak area (SE Turkey):* Marine and Petroleum Geology*, v. 93, p. 95-112 (Postprint).*
https://doi.org/10.1016/j.marpetgeo.2018.02.035

3.1. Abstract

Southeast Turkey is the main oil-producing region of the country, located at the northwestern part of the Zagros Basin. In this study, we investigated the geochemical characteristics of both surface and subsurface hydrocarbon occurrences in the Batman-Mardin-Şırnak area in southeast Turkey to determine whether a genetic relationship exists between the two. For this, thirty solid bitumens from twenty-two different veins along with ten heavy oils and thirteen oil seepage samples from nearby oilfields and seeps were studied using diverse geochemical tools. Firstly each of the different hydrocarbon types was considered individually with respect to source organofacies, level of thermal maturity and degree of biodegradation. The results obtained from the source-related parameters demonstrate a marine algal source for all investigated samples. Also, lithology determination based on various diasterane, tricyclic terpane, hopane and homohopane parameters, suggests a carbonate source for all samples, except for the

Dadaş and İşkar seeps (clastic). Thereafter, considering the influences caused by thermal and biological alteration processes, all heavy oils, less mature solid bitumens as well as the less biodegraded seep oils were selected to be correlated using selected additional parameters. Homohopane distributions reveal that solid bitumens, compared to heavy oils and seeps, are highly enriched in C_{31}- and depleted in higher homologs possibly due to cracking of high molecular weight homologues to lower ones during and/or after solidification processes. Furthermore, the similarities observed for the relative abundances of six series of aromatic hydrocarbons and their alkylated counterparts substantiate strong genetic affinities within the sample set. Finally, compound-specific stable carbon isotopes of individual components show that solid bitumens are more enriched in ^{13}C than the heavy oils which is mainly attributed to the preferential removal of light isotopes (^{12}C) during solidification. Our results strongly confirm that Turkish solid bitumens are genetically related to the nearby heavy oils, thereby providing new information on the petroleum system in this part of the southeast Anatolia.

3.2. Introduction

The Zagros Basin, as one of the world's largest petroleum provinces, extends from Turkey through Syria and Iraq into Iran. Located in the northwestern edge of the Zagros Basin, southeast Turkey is the most petroliferous region of the country and there are many surface and subsurface hydrocarbon occurrences. In the Batman-Mardin-Şırnak area located to the East of southeast Turkey solid bitumen veins, several oil seeps and diverse oilfields with heavy oil are represented.

Solid bitumens occur in large veins and vugs close to and at the erosional surface and are economically important (Lebküchner *et al*., 1972), amounting to about 82 million tons (Kar, 2006). Generally speaking, solid bitumens can form by either the thermal chemical alteration (TCA) or thermochemical sulphate reduction (TSR) of once liquid petroleum (Kelemen *et al*., 2008). As far as Turkish solid bitumens are concerned, mainly TCA processes are important. The solid bitumens are ostensibly generated from the same source but show different physico-chemical characteristics depending upon

their geographic locations. Various secondary alteration processes affect composition, it was shown that post-emplacement thermal stress, increasing from west to east, plays the major role in controlling the chemical composition of solid bitumens across the region (Hosseini *et al*., 2017). This is in accordance with the regional tectonic framework (Egeran, 1951; Harput *et al*., 1992; Yilmaz *et al*., 1993).

Although several large oilfields have been discovered in the Zagros Basin, e.g. the Rumaila oilfield in Iraq with 17 bbls oil in place, subsurface accumulations in southeast Turkey are very small by Middle Eastern standards, e.g. the Batı Raman oilfield with 1.85 bbls oil in place. Virtually most of the traps are structurally-controlled and reservoirs occur in fractured carbonate units. Although there are a few gas and condensate reservoirs (40 to 45º API) e.g. the Barbes field (Katin Formation, Devonian); oils produced in southeastern Turkey may be grouped as medium (25 to 35º API) or heavy (10 to 20º API) based on API gravity. The geological age of the respective reservoirs revealed that most of the medium gravity oils were trapped in the Middle Cretaceous sedimentary units, whereas the younger reservoirs (Upper Cretaceous-Paleocene) contained either medium or heavy oils (Nairn and Alsharhan, 1997).

Here we focus on the geochemical characteristics of both surface/near surface and subsurface hydrocarbon occurrences in southeast Turkey to determine whether a genetic relationship exists between them. In this context, the most important solid bitumen veins in the region along with nearby oil and oil seepage samples have been investigated. Although potential source rocks for the studied samples have not been analysed here, biomarkers in seeps, oils as well as solid bitumens have been used to infer the lithology, organic matter input, and depositional environment of the generative source facies (cf. Moldowan *et al*., 1985; Peters *et al*., 2008). While solid bitumens add complexity to the geochemical correlation studies mostly due to their highly variable and refractory character, genetic relationships between solid bitumens and oils can be established as long as the influences caused by alteration processes are taken into account (Peters *et al*., 2005).

Literature review reveals that various correlation studies have been conducted successfully since John Hunt and co-workers' pioneering work from over 60 years ago. They correlated oils and solid bitumens of the Uinta Basin using chemical data such as infrared spectra and elemental analyses, various physical properties as well as geological evidence, and identified the source rocks of the Uinta Basin hydrocarbons (Hunt *et al*., 1954). Many years later Williams (1974) and Dow (1974), using carbon isotope ratio measurement, gas chromatography, optical rotation measurement, and infrared spectrophotometry techniques, established a correlation between source rock units (Ordovician, Mississippian and Pennsylvanian) and oil families of the Williston Basin. Although later studies became progressively more analytically sophisticated, the concepts and approaches established by Hunt, Williams and Dow are still valid (Curiale, 2008). Despite the fact that the majority of previously published correlation studies have relied heavily on saturated biomarkers, there are several publications focusing on other geochemical parameters such as aromatic hydrocarbons (e.g. Pu *et al*., 1990; Jinggui *et al*., 2005) or compound-specific stable carbon isotope ratios (e.g. Odden *et al*., 2002; Dawson *et al*., 2007; Li *et al*., 2009; Murillo *et al*., 2016).

As far as southeast Turkey is concerned, several geochemical studies have been conducted comparing surface and subsurface hydrocarbon occurrences. Connan and co-workers have studied the bitumens present in Neolithic artefacts of archaeological sites in the region, compared them with oil seeps and crude oils using geochemical approaches and found that those bitumens likely were sourced from Silurian shales; they also determined different oil families of southeast Anatolian oils (Connan *et al*., 2006). Kavak compared solid bitumens from the Şırnak area with two oil samples from the Raman and Dinçer oil fields using bulk and molecular parameters and suggested similarities amongst them (Kavak, 2011). Kara-Gülbay and Korkmaz, using the same approach, correlated four oils with three solid bitumen veins and suggested the Upper Jurassic/Lower Cretaceous carbonates of the Cudi Group to be a common source (Kara-Gülbay and Korkmaz, 2012). However, others have reported the hydrocarbon potential of this unit as being low (Yalçın Erik and Özcelik, 2007). Mueller *et al*. (1995) studied solid bitumens from the Seridahli vein and five oils from different oilfields and on the basis of

biomarker parameters concluded that there was no genetic relationship between the studied oils and solid bitumens. A relatively recent report suggested a Middle Jurassic source rock (Yolaçan Fm.) as the origin of the heavy oils and solid bitumens (Çorbacıoğlu, 2015). Literature review reveals that the origin(s) of the hydrocarbon occurrences in the study area i.e. the Batman-Mardin-Şırnak area, is(are) still under debate and remain inconclusive. Recently, we have investigated Turkish solid bitumens in detail using conventional and advanced geochemical tools, focusing on the role of thermal stress in controlling their composition (Hosseini *et al*., 2017). In the current contribution we extend the investigation to include nearby heavy oil and oil seep occurrences in order to investigate possible genetic affinities, thereby providing new information on the formation mechanism of Turkish solid bitumens.

3.3. Geological Setting and Sample Set

The tectonic history of southeast Turkey has been documented in detail (Şengör and Yilmaz, 1981; Hempton, 1985; Yilmaz *et al*., 1993; Gorur and Tuysuz, 2001; Okay, 2008). During the Alpine orogeny the region underwent two major episodes of deformation, firstly in the Late Cretaceous and then in the Middle Eocene-Late Miocene. The latter episode occurred as a result of the progressive elimination and complete closure of the ocean(s) which led to the collision between Eurasia and the Arabian plate (Yilmaz *et al*., 1993). Due to this main phase of the Alpine orogeny compressional folds developed; all the hydrocarbon accumulations so far discovered in SE Turkey are held in structural traps formed during this last phase of the Alpine movements (Ala and Moss, 1979).

Thirty solid bitumen samples from twenty-two different veins were selected from surface outcrops. All of them are located in the Şırnak province of SE Turkey and found as fault and crack fills in NE-SW and NW-SE trending veins and fractures (Fig. 3.1.a). They are distributed in sedimentary units of different ages i.e. in the Cudi, Mardin, Adiyaman, Şırnak as well as Midyat Groups (Fig. 3.1.c), and there is no regularity in occurrence and form of the bitumens as a function of stratigraphy (Lebküchner, 1969,

Hosseini *et al*., 2017). For example Harbul and Silip veins (Gerçüş Fm.) or Milli and Kumçatı veins (Germav Fm.) have the same host rock but they are different in appearance and transformation level (Fig. 3.1.b).

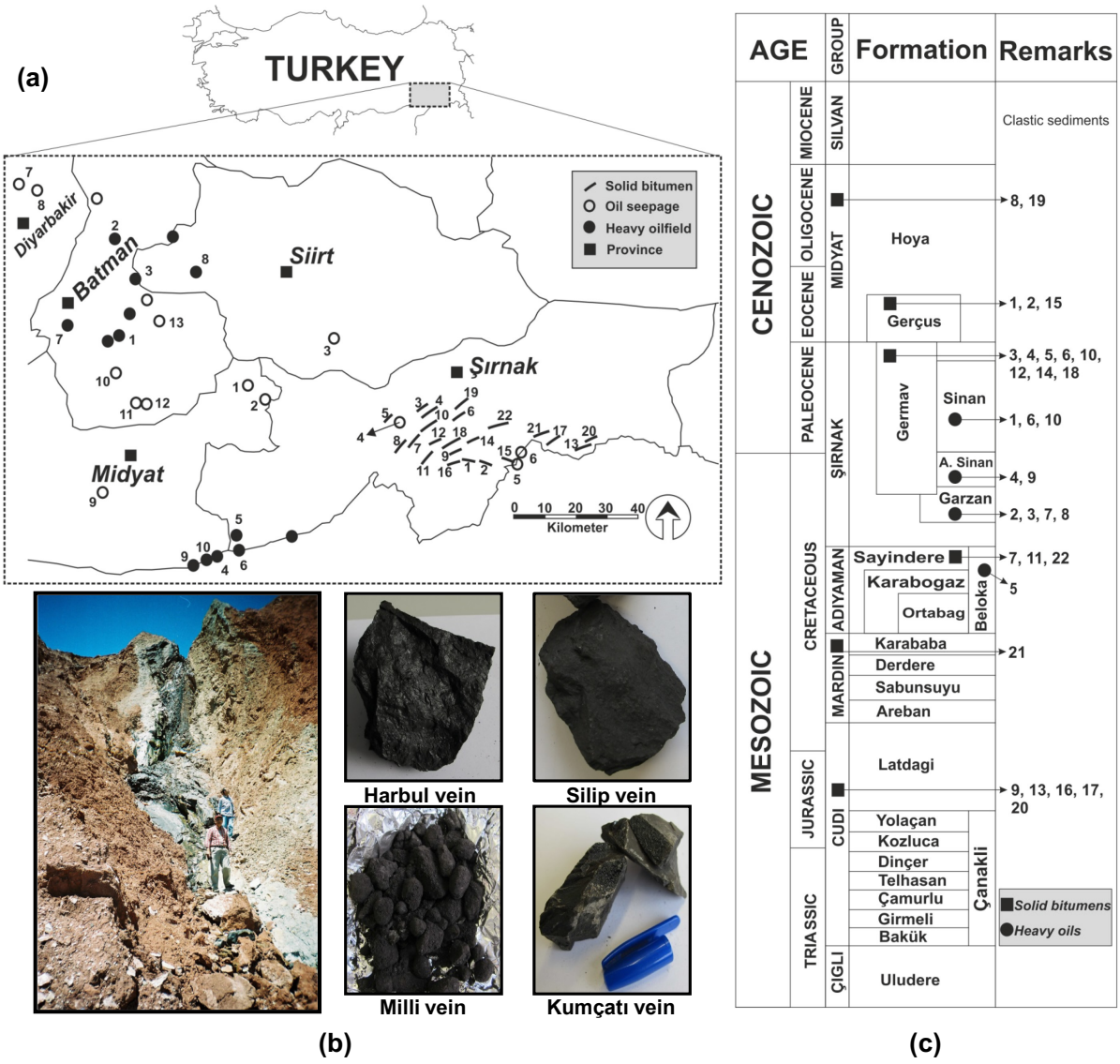

Fig. 3.1: a) Geographic location of solid bitumen's veins as well as oil seepages and heavy oilfields in the study area. The related names are given in Table 3.1. **b)** Left: The dyke-shape Harbul vein in the Gerçüş Formation as host rock; Right: Some of solid bitumens in hand specimen to show their different appearance (Hosseini *et al*., 2017). **c)** The stratigraphic column of SE Turkey displaying the reservoir formations for studied oils as well as host rocks for solid bitumen veins.

Tab. 3.1. Bulk parameters of different sample types from SE Turkey. Estimated biodegradation levels are given as well.

Type	No.	Sample Name	TOC (wt.%)	HI*	Tmax (°C)	EOM*	Sat. (%)	Aro. (%)	Res. (%)	Asph. (%)	Sat./Aro.	Bio.*
Solid Bitumen	01	Üçkardeşler+	50.5	569	433	886	6	16	38	40	0.39	0
	02	Harbul-1+	51.0	619	434	561	3	14	45	38	0.24	0
		Harbul-2+	54.3	546	435	892	7	12	40	41	0.60	0
	03	Seqürük-1+	39.3	586	437	367	3	13	40	43	0.24	0
		Seqürük-2+	42.0	485	437	539	7	13	33	47	0.55	0
	04	Avgamasya-1+	38.5	474	440	236	5	21	47	27	0.24	1
		Avgamasya-2+	37.3	241	450	104	13	36	33	18	0.37	2
		Avgamasya-3	33.7	252	449	141	10	33	37	19	0.31	2
	05	Kumçatı+	2.4	324	443	285	13	20	46	21	0.62	0
	06	Milli-1+	10.0	14	451	63	9	20	37	33	0.46	1
		Milli-2	36.0	205	453	105	12	33	40	15	0.37	0
	07	Divin	41.3	15	455	3	39	7	49	4	-	0
	08	Çağlayan+	53.0	189	456	79	23	39	30	9	0.59	1
	09	Ispindoruk	48.9	117	462	24	30	45	15	10	0.66	2
	10	Seridahli-1+	20.1	133	464	24	25	47	22	6	0.53	0
		Seridahli-2+	41.8	140	465	45	23	30	16	31	0.77	0
	11	Hesana	50.1	110	465	24	29	47	19	6	0.61	0
	12	Nivekara	18.0	82	470	40	25	34	30	10	0.75	1
	13	Ortasu-1+	36.0	9	550	3	11	34	25	30	0.33	2
		Ortasu-2	4.0	26	478	12	22	38	28	11	0.58	0
	14	Karatepe-1+	37.7	25	550	4	10	42	14	34	0.24	0
		Karatepe-2+	46.3	76	480	16	28	48	14	10	0.58	0
	15	Silip+	42.2	28	487	289	-	-	-	17	-	3
	16	Rutkekurat+	22.2	57	487	16	16	44	16	25	0.35	0
	17	Taşdelen+	38.5	33	517	3	15	65	13	6	0.23	0
	18	Anılmış	36.6	28	519	4	14	60	18	8	0.24	0
	19	Herbiş+	30.5	3	550	1	20	12	37	32	1.72	0
	20	Roboski+	12.2	21	562	3	14	63	20	3	0.22	0
	21	Anıttepe+	32.3	15	588	3	24	53	15	8	0.45	0
	22	Besta+	13.3	18	597	6	20	52	18	10	0.39	0
Oil Seepage	01	Kerbent	-	-	-	-	21	18	30	30	1.16	3
	02	Zengen	-	-	-	-	13	19	39	30	0.68	6
	03	Eruh	-	-	-	-	10	18	37	35	0.56	4
	04	Kumçatı	-	-	-	-	10	22	49	19	0.46	1
	05	Silip	-	-	-	-	12	28	39	20	0.44	8
	06	Kayatepe	-	-	-	-	15	21	40	24	0.71	1
	07	Dadaş	-	-	-	-	16	1	28	55	-	7
	08	İşkar	-	-	-	-	22	17	48	14	1.30	7
	09	Yeşilli	-	-	-	-	4	6	31	59	0.78	5
	10	Bagas	-	-	-	-	13	29	38	20	0.44	4
	11	Tala	-	-	-	-	4	2	33	61	2.60	5
	12	Gerçüş	-	-	-	-	4	14	45	37	0.29	5
	13	Badzivan	-	-	-	-	9	13	43	35	0.68	9
Heavy Oil		**Oilfield Name**	**Reservoir Fm.**	**Res. Depth (m)**	**Res. Temp. (ºC)**	**API Gravity**						
	01	Silvanka Sinan #1	Sinan	1302	51	15.7	20	26	44	11	0.76	0
	02	Raman #8	Garzan+Mardin	1334	60	18.0	21	30	36	13	0.71	0
	03	Germık #1	Garzan	1970	71	18.8	29	28	30	14	1.03	0
	04	Çamurlu #2	Alt Sinan	1336	48	12.0	16	26	42	16	0.61	0
	05	Güney Dinçer #1	Beloka	1576	63	15.7	15	30	35	20	0.52	0
	06	Batı Kozluca #1	Sinan	1472	56	12.6	14	30	39	17	0.47	0
	07	Batı Raman #1	Garzan	1342	66	13.0	14	23	42	21	0.58	0
	08	Mağrip #1	Garzan+Alt Germav	1690	88	18.5	35	30	23	12	1.16	0
	09	Doğu Sınırtepe #1	Alt Sinan	1325	50	15.9	21	30	37	12	0.70	0
	10	Ikiztepe #1	Sinan	1359	46	11.3	13	24	40	23	0.54	0

* **Units: HI** = mg HC/g TOC; **EOM** = mg/g TOC; **Bio.** = Biodegradation level based on Peters and Moldowan (1993).

\+ RE, solvent extraction and fractionation data are taken from Hosseini *et al*. (2017).

Ten oils and thirteen oil seepage samples from proximal oilfields and seeps were collected. All selected oils are heavy (11 to 19º API) and their geographic location is shown in Figure 3.1.a. Except for the Güney Dinçer oil which is reservoired in the Beloka Formation (Adiyaman Group), other reservoirs are the Sinan and Garzan formations of the Şırnak Group (Fig. 3.1.c). The dolomitic limestone of the Sinan Formation (Late Maastrichtian – Paleocene) was deposited under shallow-marine conditions and has a thickness ranging from 15 to 65 m, with an average porosity of 5% and permeability less than 5 mD. The Garzan Formation (Late Maastrichtian), is a fractured, bioclastic to reefal limestone of shallow-marine origin and has an average thickness of 50 m with porosity ranging from 6 to 20% and permeability from 1 to 500 mD (Nairn and Alsharhan, 1997).

3.4. Analytical Methods

3.4.1. Rock-Eval pyrolysis & TOC analysis

Rock-Eval pyrolysis was conducted on the finely ground solid bitumens using a Rock-Eval 6 instrument (Behar *et al*., 2001). The temperature program started isothermally at 300°C for 3 minutes subsequently increased to 650°C at a heating rate of 25°C/min. The quality of data was checked by analyzing a standard sample at every tenth sample. For determination of total organic carbon (TOC) contents a Leco SC-632 instrument was employed. Prior to analysis, carbonate was removed from the finely crushed samples using dilute HCl. The amount of carbon in the decarbonated sample was measured as carbon dioxide by an IR-detector (Weiss *et al*., 2000).

3.4.2. Thermovaporisation- and pyrolysis-gas chromatography

All solid bitumens, four heavy oils and four seep oils were analyzed by Tvap & Py-GC techniques. In the case of seep oils and heavy oils the Tvap is equivalent to whole oil gas chromatography. For Tvap-GC analysis, milligram quantities of each sample were

loaded in a glass tube (30 mm long; internal diameter ~1.5 mm) with pre-cleaned quartz wool and then closed by a H_2 flame. After loading the sealed glass tube into the system, it was cracked at 300°C and released products were collected at -196°C in a cryogenic trap. Thereafter, they were transferred by helium flow (30 ml/min) into a HP-Ultra 1 fused silica capillary column (50 m length, 0.32 mm internal diameter and 0.52 μm film thickness) mounted in an Agilent Technology (AT) 6890A gas chromatograph equipped with a flame ionization detector (FID). For Py-GC analysis, whole samples were inserted or injected into a glass tube with both ends open (non-isothermal open-system Py-GC). The sample was heated at a temperature of 300°C for 5 min in order to release and vent the free hydrocarbons. Then pyrolysis was carried out by heating from 300 to 600°C at 50°C/min and holding for 2 min. The products were collected in a cryogenic trap from which they were later injected on to the capillary column by ballistic heating. For both methods, Tvap- and Py-GC, hydrocarbon peaks were identified by comparison with reference chromatograms and quantification was conducted by external standardization with *n*-butane.

3.4.3. Solvent extraction & hydrocarbon fractionation

The finely crushed solid bitumens and the oil seepage samples were extracted in a Soxhlet apparatus using dichloromethane:methanol 99:1 (v:v) as solvent. After asphaltene precipitation from extracted bitumens and crude heavy oils with *n*-hexane (Theuerkorn *et al*., 2008), the maltenes were separated into saturate, aromatic and resin fractions using automated medium pressure liquid chromatography (MPLC) (Radke *et al*., 1980).

3.4.4. Gas chromatography

Identification and quantification of constituents of the aliphatic hydrocarbon fractions was conducted using a gas chromatograph (AT 6890A), equipped with an Agilent-Ultra 1 capillary column (50 m × 0.20mm i.d., 0.33 μm f.t.) and a flame ionization detector.

The GC oven was programmed from 40°C (2 min isothermal) to a final temperature of 300°C (65 min isothermal) at a heating rate of 5°C/min with a constant Helium flow as carrier gas (1ml/min). 5α-Androstane was used as internal standard.

3.4.5. Gas chromatography-mass spectrometry

GC-MS analyses were conducted on the aliphatic and aromatic hydrocarbon fractions using an AT 6890A GC equipped with a PTV injection system and a fused silica capillary column (BPX5; 50 m × 0.22 mm i. d., f. t. = 0.25 μm). The initial GC oven temperature was programmed from 50°C for 1 min, and then increased to 310°C at 3°C/min, followed by an isothermal phase of 10 minutes. Helium was used as carrier gas at a constant flow rate of 1ml/min. For compound identification, the GC unit was connected to a Finnigan MAT 95 XL mass spectrometer operating in the electron impact mode (70 eV). 5α-Androstane and 1-ethylpyrene were used as internal standards for saturate and aromatic fractions, respectively.

3.4.6. Gas chromatography-isotope ratio mass spectrometry

Compound-specific stable carbon isotope signatures were determined on the aliphatic fractions of different sample types. The carbon isotopic composition of individual *n*-alkanes was measured using a GC unit (AT 6890) coupled to a MAT 253 mass spectrometer via a combustion interface (GC-C/TC III). Combustion was done in a microvolume ceramic tube with CuO/Ni/Pt wires at 940 °C. A HP Ultra 1 capillary column (50 m × 0.2 mm i.d., 0.33 μm f.t.) was used in the GC unit. The temperature program started at 40 °C (for 2 min), then increased to 300 °C at 4 °C/min and was held at this temperature for 45 min. The initial temperature of the injector was set to 230 °C and by injection it was heated to 300 °C at a rate of 700 °C/min and held at this condition for the rest of the analysis time. Each sample was analyzed at least three times, and the standard deviations were from 0.01 to 0.46‰. The $\delta^{13}C$ values of individual *n*-alkanes are given in the delta notation relative to Pee Dee Belemnite (PDB) and data quality was

checked regularly by certified standards containing mixtures of *n*-alkanes with known isotopic composition.

3.5. Results and Discussion

To establish a geochemical correlation between different hydrocarbon types, equivalent or at least similar levels of thermal maturity and biodegradation are required (Peters *et al*., 2005). Therefore, firstly geochemical results of the surficial and subsurface hydrocarbons from SE Turkey are considered separately, focusing on the related organofacies as well as the level of transformation by respective alteration processes. Thereafter, selected samples are correlated using additional parameters.

3.5.1. Heavy oils

The results of bulk fraction separation (asphaltene, saturates, aromatics, resins) are presented alongside API gravity, reservoir formation, temperature and depth (Table 3.1). The aliphatic hydrocarbons are a subordinate fraction, with polar compounds being the major constituents, and the oil samples are classified as naphthenic oils according to the criteria provided by Tissot and Welte (1984). It is clear that the relative abundances of saturate, aromatic, resin and asphaltene (SARA) fractions in the studied heavy oils are related to their API gravities. Those with relatively high API gravities show the highest abundance of the saturate fraction and lowest of polar compounds, while the reverse is true for oils with lower API gravities (Fig. 3.2.a).

The macromolecular building blocks in resins and asphaltenes can be analysed using open system Py-GC (Horsfield *et al*., 1991; Muscio *et al*., 1991). Two selected pyrograms from the solid bitumens, heavy oils and seep oils are given in Figure 3.3. All four analyzed heavy oils i.e. Silvanka Sinan, Germik, Güney Dinçer and Batı Kozluca, show closely similar patterns; they are dominated by *n*-alk-1-ene/*n*-alkane doublets (*n*-alk-1-enes > *n*-alkanes), with simple aromatic compounds such as BTEX (benzene,

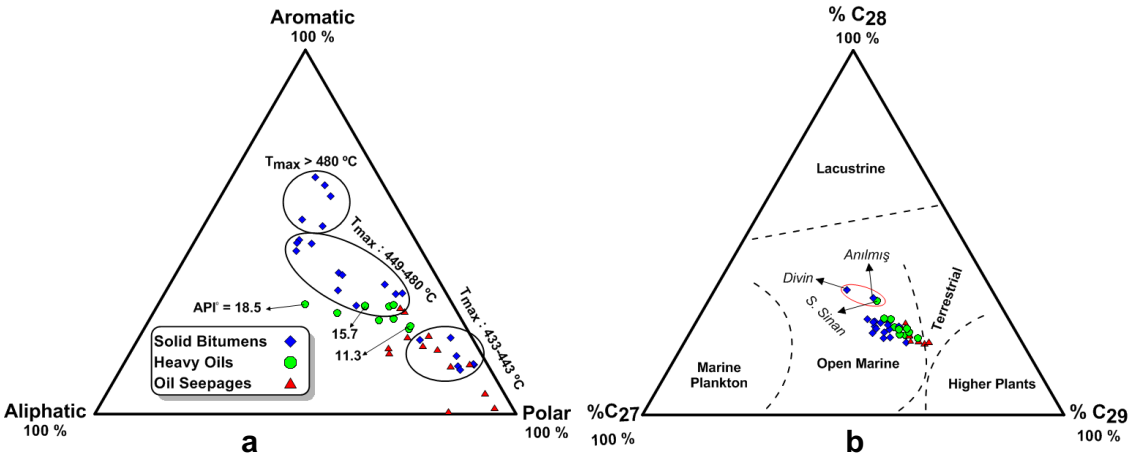

Fig. 3.2: a) The bulk composition of different petroleum types from SE Turkey using relative abundances of SARA fractions; T_{max} ranges of solid bitumens as well as API gravities for some of oils are shown. **b)** Source identification using regular sterane distributions (C_{27}-C_{28}-C_{29}).

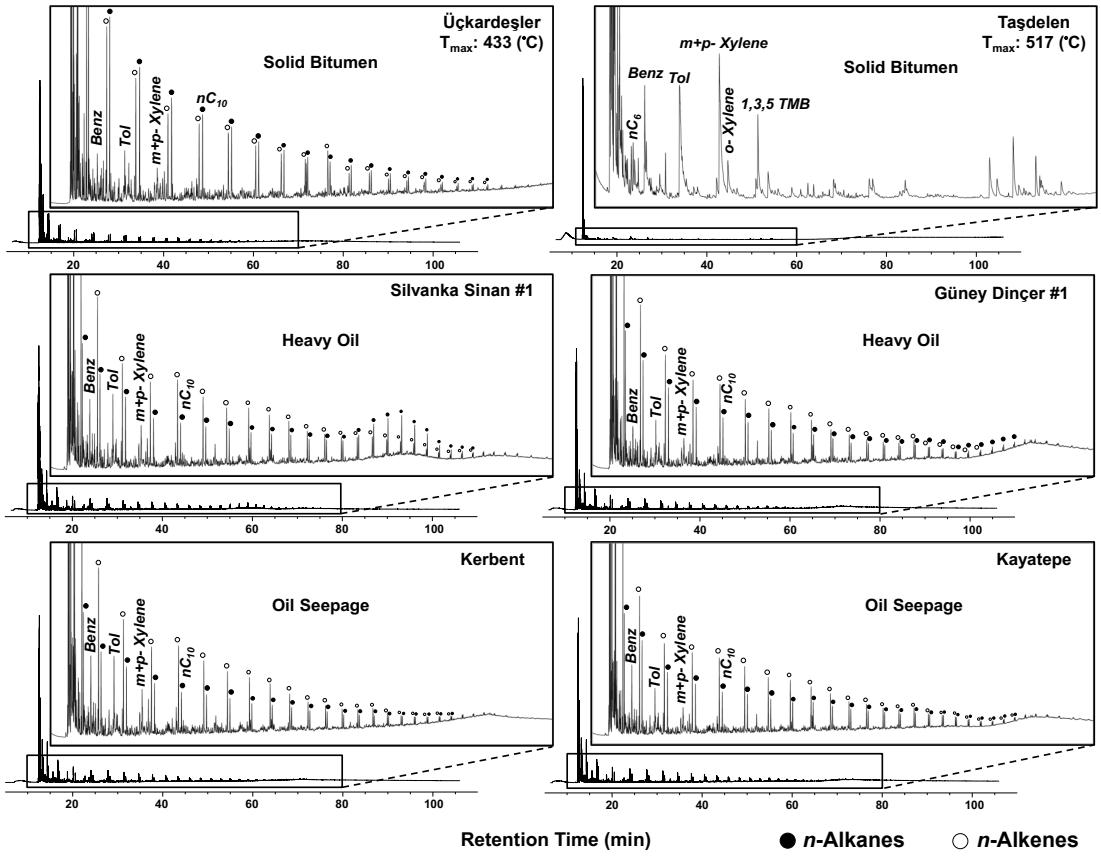

Fig. 3.3. Open system pyrolysis gas chromatograms of different sample types from SE Turkey.

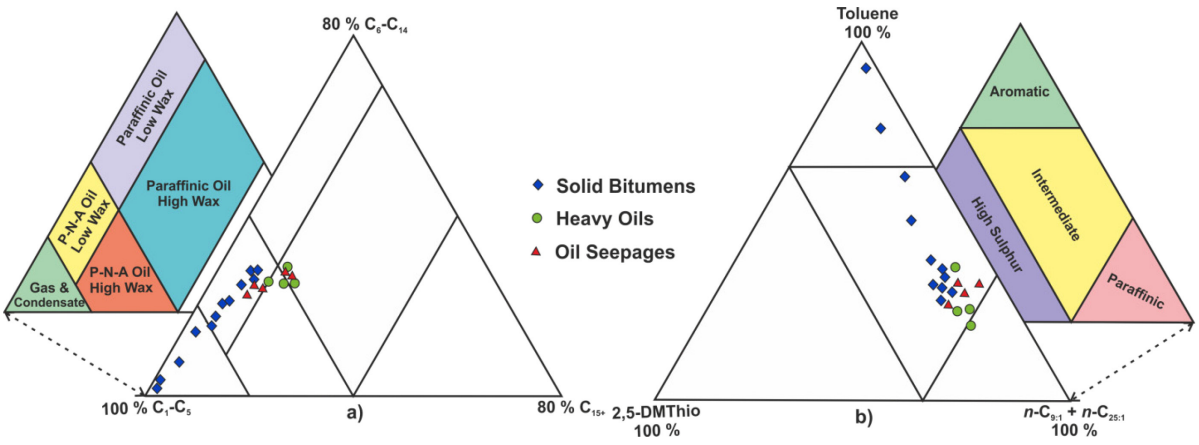

Fig. 3.4. a) Distribution patterns of total C_1-C_5 resolved pyrolysate, C_6-C_{14} *n*-alkenes plus *n*-alkanes and C_{15+} *n*-alkenes plus *n*-alkanes in different sample types from SE Turkey (after Horsfield, 1989); **b)** Differentiation of pyrolysate composition using relative proportions of non-1-ene plus pentacos-1-ene, toluene and 2,5-dimethylthiophene (after di Primio and Horsfield, 1996).

toluene, ethylbenzene and xylenes) in low abundance. The chain length distribution falls close to the junction of four oil-based Petroleum Type Organofacies (Fig. 3.4.a). Turkish heavy oils are known to be sulphur-rich (e.g. Mueller *et al*., 1995; Nairn and Alsharhan, 1997; Kavak, 2011). Interestingly, the amounts of sulphur compounds in resolved pyrolysates, shown in Fig. 3.4.b, are relatively low, falling in the Intermediate category. This implies that sulphur components in the heavy oils are not in a form that is labile and degradable by pyrolysis, and instead likely occur mainly in refractory structures and condensed ring systems.

The *n*-alkanes and isoprenoids are the most abundant components in saturated fractions of heavy oils exhibiting a unimodal distribution from ~*n*-C_{10} to ~*n*-C_{35}, with a maximum at around *n*-C_{15} to *n*-C_{17} (Fig. 3.5). The low molecular weight hydrocarbons (LMWH) (<*n*-C_{20}) are more abundant than the high molecular weight hydrocarbons (HMWH) (>*n*-C_{25}), revealing a non-waxy character (Tab. 3.2).

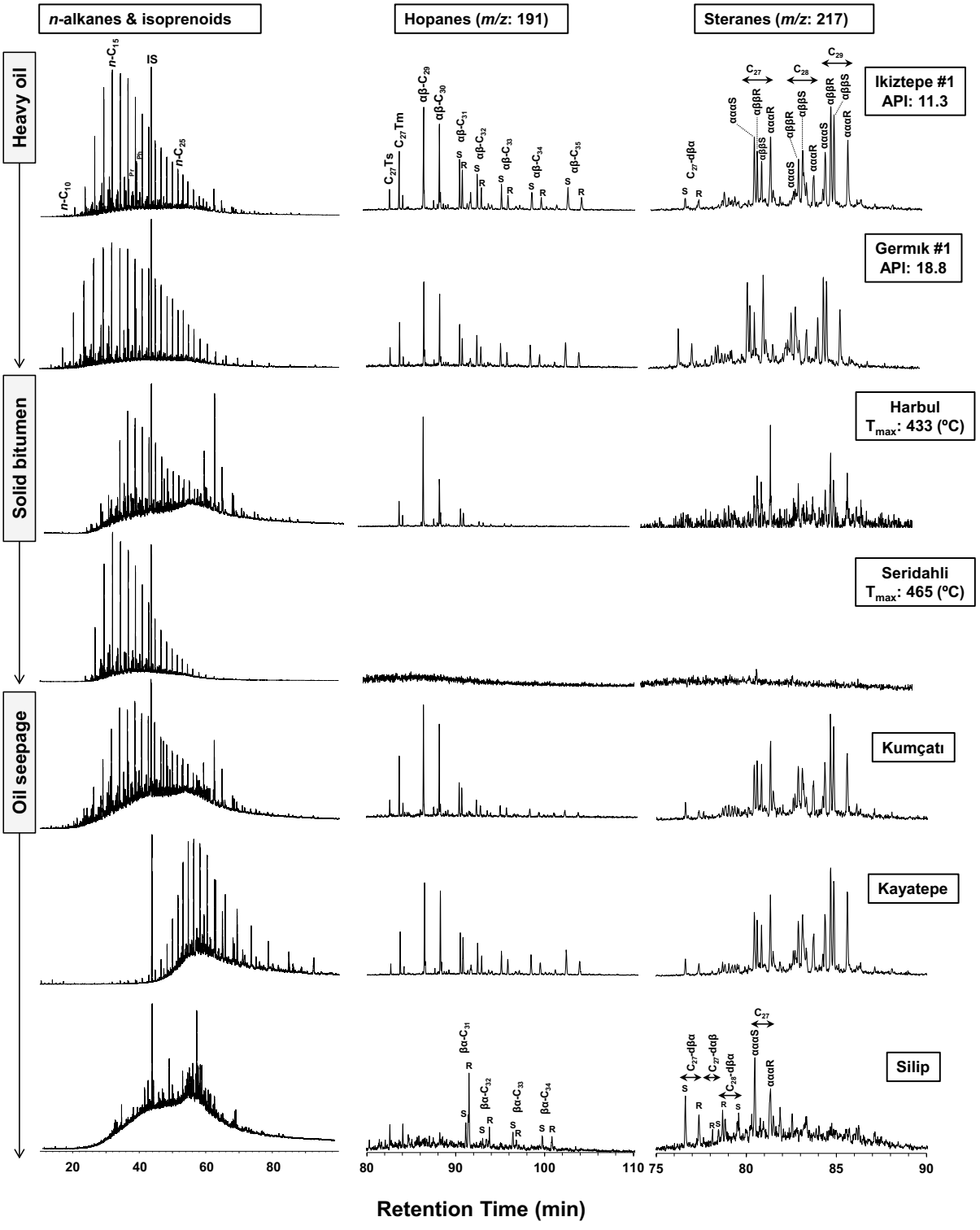

Fig. 3.5. The *n*-alkane, isoprenoid, hopane and sterane distributions in selected samples from surface and subsurface petroleum occurrences in SE Turkey.

Tab. 3.2. Source-related biomarkers obtained from GC and GC-MS data of different sample types in SE Turkey.

		n-alkanes & isoprenoids						Steranes					Terpanes				
	Sample Name	CPI*	Pr/Ph	Pr/nC_{17}	Ph/nC_{18}	TAR*	L/H*	%C_{27}	%C_{28}	%C_{29}	C_{28}/C_{29}	C_{30} SI*	$C_{22/3}/C_{21/3}$	$C_{24/3}/C_{23/3}$	$C_{24/4}/C_{23/3}$	C_{29}/C_{30} H	C_{35} HHI*
Solid Bitumens	Üçkardeşler	0.98	0.54	0.13	0.28	0.08	8.35	33	24	43	0.52	0.05	0.70	0.36	1.96	1.27	0.03
	Harbul-1	1.05	0.49	0.18	0.34	0.26	3.27	32	21	47	0.58	0.07	0.97	0.45	2.58	2.11	0.05
	Harbul-2	0.95	0.73	0.14	0.21	0.09	5.68	29	25	46	0.51	0.04	0.85	0.47	2.89	1.48	0.04
	Segürük-1	1.08	0.69	0.10	0.15	0.05	12.60	32	26	42	0.69	0.05	0.61	0.57	3.23	1.68	0.04
	Segürük-2	1.03	1.18	0.21	0.20	0.07	9.34	31	25	44	0.57	0.04	1.03	0.53	3.02	1.15	0.04
	Avgamasya-1	0.95	0.84	0.21	0.19	0.12	6.10	34	22	44	0.52	0.06	0.80	0.46	2.95	1.67	0.03
	Avgamasya-2	1.18	1.37	1.29	0.44	0.71	1.16	31	23	46	0.49	0.04	0.63	0.57	1.61	-	-
	Avgamasya-3	0.99	0.94	1.88	0.82	0.52	1.79	30	23	47	0.56	0.04	0.70	0.51	1.56	1.16	0.06
	Kumçatı	1.06	1.42	0.39	0.28	0.29	2.90	31	21	48	0.47	0.04	0.71	0.46	1.87	1.28	0.02
	Milli-1	1.04	0.95	0.42	0.32	0.26	3.08	33	24	43	0.58	0.05	0.85	0.66	1.85	-	-
	Milli-2	1.03	1.66	0.15	0.10	0.09	9.23	27	24	49	0.48	0.03	0.68	0.57	1.83	1.36	0.08
	Divin	0.97	1.31	0.17	0.16	0.01	35.25	34	34	32	0.56	-	0.56	0.89	0.98	-	-
	Çağlayan	1.18	1.43	0.15	0.11	0.10	8.92	26	22	52	0.52	0.07	0.78	0.71	2.12	-	-
	Ispindoruk	1.01	0.94	-	0.84	0.77	1.13	-	-	-	-	-	-	-	-	-	-
	Seridahli-1	1.04	0.75	0.05	0.08	0.04	15.67	-	-	-	-	-	-	-	-	-	-
	Seridahli-2	1.02	1.02	0.12	0.14	0.06	11.36	-	-	-	-	-	-	-	-	-	-
	Hesana	1.05	1.76	0.13	0.09	0.03	21.66	34	26	40	0.76	-	-	-	-	-	0.13
	Nivekara	1.11	0.00	0.00	0.52	0.23	4.21	29	25	46	0.43	0.06	0.95	0.55	1.95	1.33	0.09
	Ortasu-1	0.90	3.31	0.44	0.49	-	-	-	-	-	-	-	-	-	-	-	-
	Ortasu-2	1.08	1.48	0.11	0.09	0.09	9.37	33	25	42	0.70	-	-	-	-	1.05	-
	Karatepe-1	1.25	1.59	0.16	0.13	0.01	-	-	-	-	-	-	-	-	-	-	-
	Karatepe-2	1.02	1.59	0.13	0.09	0.12	5.99	-	-	-	-	-	-	-	-	-	-
	Silip	0.89	1.17	0.87	0.65	0.13	5.37	27	20	53	0.46	-	0.91	0.92	4.07	-	-
	Rutkekurat	1.09	2.54	0.23	0.25	0.01	-	-	-	-	-	-	-	-	-	-	-
	Taşdelen	1.02	-	-	-	0.07	12.06	-	-	-	-	-	-	-	-	-	-
	Anılmış	1.23	1.21	0.15	0.13	0.01	-	29	32	39	0.74	-	-	-	-	1.15	0.13
	Herbiş	0.81	-	0.09	-	0.01	32.76	-	-	-	-	-	-	-	-	-	-
	Roboski	1.12	1.03	0.41	0.51	0.04	12.72	-	-	-	-	-	-	-	-	-	-
	Anıttepe	0.57	-	-	-	-		-	-	-	-	-	-	-	-	-	-
	Besta	1.00	0.77	0.14	0.18	0.09	7.86	29	26	45	0.54	0.09	-	-	-	-	-
Seep Oils	Kerbent	-	0.30	1.69	-	-	5.08	26	22	52	0.41	0.04	0.72	0.37	2.12	1.25	0.14
	Zengen	-	0.00	-	0.54	-	-	-	-	-	-	-	0.69	0.32	1.75	-	-
	Eruh	-	0.60	-	-	-	-	26	20	54	0.35	0.03	0.81	0.17	1.77	1.17	0.17
	Kumçatı	0.93	1.03	0.49	0.45	0.20	2.96	27	24	49	0.48	0.04	0.55	0.52	1.72	1.09	0.09
	Silip	-	0.00	-	-	-	-	-	-	-	-	-	0.63	0.39	0.59	-	-
	Kayatepe	0.94	0.48	0.64	1.11	49.26	0.01	25	25	50	0.47	0.04	1.18	0.56	2.26	1.01	0.17
	Dadaş	-	0.60	0.25	0.60	-	-	-	-	-	0.18	0.29	-	-	-	-	0.18
	İşkar	1.28	0.94	0.56	0.75	0.25	3.46	-	-	-	0.17	0.18	0.35	0.82	0.26	-	0.10
	Yeşilli	-	-	-	-	-	-	23	20	57	0.32	0.05	0.95	0.30	1.59	1.11	0.13
	Bagas	-	0.63	1.71	3.98	-	-	26	22	52	0.40	0.07	0.41	0.69	0.81	0.66	0.10
	Tala	-	-	-	-	-	-	22	20	58	0.31	0.04	1.96	0.49	2.76	1.25	0.14
	Gerçüş	-	-	-	-	-	-	24	20	56	0.34	0.03	1.01	0.35	1.72	1.17	0.14
	Badzivan	-	-	-	-	-	-	-	-	-	0.51	-	0.71	0.43	1.41	-	-
Heavy Oils	Silvanka Sinan	0.90	0.57	0.48	0.85	0.32	2.25	29	31	40	0.68	0.04	0.82	0.34	0.56	1.11	0.18
	Raman	0.94	0.60	0.26	0.47	0.25	2.86	28	24	48	0.46	0.04	0.79	0.30	1.22	1.16	0.17
	Germık	0.93	0.60	0.28	0.49	0.27	3.12	28	26	46	0.48	0.05	0.38	0.42	0.72	1.07	0.17
	Çamurlu	0.92	0.59	0.35	0.65	0.23	2.86	29	27	44	0.56	0.05	0.62	0.42	0.98	1.09	0.17
	Güney Dinçer	0.97	0.62	0.20	0.37	0.18	3.83	27	22	51	0.41	0.04	1.03	0.42	1.70	1.37	0.15
	Batı Kozluca	0.99	0.57	0.21	0.42	0.16	3.92	28	22	50	0.42	0.03	1.04	0.43	1.32	1.46	0.15
	Batı Raman	0.94	0.50	0.25	0.57	0.24	2.93	25	23	52	0.43	0.03	0.92	0.38	1.37	1.06	0.15
	Mağrip	0.92	0.62	0.29	0.51	0.24	3.08	27	23	50	0.46	0.03	0.65	0.35	1.28	1.25	0.14
	Doğu Sınırtepe	1.01	0.61	0.27	0.51	0.18	4.45	24	21	55	0.36	0.03	0.85	0.39	1.33	1.39	0.17
	Ikiztepe	1.02	0.60	0.26	0.51	0.18	4.16	26	24	50	0.41	0.03	0.77	0.37	1.35	1.20	0.14

* **CPI** = $[(C_{23}+C_{25}+C_{27})+(C_{25}+C_{27}+C_{29})]/2(C_{24}+C_{26}+C_{28})$; **TAR** = Terrigenous/aquatic ratios of *n*-alkanes: $(C_{27}+C_{29}+C_{31})/(C_{15}+C_{17}+C_{19})$; **L/H** = Low molecular weight *n*-alkanes/High molecular weight *n*-alkanes;**C_{30} SI** = $C_{30}/(C_{27}-C_{30})$ Sterane Index; **C_{35} HHI** = $\sum C_{35}/\sum C_{31-35}$ Homohopane index.

The widely used source-sensitive parameters are listed in Table. 3.2. The Carbon Preference Index (CPI) values around unity indicate that the heavy oils are thermally mature and/or derived from marine algal organic matter (Powell and Mokirdy, 1973). The low values for the Pr/Ph, Pr/*n*-C_{17} and Ph/*n*-C_{18} ratios imply anoxic conditions of the depositional environment and demonstrate a mature marine algal source (kerogen Type II) (Didyk *et al*., 1978). The same inferences are observed using the cross-plot of Pr/Ph against the C_{29}/C_{27} ratio of regular steranes (Fig 3.6.a). The dibenzothiophene/phenanthrene ratios are >1 for all heavy oils, suggesting they were generated by a marine carbonate source (Hughes *et al*., 1995). Compared with the other samples, the value of this ratio is quite high in the Silvanka Sinan oil (7.5), possibly due to a different lithofacies of the source unit (Fig 3.6.b).

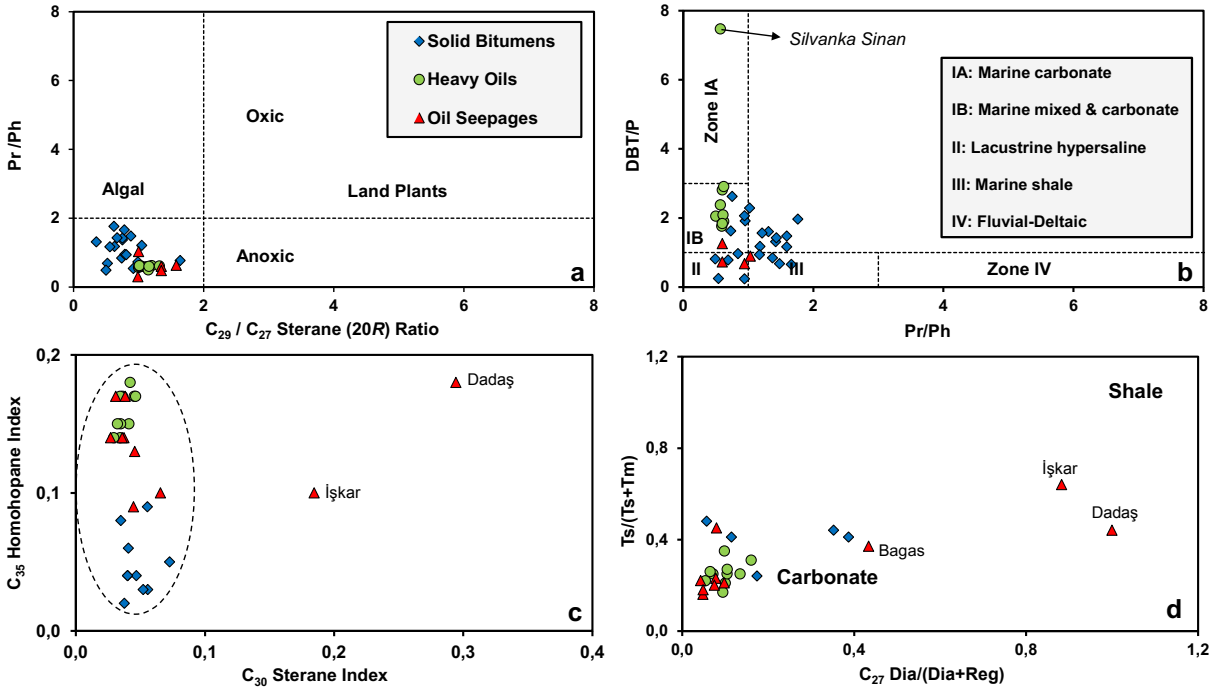

Fig. 3.6. Characterization of depositional environment and lithology of the source unit(s) using saturated and aromatic parameters in different petroleum occurrences from SE Turkey: **a)** Pr/Ph versus C_{29}/C_{27} (20*R*) sterane ratios; **b)** DBT/P versus Pr/Ph ratios; **c)** the C_{35} homohopane index versus C_{30} sterane index, and **d)** the C_{27} Dia/(Dia+Reg) sterane versus $T_s/(T_s+T_m)$ ratios.

The relative abundance of regular steranes decreases in the order $C_{29} > C_{27} > C_{28}$ in all heavy oils, except for the Silvanka Sinan sample, but all samples plot in the area indicating a marine environment in the sterane ternary diagram (Fig. 3.2.b) (Waples and Machihara, 1991). The high relative amount of C_{28} steranes in the Silvanka Sinan oil which is clearly separated from other samples may suggest a relatively younger source as C_{28} sterane abundances are thought to have increased through geological time (Grantham and Wakefield, 1988). Furthermore, the presence of C_{30} steranes in all heavy oils implying to the contribution of marine-derived organic matter in the source unit(s), is entirely consistent with inferred results noted above (Tab. 3.2) (Peters *et al*., 1986). The low Pr/Ph (<1) and high Ph/*n*-C_{18} ratios (>0.3) pointing to carbonate-derived oils, are consistent with the high sulphur contents, low API gravities as well as low to medium values of saturate/aromatic ratios (0.47-1.16) (Tab. 3.1) (Mueller *et al*., 1995; Hughes, 1984; Ten Haven *et al*., 1988).

The lower sensitivity of tricyclic terpanes to alteration processes relative to other types of biomarkers in saturated fractions i.e. hopanes and steranes, make them suitable for correlation studies (Sofer, 1988). Hydrocarbons generated from carbonate source rocks are distinguished by high C_{22}/C_{21} and low C_{24}/C_{23} tricyclic terpanes (Peters *et al*., 2008). Based on these ratios the investigated samples are inferred to originate from carbonate and/or evaporite source rocks (Tab. 3.2). Moreover, low values of the T_s/T_m ratios and C_{27} Dia/(Dia+Reg) steranes, high amounts of C_{24} tetracyclic/C_{23} tricyclic terpane ratios, low values of the C_{30} sterane index as well as C_{29}/C_{30} hopane ratios >1 are entirely in accordance with the inferred results (see Tab. 3.2 and Fig. 3.6.c-d) (Connan *et al*., 1986; Clark and Philp, 1989; Peters *et al*., 2005).

It is widely accepted that hydrocarbon biodegradation processes may be active in reservoirs at temperatures below ~80ºC (e.g. Connan, 1984). With one exception the temperatures of the reservoirs hosting the investigated heavy oils are clearly below this threshold (Table 3.1) and thus would be regarded as being amenable to the activity of petroleum-degrading microorganisms. Surprisingly however, there is no evidence of biodegradation based on the criteria introduced by Peters and Moldowan (1993) (Fig. 3.5). This might be either due to high salinity of the formation water (Nairn and

Alsharhan, 1997) and/or the presence of sterilized hydrocarbon traps according to the paleopasteurization concept (Wilhelms *et al*., 2001) as the investigated area experienced significant uplifts through geological time.

Since the investigated heavy oils are undegraded and genetically related, the API gravity can be used as a maturity indicator (Peters and Moldowan, 1991). Also, the maturity-sensitive parameters obtained from aliphatic and aromatic hydrocarbons are presented in Tab. 3.3. Saturated biomarker maturity parameters are at epimerisation and isomerisation equilibrium or close to it, and thus provide information on the minimum maturity level only. The T_s/T_m ratios increase with increasing API gravity and depth, except for the Raman oil which has a higher API gravity (18) compared to other oils but a relatively low value of T_s/T_m ratio (0.23). The saturate/aromatic ratios display the same variation and increase with increasing API gravities.

It is well known that a significant decrease in concentration of saturated biomarkers occurs with increasing maturation levels and their dynamic ranges are limited to rather low maturation levels (Mackenzie and Maxwell, 1981; Radke, 1988). In contrast, aromatic hydrocarbons are more thermally resistant and their distributions change in a regular fashion with increasing maturity up to high levels (Radke, 1987). Variations of different maturation parameters obtained from aromatic hydrocarbons, except for MPI 1, correlate well with API gravity (Fig. 3.7.a). Based on API gravity, saturated hydrocarbon biomarkers, naphthalene- and phenanthrene-based parameters such as TMNR, TeMNR, MPI-1, MPI-2 and R_c, the Silvanka Sinan oil displays the same maturation level as the other oils, however, it is highly mature using dibenzothiophene-based maturity parameters (Tab. 3.3).

3.5.2. Oil seepages

The bulk composition of the thirteen seep oils is dominated by polar compounds (58 to 95%), as expected (Fig. 3.2.a). The amounts of polar compounds do not show systematic changes with biodegradation and it appears that other factors such as maturity

Tab. 3.3: Thermal maturity indicators calculated based on saturate and aromatic fractions in all investigated samples from SE Turkey.

		Saturates					Aromatics								
	Sample Name	**T_s/T_m**	**M/(M+H)**	**C_{31} H**	**20*S* C_{29}**	**ββ-C_{29}**	**TMNR**	**TeMNR**	**MPI 1**	**MPI 2**	**MDR**	**MDBT Ratio 2**	**R_m**	**R_c**	**DBT/Phen**
Solid Bitumens	**Üçkardeşler+**	0.04	0.04	0.53	0.52	0.55	0.77	0.90	0.96	1.01	3.62	2.07	0.78	0.90	0.24
	Harbul-1+	0.06	0.04	0.59	0.46	0.60	0.36	0.52	0.79	0.89	0.81	0.86	0.59	0.83	0.81
	Harbul-2+	0.06	0.05	0.54	0.42	0.60	0.60	0.76	1.10	1.14	0.98	0.98	0.61	0.98	1.62
	Seğürük-1	0.06	0.05	0.52	0.45	0.62	0.37	0.61	0.66	0.77	0.90	0.93	0.60	0.75	0.78
	Seğürük-2	0.10	0.04	0.52	0.41	0.62	0.39	0.64	0.75	0.82	0.81	0.87	0.59	0.80	1.17
	Avgamasya-1+	0.09	0.05	0.54	0.47	0.60	0.50	0.69	0.62	0.65	1.36	1.21	0.66	0.72	0.96
	Avgamasya-2+	-	0.06	0.51	0.51	0.59	0.66	0.86	0.59	0.63	1.92	1.47	0.71	0.71	0.84
	Avgamasya-3	0.70	-	0.57	0.48	0.63	0.67	0.81	0.64	0.65	1.83	1.41	0.70	0.74	0.23
	Kumçatı+	0.26	0.06	0.56	0.45	0.64	0.49	0.76	0.58	0.62	1.74	1.42	0.70	0.71	1.31
	Milli-1+	-	0.06	0.56	0.49	0.63	0.74	0.82	0.99	1.03	6.43	1.93	1.37	0.91	1.91
	Milli-2	-	-	0.54	0.48	0.62	0.68	0.88	0.73	0.78	2.49	1.74	0.73	0.79	0.65
	Divin	-	-	-	0.42	0.47	0.63	0.76	0.26	0.29	1.61	1.50	0.69	0.50	1.60
	Çağlayan+	-	-	-	0.48	0.60	0.55	0.86	0.87	0.97	2.03	1.46	0.71	0.86	1.42
	Ispindoruk	-	-	-	-	-	0.81	0.92	1.36	1.49	4.90	1.78	0.91	1.13	2.06
	Seridahli-1+	-	-	-	-	-	0.76	0.88	1.12	1.32	8.80	2.13	3.26	1.01	2.62
	Seridahli-2+	-	-	-	-	-	0.80	0.90	1.24	1.39	4.24	1.71	0.82	1.07	2.28
	Hesana	0.79	-	0.50	0.53	0.62	0.80	0.92	1.37	1.51	4.65	1.73	0.87	1.14	1.96
	Nivekara	0.18	-	0.58	0.43	0.57	0.90	0.93	1.39	1.48	13.75	2.17	15.35	1.13	1.51
	Ortasu-1+	-	-	-	-	-	0.94	0.97	1.18	1.25	7.31	1.67	1.87	0.96	1.52
	Ortasu-2	0.70	-	0.45	0.43	0.59	0.94	0.96	1.77	1.76	30.53	2.54	-	-	0.67
	Karatepe-1+	-	-	0.50	-	-	0.96	0.98	1.74	1.66	12.54	1.59	11.07	1.26	1.47
	Karatepe-2+	-	-	-	-	-	0.93	0.96	1.47	1.44	28.26	1.84	-	-	1.16
	Silip+	-	0.08	0.57	0.52	0.62	0.62	0.77	0.76	0.80	1.92	1.48	0.71	0.80	0.93
	Rutkekurat+	-	-	-	-	-	0.95	0.98	1.83	1.81	12.04	1.73	9.58	1.33	1.80
	Taşdelen+	-	-	0.61	-	-	0.93	1.00	1.98	2.01	38.18	2.13	-	-	2.96
	Anılmış	-	-	0.49	0.52	0.54	0.97	0.97	1.80	1.74	14.09	1.62	16.74	1.29	1.56
	Herbiş+	-	-	-	-	-	-	-	0.30	0.36	13.98	4.39	16.28	-	0.33
	Roboski+	-	-	0.44	-	-	-	-	1.59	1.59	36.12	2.27	-	-	5.12
	Anıttepe+	-	-	-	-	-	-	-	0.84	0.77	31.77	2.25	-	-	3.55
	Besta+	-	-	0.57	0.47	0.53	-	-	1.14	1.22	42.67	2.50	-	-	11.36
Seep Oils	**Kerbent**	0.79	0.06	0.55	0.58	0.47	0.45	0.48	0.49	0.47	0.64	0.77	0.56	0.66	-
	Zengen	-	-	-	-	-	-	-	-	-	-	-	-	-	-
	Eruh	0.19	0.05	0.53	0.58	0.46	0.16	0.50	0.73	0.92	1.19	1.11	0.64	0.79	1.25
	Kumçatı	0.27	0.06	0.56	0.56	0.47	0.44	0.65	0.42	0.37	1.30	1.17	0.66	0.62	0.89
	Silip	-	-	0.30	-	-	0.45	0.52	0.76	0.55	1.28	1.11	0.65	0.77	0.98
	Kayatepe	0.26	0.05	0.53	0.55	0.46	-	-	0.60	0.72	1.16	1.08	0.64	0.72	0.00
	Dadaş	0.78	0.39	0.52	0.56	0.52	0.68	0.71	1.07	1.10	2.80	1.74	0.74	0.97	0.72
	İşkar	-	-	0.58	0.50	0.56	0.28	0.13	0.88	0.88	1.96	1.36	0.71	0.86	0.67
	Yeşilli	0.24	-	0.54	0.47	0.58	0.44	0.34	0.24	0.25	1.29	1.13	0.65	0.51	0.73
	Bagas	0.60	-	0.55	0.53	0.70	0.38	0.32	1.56	1.75	-	-	-	-	-
	Tala	0.29	-	0.56	0.51	0.59	-	-	-	-	-	-	-	-	-
	Gerçüş	0.22	-	0.56	0.44	0.61	-	-	-	-	-	-	-	-	-
	Badzivan	-	-	-	-	-	-	-	-	-	-	-	-	-	-
Heavy Oils	**Silvanka Sinan**	0.33	0.05	0.59	0.47	0.62	0.53	0.59	1.07	0.95	15.94	2.46	25.85	0.92	7.47
	Raman	0.23	0.04	0.58	0.47	0.62	0.50	0.65	0.86	0.89	2.56	1.54	0.74	0.84	2.81
	Germık	0.43	0.04	0.59	0.46	0.62	0.52	0.59	0.80	0.79	1.97	1.39	0.71	0.81	1.90
	Çamurlu	0.32	0.04	0.58	0.44	0.62	0.47	0.65	0.96	1.06	1.24	1.12	0.65	0.90	1.76
	Güney Dinçer	0.34	0.05	0.54	0.45	0.62	0.46	0.60	0.83	0.93	1.61	1.27	0.68	0.83	2.91
	Batı Kozluca	0.29	0.04	0.55	0.46	0.62	0.42	0.64	0.85	1.00	1.13	1.07	0.63	0.85	2.38
	Batı Raman	0.21	0.04	0.56	0.43	0.63	0.38	0.59	0.77	0.81	1.11	1.06	0.63	0.80	2.05
	Mağrip	0.36	0.04	0.55	0.47	0.62	0.61	0.67	0.96	1.10	2.13	1.44	0.72	0.92	1.90
	Doğu Sınırtepe	0.53	0.05	0.54	0.44	0.63	0.48	0.69	0.92	1.06	1.51	1.24	0.68	0.89	2.09
	Ikiztepe	0.35	0.04	0.56	0.46	0.62	0.43	0.66	0.86	0.98	1.25	1.13	0.65	0.85	1.84

T_s/T_m = 18α(H)-22,29,30 –trisnorneohopane (T_s)/ 22,29,30 –trisnorhopane (T_m); **M/(M+H)** = 17β(H),21α(H)-moretane/(17β(H),21α(H)-moretane + 17α(H),21β(H)-hopane); **C_{31} H** = 22*S*/(22*S* + 22*R*)-17α(H),21β(H)-C_{31} hopanes; **20*S* C_{29}** = 20*S*/(20*S* + 20*R*)-14α(H),17α(H)-C_{29} steranes; **ββ-C_{29}** = 14β(H),17β(H)/(14β(H),17β(H) + 14α(H),17α(H))-C_{29} steranes (20*R* + 20*S*); **TMNR** = 1,3,7-TMN/(1,3,7 + 1,2,5-TMN); **TeMNR** = 1,3,6,7-TeMN/(1,3,6,7 + 1,2,5,6+1,2,3,5-TeMN); **MPI 1** = 1.5(2-MP+3-MP)/(P+1-MP+9-MP); **MPI 2** = 3×2-MP/(P+1-MP+9-MP); **MDR** = 4-MDBT/1-MDBT; **MDBT Ratio 2** = (2-MDBT + 3-MDBT + 4-MDBT)/(1-MDBT + 2-MDBT + 3-MDBT); **R_m** = 0.4 + (0.3×MDR) - (0.094×MDR^2) + (0.011×MDR^3); **R_c** = (0.6×MPI-1)+0.37.
+ Most of maturity parameters are taken from Hosseini *et al*. (2017).

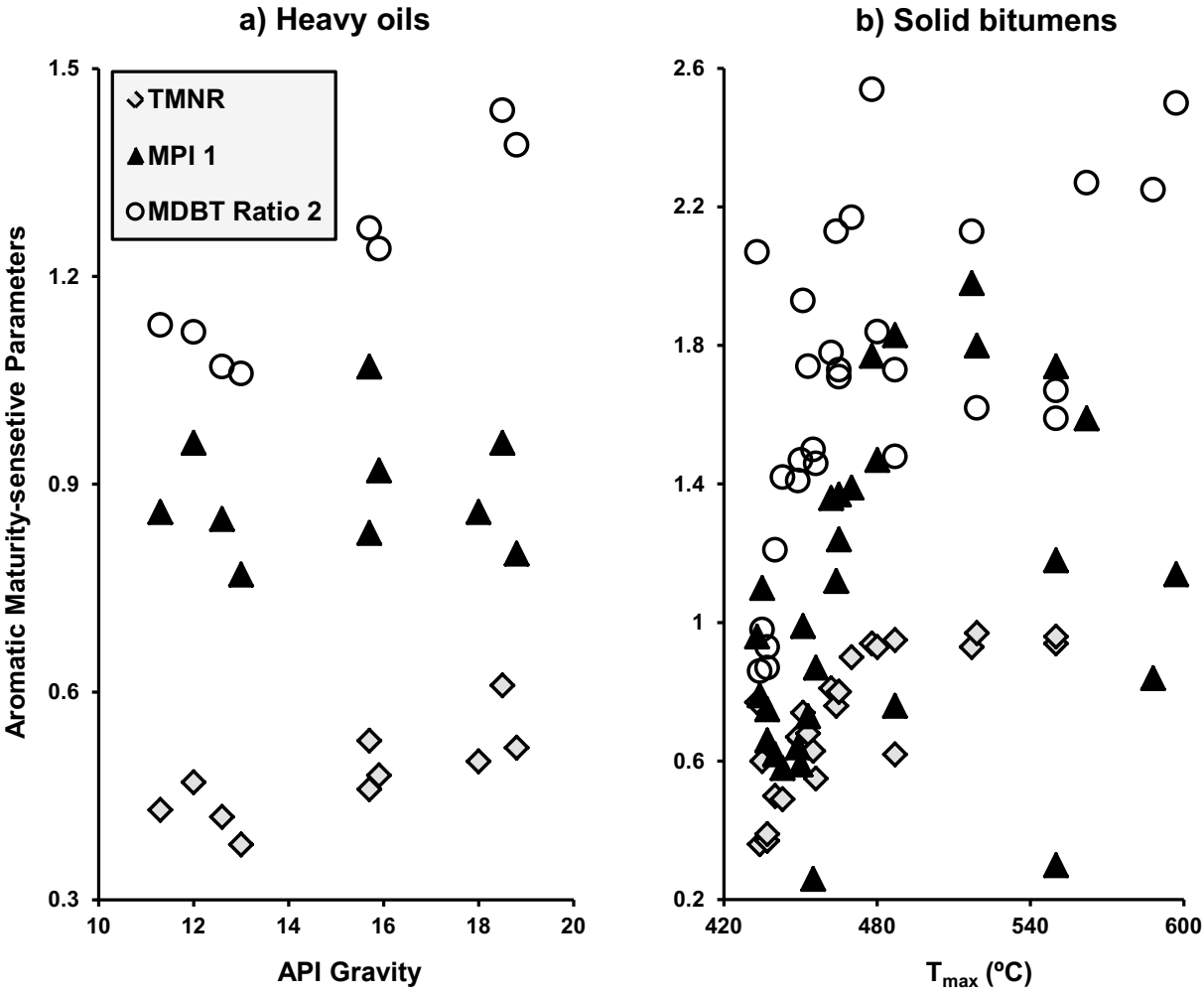

Fig. 3.7. Correlation of maturity parameters based on aromatic hydrocarbons versus: **a)** API gravities for the studied heavy oils; **b)** T_{max} values for the studied solid bitumens.

or source are likely to play a role. Various levels of biodegradation from "light" to "very heavy" are observed using the PM biodegradation scale (Tab. 3.1) (Peters and Moldowan, 1993). The gas chromatograms of saturated hydrocarbons indicate that *n*-alkanes are preserved well in the Kumçatı and Kayatepe seeps ("light" biodegradation) (Fig. 3.5). In "moderately" biodegraded seeps (levels 3 to 5), only traces of *n*-alkanes and acyclic isoprenoids (if any) remain whereas steranes and hopanes are intact. In the "heavily" and "very heavily" biodegraded seeps (levels 6 to 9) *n*-alkanes and acyclic isoprenoids are absent, and steranes and/or hopanes are either partly degraded or absent

depending on the biodegradation level. For example in the Silip seep (level ~8), regular steranes and hopanes are strongly depleted whereas βα-homohopanes and diasteranes are preserved well (Fig. 3.5). The macromolecular components, revealed by Py-GC of selected seeps i.e. the Kerbent, Kumçatı, Silip and Kayatepe, show close similarities with the heavy oils (Fig. 3.3). As was the case for the heavy oils, *n*-alk-1-enes and *n*-alkanes dominate the GC-resolvable pyrolysis products, and *n*-alk-1-enes are more abundant than *n*-alkanes. Also the aromatic compounds are minor and present in low abundances. This applies to samples showing high or low levels of biodegradation.

Molecular distributions of *n*-alkanes and isoprenoids in heavily biodegraded seeps could not be used for correlation purposes as the required components are absent. However, as displayed by the slightly biodegraded seeps such as Kumçatı, there is a unimodal distribution of *n*-alkanes from *n*-C_{11} to *n*-C_{34}, with a maximum at *n*-C_{16} to *n*-C_{18}, pointing to a mature algal source. Based on source-related parameters obtained from aliphatic and aromatic hydrocarbons the source unit(s) of seeps is a marine carbonate deposited under anoxic conditions (see Tab. 3.2 and Fig. 3.6.a-d). A few exceptions are observed. The *n*-alkane distribution in the Kayatepe seep displays a unimodal distribution from *n*-C_{15} to *n*-C_{38} with a maximum at *n*-C_{28}, that could be tied to several causes. It could indicate a major terrestrial contribution to the sedimentary units, i.e. is related to source organofacies; Also, the depletion of lower homologues of *n*-alkanes due to either light biodegradation or migration fractionation could explain the bias to high molecular weight alkanes (Fig. 3.5). Lithology determination based on various diasterane, tricyclic terpane, hopane and homohopane parameters, suggests a clastic source or a different lithofacies of the same source for the Dadaş, İşkar and Bagas seeps (Tab. 3.2 and Fig. 3.6.c-d). It is noteworthy that the Dadaş and İşkar seeps are located in the northernmost part of the study area and are possibly therefore most likely to be genetically distinct from others in the south. These seeps might be related to the Silurian shales which occur in the Dadaş Formation (Soylu, 1987), and sourced some oilfields e.g. the Kurkan-Karakoy (Connan *et al*., 2006).

Since the studied seep oils have various levels of biodegradation, estimation of their maturity is complicated. For instance, in the Badzivan and Zengen seeps maturity

evaluation is possible neither by molecular ratios for saturates nor by aromatics due to the heavy extent of biodegradation. However, based on maturation parameters obtained from aliphatic fractions other seeps display more or less the same maturation level as the heavy oils, except for the T_s/T_m ratios in the Kerbent, Dadaş and Bagas seeps (0.6-0.79). The relatively higher values of this ratio in these seeps might be attributed to either a higher level of maturity or because T_m is more readily biodegraded than is T_s (Bost *et al*., 2001). Also the effect of source on this ratio cannot be ruled out. While maturity assessment using different aromatic compounds in seeps indicates that the Dadaş and Bagas seeps have the highest maturation levels, other seeps have lower or similar maturities relative to the heavy oils (Tab. 3.3). We conclude that among the studied oil seepage samples the Kumçatı and Kayatepe seeps, being least biodegraded, are the best choices to be used along with heavy oils and solid bitumens for correlation purposes.

3.5.3. Solid bitumens

The most relevant bulk parameters of solid bitumens obtained from Rock-Eval pyrolysis, TOC content, extractability and fractionation results are given in Table 3.1. There is a wide range (between 2 to 54%) of TOC contents without any obvious relation to the geographic location of the veins. Considering T_{max} values, there is a clear maturity trend across the region increasing from west to east in direction of the tectonically active zone. Also the hydrogen content, presented by the HI parameter and extractability of organic matter are controlled mainly by maturity and decrease with increasing T_{max} values (Hosseini *et al*., 2017). The distribution of SARA abundances is controlled by maturation processes as well (Fig. 3.2.a). The least mature samples (T_{max} range: 433-443 ºC) contain the highest and lowest amounts of polar and aliphatic compounds, respectively. The concentrations of high molecular weight compounds decrease with increasing maturity due to thermal cracking. The overmature solid bitumens (T_{max} > 480 ºC) show the highest amounts of aromatic fractions and the saturate/aromatic ratios are low throughout the entire series (Tab. 3.1).

The macromolecular components, as revealed by Py-GC, show that the less mature bitumens have the same composition as heavy oils. As it can be seen in Figure 3.3, the Üçkardeşler vein is dominated by *n*-alkane/*n*-alk-1-ene doublets along with low abundances of simple aromatic compounds (*n*-alkane > *n*-alk-1-ene). On the other hand in highly mature solid bitumens, due to thermal cracking, a progressive shortening of hydrocarbon chains takes place; the *n*-alkane/*n*-alk-1-ene doublets are depleted and aromatic compounds become dominating (Fig. 3.3). As maturation proceeds, the proportion of gaseous pyrolysates progressively increases for highly mature solid bitumens which are accompanied by increasing proportions of aromatic moieties (Fig. 3.4.b).

As observed for the heavy oils, the *n*-alkanes and isoprenoids in solid bitumens of low thermal maturity are dominated by aliphatic hydrocarbons, showing a unimodal distribution from ~*n*-C_{12} to ~*n*-C_{33}, with maxima around *n*-C_{15} to *n*-C_{17} (Fig. 3.5). This is consistent with a genetic affiliation to the heavy oils. Furthermore, the LMWHs > HMWHs ratios, Pr/Ph, Pr/*n*-C_{17} and Ph/*n*-C_{18} ratios as well as source-sensitive parameters from biomarker analysis confirm an algal marine carbonate source for the solid bitumens (Tab. 3.2, Fig. 3.2.b and Fig. 3.6).

Turkish solid bitumens are showing various levels of maturity. The maturity and its role in controlling the chemical composition of solid bitumens has recently been reported by the authors elsewhere (Hosseini *et al*., 2017). Maturity assessment using source-related parameters obtained from saturated biomarkers is not possible, except for the T_s/T_m ratios (Tab. 3.3). Although these ratios are not detectable in high thermally-degraded solid bitumens, their values (0.04 – 0.79) increase with increasing thermal stress toward the eastern part of the study area. The aromatic maturity-related parameters are plotted against T_{max} values in Fig. 3.7.b. The methylnaphthalene as well as methyldibenzothiophene ratios are in good agreement with T_{max} values whereas the methylphenanthrene index increases with increasing T_{max} values then decreases at higher maturation levels. The same trend has been reported for the methylphenanthrene index in a maturity series of shales and coals containing type III organic matter (Radke and Welte, 1981).

Although some of the solid bitumens, e.g. from the Avgamasya, Milli and Silip veins, show a certain unresolved complex mixture (UCM or hump) possibly due to local weathering, the presence of *n*-alkanes in nearly all solid bitumens of different transformation levels exclude a severe influence of biodegradation (Mueller *et al*., 1995; Kavak *et al*., 2010 Kavak, 2011; Hosseini *et al*., 2017) (Fig. 3.5). This probably indicates that most of the solid bitumen veins were formed at elevated temperatures precluding the activity of hydrocarbon-degrading microorganisms.

Based on the results discussed so far, all heavy oils, less mature solid bitumens i.e. the Üçkardeşler, Harbul, Segürük, Kumçatı and Seridahli veins as well as low-biodegraded seep oils i.e. the Kumçatı and Kayatepe appear to derive from the same organofacies and also exhibit similar levels of maturation (except for the Seridahli bitumen which is highly mature) and biodegradation; therefore they can be used for correlation purposes. In the following section, selected samples are compared using additional geochemical parameters.

3.5.4. Correlation criteria

3.5.4.1. Homohopane distribution

The distribution of C_{31}-C_{35} 17α,21β(H)-homohopanes are known to be sensitive to the redox conditions of the depositional environment and can be used in correlation studies. Although their precursors, hopanoids, are resistant to degradation during diagenesis, post-generation alteration processes may change their relative distributions (Peters and Moldowan, 1991). The distributions of extended hopanes in different petroleum types are shown in Figure 3.8 and the mass chromatograms (*m/z* 191) of selected samples are displayed in Figure 3.5. All heavy oils and two selected seeps i.e. Kumçatı and Kayatepe, are displaying very similar homohopane distributions, suggesting a strong genetic affinity. Interestingly, low-thermally degraded solid bitumens (T_{max} range: 433 to 443 ºC), are highly enriched in C_{31}- and depleted in higher homologs i.e. C_{33}-, C_{34}- and C_{35}-homohopanes compared to heavy oils and seeps. Since based on the aforementioned

source-sensitive parameters solid bitumens and heavy oils probably are generated from the same or at least a very similar source, different patterns might be attributed to transformation processes that are active during and/or after solidification. These processes may lead to cracking of high molecular weight homologs of homohopanes to lower ones. The same process has been reported to occur during catagenesis of source rocks (Peters and Moldowan, 1991). Biomarkers can occur in a bound form in crude oils and source rocks (Love *et al*., 1995; Rullkötter and Michaelis, 1990), especially in sulphur-rich systems (Schaeffer-Reiss *et al*., 1998) with attachment being from the alkyl chain in the case of the hopanes. Thermal cracking of weak S-C or stronger C-O at the beta carbon atom could release C_{31} hopanes in abundance.

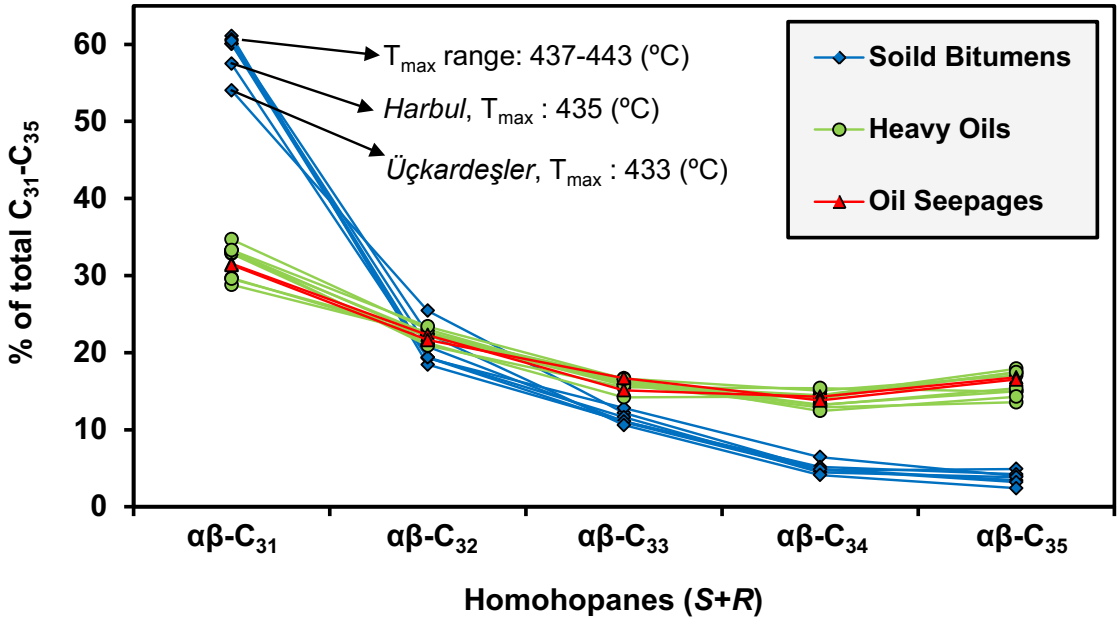

Fig. 3.8. Homohopane distributions for different petroleum occurrences from SE Turkey.

3.5.4.2. Aromatic hydrocarbon distributions

Most of the previously published correlation studies on Turkish petroleum systems focused on the saturated hydrocarbons, while little information has been reported on the aromatic compounds. They are major components of the petroleum types studied,

typically accounting for about 20 to 45% of the total hydrocarbons (Tissot and Welte, 1984). In our sample set the aromatic fraction shows wide variations from 1% in the Dadaş oil seep up to 65% in Taşdelen bitumen which is one of the most thermally-degraded veins. In heavy oils they form 23 to 30% of the total hydrocarbons and in solid bitumens their abundances depend on maturation level and increase with increasing maturity. In selected oil seeps they form about 20% and in less mature solid bitumens (T_{max} range: 433 to 443 ºC) they are present from 12 to 20%, very close to their abundances in heavy oils (Tab. 3.1).

Aromatic compound distributions can be used for correlation purposes as they show obviously different distributions depending on the organic matter source input (Pu *et al*., 1990; Jinggui *et al*., 2005). Therefore, it is expected that different sample types that originate from a common source show some similarities in aromatic hydrocarbon distributions. The relative abundances of six series of aromatic hydrocarbons i.e. dibenzothiophenes, naphthalenes, phenanthrenes, aromatic steroids, biphenyls as well as fluorenes, and their alkylated derivatives in selected samples are displayed in Figure 3.9 (see Tab. 3.4 for all samples). The most abundant compounds in aromatic fractions of heavy oils and solid bitumens are dibenzothiophenes, naphthalenes and phenanthrenes (Fig. 3.9.a). Combined together, they form 82 to 99% of the total abundances. The major difference is at their relative amounts of naphthalenes and phenanthrenes. Heavy oils contain a higher proportion of naphthalenes relative to phenanthrenes while the opposite is true for solid bitumens. This can be attributed to the compositional changes that have occurred during and after the solidification processes as alkylnaphthalenes are more susceptible to alteration processes than alkylphenanthrenes (Fisher *et al*., 1998; Volkman *et al*., 1984). Apart from that, the aromatic hydrocarbon distributions in heavy oils and low-thermally degraded solid bitumens are quite similar. The selected seep oils displayed in Fig. 3.9 represent the least biodegraded seeps and also have an equivalent maturation level (e.g. R_c: 0.6 -0.7). The aromatic compound distribution in the Kumçatı and Kerbent seeps is similar to those of heavy oils and solid bitumens as well (Fig. 3.9.a). The main difference is the relative abundance of aromatic steroids, as expected. Since aromatic steroids are known to be highly resistant to biodegradation processes, their relative

Tab. 3.4. Relative abundances of the major series of aromatic hydrocarbon compounds and their alkylated counterparts in different sample types of SE Turkey.

		Aromatic HC Distributions%						Naphthalenes%					Phenantrenes%				Dibenzothiophenes%				Aro. ST%		Fluorenes%			Biphenyles%		
	Sample Name	N	P	DBT	AS	F	B	N	M-	DM-	TM-	TeM-	P	M-	DM-	TM-	DBT	M-	DM-	TM-	MA-	TA-	F	M-	DM-	BP	M-	DM-
Solid Bitumens	Üçkardeşler	22	51	19	1	3	4	0	2	31	55	11	13	35	37	16	7	28	43	22	23	77	13	41	45	8	43	49
	Harbul-1	4	15	71	8	2	0	0	1	11	29	59	3	28	45	25	1	29	45	25	43	57	5	34	61	4	28	68
	Harbul-2	16	23	52	6	2	1	2	14	26	43	15	10	31	40	19	8	30	41	21	40	60	6	38	55	8	38	53
	Seqürük-1	8	24	64	3	1	0	0	1	15	45	40	4	28	44	25	3	22	45	30	0	100	3	29	68	2	23	76
	Seqürük-2	11	28	55	4	2	1	0	3	22	40	35	4	23	45	28	2	20	45	33	0	100	5	25	70	2	26	72
	Avgamasya-1	7	28	62	1	2	0	0	0	11	47	42	4	27	43	26	2	21	46	32	0	100	2	23	75	1	26	73
	Avgamasya-2	7	34	55	0	3	0	0	0	8	54	38	3	27	46	24	1	16	50	34	0	100	3	27	70	0	12	88
	Avgamasya-3	9	38	49	1	3	1	0	0	8	56	36	10	39	36	15	1	28	49	22	0	100	5	37	58	0	16	83
	Kumçatı	14	36	43	3	3	1	0	3	14	49	34	4	23	44	29	2	15	46	37	0	100	3	29	68	5	23	72
	Milli-1	5	27	63	1	3	1	0	3	19	51	27	12	28	39	21	12	26	40	23	0	100	9	37	54	2	26	72
	Milli-2	7	35	54	0	3	1	0	0	5	56	39	5	41	38	16	1	25	50	24	0	100	3	34	63	0	10	90
	Divin	3	25	71	0	1	0	0	3	12	49	36	56	20	18	6	35	28	28	9	0	0	6	40	55	10	21	69
	Çağlayan	14	24	58	0	3	0	0	1	22	58	19	7	32	41	20	4	26	44	26	0	0	5	31	64	0	32	68
	Ispindoruk	21	20	53	0	5	1	0	6	35	49	11	9	37	38	16	8	28	43	21	0	0	6	35	59	7	40	53
	Seridahli-1	7	19	68	0	5	1	0	0	18	65	17	6	32	42	20	5	26	49	20	0	100	3	29	68	1	24	75
	Seridahli-2	11	23	60	0	4	2	0	3	29	52	17	6	29	44	22	5	23	47	25	0	0	5	30	64	4	34	63
	Hesana	19	21	54	0	5	1	0	5	32	51	12	9	37	39	15	7	28	44	21	0	0	6	35	59	4	35	60
	Nivekara	10	25	53	0	5	8	0	5	33	51	11	11	39	36	14	9	28	43	20	0	100	6	38	56	4	37	59
	Ortasu-1	4	23	70	0	3	1	28	37	26	8	2	41	40	18	2	24	35	35	7	0	0	5	40	55	37	35	28
	Ortasu-2	15	35	43	0	3	4	0	8	39	44	8	12	40	35	13	8	28	42	21	0	0	2	27	70	6	41	53
	Karatepe-1	6	23	60	0	8	3	0	13	53	31	3	24	42	29	5	16	32	38	13	0	0	14	43	42	7	37	56
	Karatepe-2	10	26	46	0	7	11	0	5	40	46	8	12	33	41	14	8	23	43	27	0	0	7	35	58	3	34	63
	Silip	9	28	60	1	3	1	0	2	18	53	26	6	22	42	31	2	17	46	36	0	100	0	28	72	12	53	35
	Rutkekurat	15	20	56	0	7	2	1	16	45	33	5	14	35	39	11	10	26	43	21	0	0	6	36	57	11	37	51
	Taşdelen	10	16	67	0	5	1	1	33	55	10	1	32	47	19	2	22	41	30	6	0	0	13	42	45	16	48	36
	Anılmış	7	24	57	0	9	3	0	19	53	26	2	25	45	26	4	20	35	34	11	0	0	15	44	41	9	44	47
	Herbiş	0	24	76	0	0	0	0	0	0	0	0	60	27	13	0	6	28	48	18	0	0	0	0	0	0	0	0
	Roboski	3	11	80	0	5	0	2	39	51	8	0	38	43	14	5	31	41	24	4	0	0	21	45	34	13	51	36
	Anıttepe	1	16	75	0	2	5	5	43	53	0	0	61	34	5	0	47	42	10	1	0	0	47	34	19	48	45	6
	Besta	0	7	90	0	2	0	0	24	76	0	0	46	37	11	7	44	39	15	2	0	0	26	39	35	0	0	0
Oil Seepages	Kerbent	2	23	53	20	2	0	0	0	0	58	42	0	12	39	49	0	6	43	51	31	69	0	0	100	0	0	0
	Zengen	0	0	0	100	0	0	0	0	0	0	0	0	0	0	0	0	0	0	0	37	63	0	0	0	0	0	0
	Eruh	6	20	54	19	0	0	0	0	0	43	57	5	25	44	26	2	24	46	29	35	65	0	0	0	0	0	0
	Kumçatı	11	38	43	8	0	0	0	3	19	49	30	3	23	40	34	2	13	44	41	0	100	0	0	0	0	0	0
	Silip	55	8	8	19	6	4	0	1	27	57	15	40	60	0	0	23	60	17	0	41	59	16	84	0	0	40	60
	Kayatepe	2	19	27	52	0	0	0	0	0	100	0	2	16	35	47	0	10	41	49	36	64	0	0	0	0	0	0
	Dadaş	28	28	40	0	0	4	0	11	48	31	9	8	35	35	23	4	28	48	21	0	0	0	0	0	0	39	61
	İşkar	12	30	13	41	3	1	0	1	19	35	44	8	27	36	29	9	27	39	25	34	66	0	38	62	0	34	66
	Yeşilli	3	29	28	40	0	0	0	0	0	38	62	1	16	44	39	1	7	36	56	58	42	0	0	0	0	0	0
	Bagas	2	2	3	93	0	0	0	0	0	38	62	0	21	20	59	0	10	45	45	37	63	0	0	0	0	0	0
	Tala	0	0	0	100	0	0	0	0	0	0	0	0	0	0	0	0	0	0	0	0	100	0	0	0	0	0	0
	Gerçüş	0	10	6	84	0	0	0	0	0	0	0	0	0	32	68	0	0	39	61	67	33	0	0	0	0	0	0
	Badzivan	0	0	0	100	0	0	0	0	0	0	0	0	0	0	0	0	0	0	0	42	58	0	0	0	0	0	0
Heavy Oils	Silvanka Sinan	19	10	60	8	2	1	2	15	40	32	12	20	28	31	20	28	43	23	6	45	55	17	36	46	15	40	45
	Raman	37	15	36	6	4	2	1	12	39	38	10	15	34	33	19	17	35	33	15	42	58	21	41	39	13	44	43
	Germık	53	14	20	4	4	5	3	13	38	35	11	10	27	38	24	16	32	34	18	38	62	17	40	43	7	22	71
	Çamurlu	43	15	26	9	3	4	0	4	30	46	19	8	24	40	28	9	28	38	25	47	53	13	38	49	2	15	83
	Güney Dinçer	31	16	43	4	4	2	0	4	36	47	12	11	34	37	19	13	31	36	20	45	55	20	40	40	6	43	51
	Batı Kozluca	29	18	41	7	3	1	0	3	36	47	14	6	22	30	42	10	30	38	21	49	51	18	36	46	5	36	59
	Batı Raman	26	16	42	11	4	1	0	4	26	46	23	11	30	36	23	14	28	36	21	44	56	11	41	48	5	38	56
	Mağrip	28	22	41	4	4	2	0	3	20	49	28	4	26	41	30	7	23	43	28	31	69	5	32	62	4	30	66
	Doğu Sınırtepe	37	15	39	4	3	1	1	10	31	42	16	8	30	38	24	9	27	41	23	45	55	12	40	48	8	45	48
	İkiztepe	32	16	42	6	3	1	1	7	28	44	20	8	30	39	24	8	27	41	24	55	45	10	38	52	5	41	54

M-: Methyl-;**DM-:** Dimethyl-; **TM-:** Trimethyl-; **TeM-:** Tertramethyl-; **Aro. ST:** Aromatic steroids **MA-:** Monoaromatic-; **TA-:** Triaromatic-.

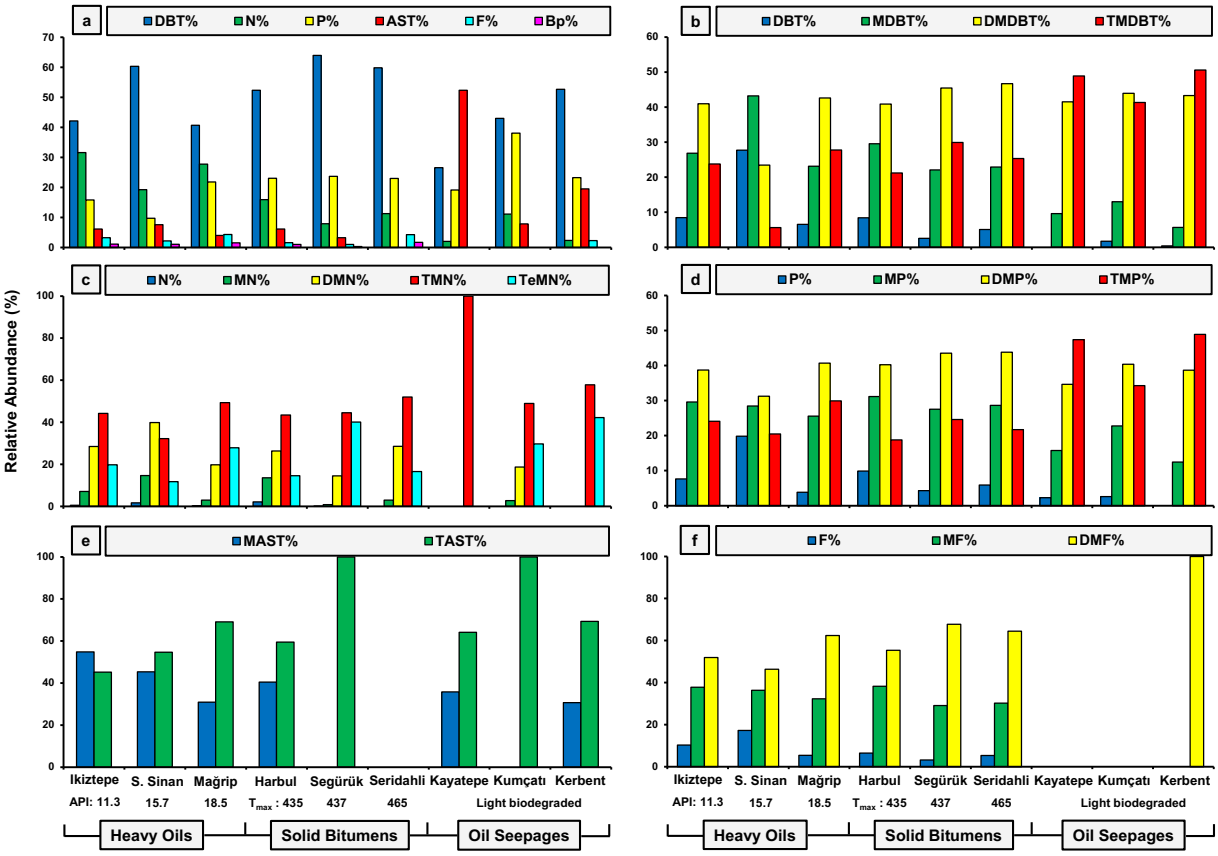

Fig 3.9. The relative abundances of aromatic hydrocarbon compounds in selected samples from each sample type of SE Turkey; **a)** All investigated aromatic compounds; **b)** Dibenzothiophenes; **c)** Naphthalenes; **d)** Phenanthrenes; **e)** Aromatic steroids; **f)** Fluorenes.

concentration increases with ongoing biodegradation. Although the Kayatepe seep is also a lightly biodegraded seep, it is significantly enriched in aromatic steroids. This might be attributed to a different source rather than alteration processes, consistent with its different *n*-alkane distribution noted above. In heavily biodegraded seeps such as Zengen or Badzivan, aromatic steroids are the only compounds preserved. Furthermore, in the Dadas seep aromatic steroids are absent which is most likely source-related, entirely in accordance with its different pattern of source-sensitive biomarkers (Tab 3.2 and Tab. 3.4).

Aromatic sulphur compounds, i.e. dibenzothiophene and its alkylated analogues are the most abundant constituents of aromatic hydrocarbon fractions in most of investigated samples (Tab. 3.4 and Fig. 3.9.a). A few exceptions are observed. Amongst heavy oils, the Germik and Çamurlu oils have the lowest amounts of dibenzothiophenes (20 and 26% respectively) and alkylnaphthalenes are the major components. Also the Silvanka Sinan oil is significantly enriched in dibenzothiophenes (60%). Among the solid bitumens there is only one sample, Üçkardeşler vein, which shows a different distribution and is enriched in phenanthrenes (51%) (Tab. 3.4). The distribution of alkylated derivatives of dibenzothiophenes in heavy oils changes in the order: DMDBT>MDBT>TMDBT>DBT, except for the Silvanka Sinan and Raman oils. While most of the solid bitumens, in particular less mature ones, display the same order as most of the heavy oils, there are some veins that display partly different distributions in the order: DMDBT>TMDBT>MDBT>DBT. Moreover, alkyldibenzothiophene distribution in high thermally-degraded veins is different and changes in favor of homologues with a lower number of methyl substituents.

Analogously to the alkyldibenzothiophenes, the alkylnaphthalenes and alkylphenanthrenes display similar distributions in heavy oils, low thermally-degraded solid bitumens as well as oil seeps with a low biodegradation level, though there are a few exceptions that are partially different. Interestingly, these exceptions are observed for the same samples that show differences regarding alkyldibenzothiophenes as mentioned above. It is noteworthy that the oil composition may considerably change after hydrocarbon generation due to a series of subsequent processes occurring during migration and/or within the reservoir (Thompson, 1987; Peters *et al*., 2005).

Aromatic steroids and non-fused diaromatic compounds i.e. fluorenes and biphenyls are found to be present in minor concentrations in heavy oils and solid bitumens, with 8 to 17% and zero to 18%, respectively. Also distribution of their alkylated counterparts is quite similar, suggesting a common source (Tab. 3.4 and Fig. 3.9.e-f). It should be noted that the aromatic steroids are below detection limit in high-thermally degraded solid bitumens and were identified in less mature solid bitumens only. In contrast, in seep oils their distributions do not change systematically. While aromatic steroids are present in all

seeps, except for the Dadaş seep, fluorenes and biphenyls are either present in low abundances or even completely absent. The presence of biphenyl, fluorene and their alkylated homologues in heavy oils and solid bitumens, even highly mature ones, and their absence in most oil seepage samples may indicate that they are more sensitive to biodegradation than thermal processes, unlike aromatic steroids. Although the aromatic compound distribution is initially controlled by the source and maturity of the organic matter (Zhang and Huang, 2005), alteration processes can significantly change it which is clearly discernible in overmature solid bitumens and highly biodegraded oil seepage samples (Volkman *et al*., 1984; Radke, 1987).

3.5.4.3. Compound-specific stable C isotope signatures of *n*-alkanes

Variations of the $\delta^{13}C$ values of individual *n*-alkanes (*n*-C_{14} to *n*-C_{34}) for selected samples of solid bitumens and heavy oils are shown in Figure 3.10. Oil seeps are excluded because their *n*-alkane abundance was too low for carbon isotope determination or mean values of triplicate measurements showed too high standard deviations. At first glance, it is evident that the *n*-alkanes in solid bitumens are more enriched in ^{13}C than the heavy oils. Solid bitumens fall within a wide range from -27 to -21‰ while that of heavy oils varies from -31 to -27‰. It is well-known that the carbon isotopic composition of hydrocarbons is initially controlled by the $\delta^{13}C$ value of source organic matter as well as the depositional setting (Schoell, 1984, Chung *et al*., 1992). Furthermore, various parameters are known to influence the isotopic fractionation during and after hydrocarbon generation e.g. thermal maturity (Rigby *et al*., 1981; Chung *et al*., 1992; Clayton and Bjorøy, 1994; Dawson *et al*., 2007), phase effects (Clayton, 1991), biodegradation as well as water washing (Stahl, 1980; Palmer, 1984; Sun *et al*., 2005; Vieth and Wilkes, 2006). It appears that the observed difference between the $\delta^{13}C$ values of the least mature solid bitumens and heavy oils can mainly be attributed to the phase effect. During the solidification processes, once-liquid petroleum undergoes a series of complex chemical and physical changes and loses its volatile constituents leading to a concomitant increase in molecular weight and decrease in H/C ratio (Bartle *et al*., 1981;

Curiale, 1986). Since molecular bonds formed by light isotopes (^{12}C) are weaker than bonds involving the heavy isotopes (^{13}C), the removal of isotopically light *n*-alkanes, during solidification is preferred, leaving the remaining saturated fraction isotopically heavier (Stahl, 1980; Clayton, 1991).

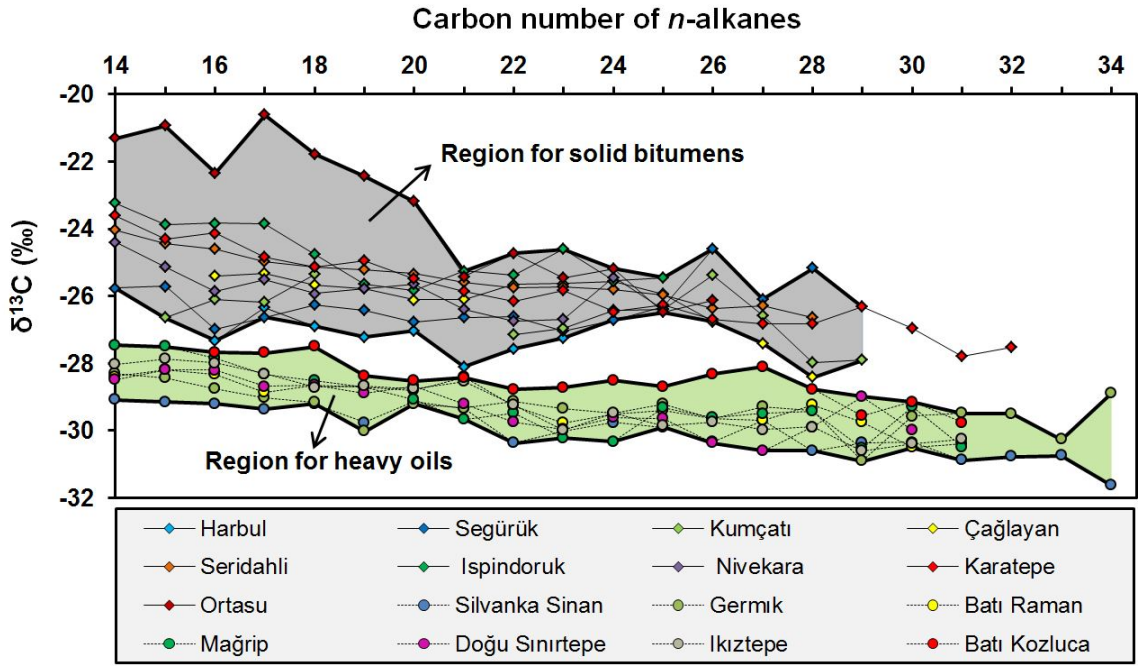

Fig. 3.10. Compound-specific $\delta^{13}C$ values of *n*-alkanes in heavy oils and solid bitumens of SE Turkey.

Studied heavy oils are, more or less, at the same maturation level as reflected by their API gravities (API gravity range: 11 to 18). Therefore, they are in the same range and no systematic variations are observed in the $\delta^{13}C$ values of the heavy oils. In contrast, variations of $\delta^{13}C$ values in solid bitumens are different and clearly controlled by their thermal degradation levels. While the less mature solid bitumens such as Harbul and Segürük, exhibit the lightest $\delta^{13}C$ values relative to other veins, the Ortasu bitumen, located in easternmost part of the investigated area, is significantly enriched in ^{13}C especially for the lower molecular weight *n*-alkanes (<*n*-C_{20}) (Fig. 3.10). Moreover, the average $\delta^{13}C$ values for *n*-C_{16} to *n*-C_{23} plotted versus the T_{max} values confirm that for the studied solid bitumens the main controlling factor is thermal maturity (Fig. 3.11).

Furthermore, in both heavy oils and solid bitumens the lower molecular weight *n*-alkanes (< *n*-C_{20}) are more enriched relative to the higher molecular weight components (> *n*-C_{20}). This is expected as the low molecular weight compounds become isotopically heavy earlier and more rapidly than the high molecular weight fractions (Fig. 3.10) (Clayton, 1991).

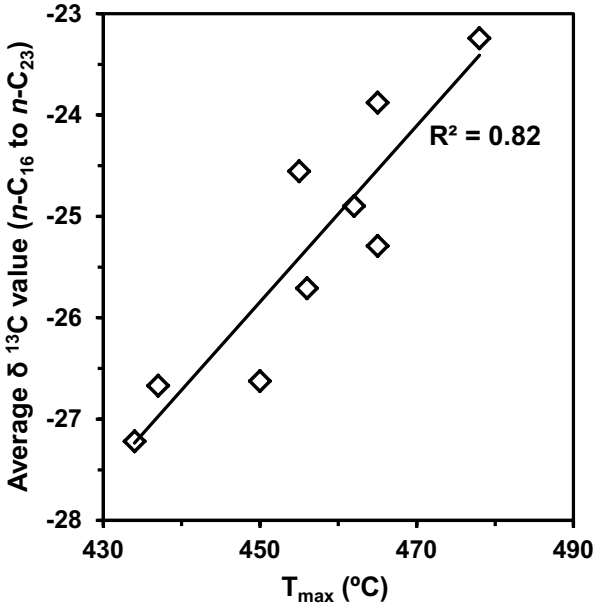

Fig. 3.11. Variation of average $\delta^{13}C$ values with maturation levels in Turkish solid bitumens.

3.6. Conclusions

A common source (algal marine carbonate) was established for all different hydrocarbon types in southeast Turkey, with two exceptions: The Dadaş and İşkar seeps appear to be derived from a clastic source and the Silvanka Sinan oil seems to have originated from a younger source. The heavy oils are undegraded, and variations of maturity-sensitive parameters correlate positively with API gravity. Solid bitumens are non- to weakly biodegraded and display levels of thermal degradation that are in accordance with the regional tectonic framework. While seep oils more or less show the

same maturation levels as heavy oils, they display various levels of biodegradation from "light" to "heavy". Thereafter, all heavy oils, less mature solid bitumens as well as less-biodegraded seep oils, originating from the same organofacies and also exhibiting similar levels of maturation, have been correlated using additional parameters. While the extended hopane distributions in heavy oils and oil seepage samples are quite similar, in solid bitumens they are quite different. They show relatively higher amounts of lower homologs (C_{31}-) relative to the higher ones (C_{33}- to C_{35}-) most likely due to thermal cracking of HMW homologues during and/or after solidification. This variation is also reflected in carbon isotopic signatures where the $\delta^{13}C$ values of individual *n*-alkanes in solid bitumens are more enriched than in heavy oils, possibly due to a "phase effect". Finally, the distribution of six series of aromatic hydrocarbons i.e. dibenzothiophenes, naphthalenes, phenanthrenes, aromatic steroids, biphenyls as well as fluorenes, and their alkylated derivatives in selected samples, again have been confirmed a genetic affinity. Based on our results it is clear that surface and subsurface hydrocarbon occurrences in the Batman-Mardin-Şırnak area of southeast Turkey are genetically related, thereby supplying new insights into the petroleum system in this part of the Zagros Basin.

3.7. Acknowledgement

We would like to thank the TKI Şırnak, especially Adil TUNÇ, Süleyman YARDIMCI, TP Batman, Ender TAPTIK, D.Ü. Enver AKIN for providing samples and MTA Yahya ÇIFTÇI for providing maps. We also would like to thank C. Karger, A. Kaminsky, F. Perssen, K. Günther and D. Noack for laboratory analyses at the GFZ.

4. ORGANIC SULPHUR COMPOUNDS – INSIGHTS INTO THEIR FORMATION USING ULTRA-HIGH RESOLUTION MASS SPECTROMETRY

This chapter is currently under review by co-authors and will be submitted afterwards: ***Hosseini, S. H.,*** *S. Poetz, B. Horsfield, H. Wilkes, M. N. Yalçın, and O. Kavak., (2018) The incorporation mechanism and thermal evolution of aromatic organosulphur compounds in heavy oils and solid bitumens from SE Turkey as revealed by ultra-high resolution APPI (+) FT-ICR MS.*

4.1. Abstract

Following our previous studies, the thermal evolution of organic sulphur compounds (OSC) in solid bitumens and heavy oils from SE Turkey are investigated using positive-ion atmospheric pressure photoionization coupled with Fourier transform ion cyclotron resonance mass spectrometry (APPI (+) FT-ICR MS). An additional focus was laid on the investigation of the incorporation mechanism and the timing of the sulphur incorporation. A suite of sulphur-rich samples including eight solid bitumens of different degradation levels from early mature (T_{max}: 433 ºC) to overmature (T_{max} > 500 ºC), as well as eight heavy oils (API gravity range: 11º to 19º) from proximal oilfields are assembled. These samples are known to be genetically related while their chemical composition is mainly governed by thermal maturity. Various bulk and molecular parameters such as the relatively low reservoirs temperature, a continual decrease in total sulphur and a concomitant increase in the aromatic hydrocarbons as well as the N_1 classes with ongoing maturation are suggesting that OSC have been incorporated into the source organic matter via bacterial sulphate reduction (BSR) mechanism at very early

diagenesis. Moreover, the existence of sulphur-rich heavy oils without any signs of biodegradation indicate that they have been yielded from kerogens with high organic sulphur content at early stage of generation arguing against a thermochemical sulphate reduction (TSR) mechanism which mainly occurs at relatively high temperatures. Furthermore, evolution of OSC in both petroleum types is quite sensitive to variations of thermal stress and OSC composition is clearly influenced by at least one of the thermally-induced reactions such as thermal cracking, cyclisation as well as aromatisation depending upon the petroleum phase and/or transformation levels. Most interestingly, there is an obvious reversal trend in high-thermally degraded solid bitumens (T_{max} > 470 ºC), most likely due to the re-incorporation of the active sulphur species released from thermally decomposing polymers by one of the many known high-temperature pathways. Finally the Venn Diagram analysis was employed for monitoring the thermal evolutionary pathways of OSC in both sample types and different maturation levels.

Keywords: Organic sulphur compounds, Solid bitumens, Heavy oils, Thermal evolution pathway, APPI (+) FT-ICR MS, SE Turkey.

4.2. Introduction

Southeastern Turkey is the most petroliferous region in the country and there are many oilfields, oil seepages and solid bitumen veins occurring in close proximity. In our previous studies on this region (Hosseini *et al*., 2017; Hosseini *et al*., 2018), the geochemical characteristics of these petroleum occurrences have been compared and documented in detail using various conventional and advanced geochemical tools. Thus, various source-sensitive parameters obtained from aliphatic and aromatic hydrocarbons as well as compound-specific stable carbon isotope signatures of *n*-alkanes indicated a strong genetic relationship between surficial solid bitumen veins and heavy oils from proximal oilfields. A marine carbonate unit, deposited under anoxic conditions, is inferred to be the source for both, entirely in accordance with other previous correlation studies in the region (e.g. Connan *et al*., 2006; Kavak, 2011; Kara-Gülbay and Korkmaz,

2012). Our results revealed that all the heavy oils and most of the solid bitumens did not experience microbial alteration, and that thermal maturation is the main factor controlling their chemical composition. Using FT-ICR MS in ESI-neg mode, it could be shown that at highest degradation levels (T_{max} >470 ºC) further condensation and aromatisation processes are not possible due to significant hydrogen deficiency (Hosseini *et al*., 2017).

According to various studies, petroleum in this region is sulphur-rich (e.g. Mueller *et al*., 1995; Nairn and Alsharhan, 1997; Kavak, 2011), though to the best of our knowledge no attempt has been made to address the question of sulphur origin in detail. Pyrolysis-gas chromatography results for solid bitumens and heavy oils have already revealed that the amounts of organosulphur compounds in resolved pyrolysates were relatively low in both cases, indicating that organosulphur compounds are not in a form that is labile and degradable by pyrolysis and substantially occur in refractory structures and condensed ring systems (Hosseini *et al*., 2018).

Organic sulphur compounds (OSC) is an important constituent in fossil fuels which has attracted much interest from organic geochemists (for a thorough review see; Sinninghe Damste and De Leeuw, 1990 and Werne *et al*., 2004). Organosulphur compounds constitute a significant fraction in petroleum from traces to more than 10 wt.%, but few commercially produced oils exceed 4% sulphur. Sulphur-rich oils are derived from carbonate or carbonate-evaporite sedimentary units whereas low-sulphur oils are derived largely from clastic ones (Tissot and Welte, 1984). OSC is present in low- to medium-molecular-weight molecules, but the largest fraction is in the high-molecular-weight components (e.g. Hunt, 1979; Tissot and Welte, 1984; Orr and White, 1990). Ho *et al*. (1974) have analyzed 79 crude oils having a range of sulphur contents from 0.05 to 7.82 % and classified them based on the distributions of sulphur-compound-types to the immature, altered and mature groups. This classification was consistent with geological data such as depth and age and with conventional bulk maturity parameter such as API gravity, %S, molecular-weight-distribution of *n*-alkanes, etc. For instance, the immature group had the highest sulphur content and contained the largest amount of nonthiophenic sulphur (the thermally labile type) and the most mature group was from deeper high-temperature reservoirs, contained less total sulphur but relatively more of the

thermally stable OSC such as dibenzothiophenes (Ho *et al*., 1974). A few years later, Radke and co-workers observed that the relative abundance and distribution of DBT and MDBT varied with increasing depth of burial in a well in a western Canada Basin containing Type III kerogen (Radke *et al*., 1982). The most suggestive maturity indication was shown as a decrease in the 4-MDBT/DBT ratio as a function of depth (Radke *et al*., 1982). Hughes (1984) reported that a characteristic distribution pattern of MDBT isomers was useful to identity oils derived from carbonate source rocks. These and many other investigations display the potential of organosulphur compounds for improving our understanding of geologic influences in determining variations in composition of petroleum fluids with relation to source and evolution history. However, seawater sulphate is known to be the ultimate source of organically bound sulphur in fossil fuels (Orr and Sinninghe Damsté, 1990). There are two major mechanisms by which organic sulphur is incorporated into kerogen: a) bacterial sulphate reduction (BSR) occurring mainly in near-surface sediments during very early diagenesis (<50 ºC) and b) thermochemical sulphate reduction (TSR) occurring in relatively hot evaporite reservoirs, through catagenesis to metagenesis (>100 ºC) (e.g. Vairavamurthy *et al*., 1995). Distinguishing these pathways is critically important. Also, it is noteworthy that the absence or presence of sulphate governs reaction pathways in high temperature petroleum reservoirs (Orr, 1974; Aizenshtat *et al*., 1995).

Since OSC in petroleum fluids is mainly present in complex macromolecules (Sinninghe Damste and De Leeuw, 1990), the ability of conventional geochemical tools such as gas chromatography-mass spectrometry (GC-MS) is limited when it comes to fully unravelling their compositional complexity, and also to elucidate the mechanism(s) of sulphur incorporation into organic matter. Recently, atmospheric pressure photoionization combined with Fourier Transform ion cyclotron resonance mass spectrometry (APPI FT-ICR MS) has been introduced to be well suited for characterisation of low polarity aromatic OSC in complex petroleum mixtures by providing molecular-level information about their composition (Purcell *et al*., 2006; Purcell *et al*., 2007). Using this approach, Walters and co-workers showed that chemical species that can give rise to TSR-solid bitumen are formed within oil and condensates

during the TSR process (Walters *et al*., 2011). In their comprehensive molecular study by combining two-dimensional gas chromatography and APPI FT-ICR MS they compared a suite of oils from lower Smackover carbonates that have experience varying degrees of thermal cracking and TSR-alteration and characterised the distribution of hydrocarbon and heteroatomic species (Walters *et al*., 2015).

Here, following our previous studies of southeastern Turkey, sulphur-containing compounds in solid bitumens and heavy oils are investigated using positive-ion APPI FT-ICR MS. In this regard, a special focus has been laid on the major forms of organosulphur compounds and the possible mechanism(s) involved in their incorporation into the investigated petroleum occurrences. Also, the thermal evolution of OSCs is discussed in both petroleum types.

4.3. Study Area and Sample Set

In our previous studies on this region the study area and complementary information about the samples have been documented in detail and interested readers are encouraged to refer to Hosseini *et al*. (2018) (see Chapter 3). Here, the required information is briefly provided.

Southeast Turkey is located in the northernmost extension of the Arabian Platform in an active collision zone and its tectonic history has been studied in detail (e. g. Yilmaz *et al*., 1993; Okay, 2008). During the Alpine orogeny southeast Turkey underwent two major episodes of deformation in the: 1) Late Cretaceous and 2) Middle Eocene-Late Miocene; the latter led to the collision between Eurasia and the Arabian plate (Yilmaz *et al*., 1993). Due to this main phase of deformation compressional folds developed; all the hydrocarbon accumulations so far discovered in this region are held in structural traps formed during this last phase of the Alpine movements (Ala and Moss, 1979). Noteworthy, it is shown that Turkish solid bitumen veins display a wide variety in character depending upon geographic location which is attributed to regional tectonic

history, as compressional pressure did not occur with the same intensity across the region and increases towards the collision zone (Hosseini *et al*., 2017).

Eight crude oils and eight solid bitumen samples from southeastern Turkey were made available for the work. The name of oilfields and solid bitumen veins are given in Table 4.1. Their geographic locations as well as the stratigraphic column of southeastern Turkey displaying the reservoir formations for selected oils and host rocks for solid bitumen veins are displayed in Figure 3.1. All selected oils are heavy, showing a narrow range of the API gravity (11 to 19º) and reservoired in fractured carbonate units. Solid bitumens are the main surficial petroleum occurrences in the region and all selected veins are located in the Şırnak province of southeast Turkey and distributed in sedimentary units of different ages from Jurassic to Eocene.

4.4. Analytical Program

Solid bitumen samples were pulverized and finely ground by a vibratory disc mill, and then extracted using dichloromethane:methanol 99:1 (v:v) at 40 ºC for 1 day in a Soxhlet apparatus. Thereafter, the analysis procedure is the same for both heavy oils and crude extracts of solid bitumens and required no liquid chromatographic preparative fractionation.

4.4.1. APPI (+)-FT-ICR MS

All analyses were conducted on a 12 Tesla FT-ICR mass spectrometer equipped with an APPI ion source from Bruker Daltonik GmbH. Nitrogen was used as drying gas at a flow rate of 3 L/min and a temperature of 210 °C and as nebulizing gas with 2.3 bar. About 20 µg/ml of the sample was diluted with methanol:*n*-hexane 9:1(v:v), and then the solution was injected into the APPI source. In the APPI source, the solvent flow rate was 20 µL/h. For each mass spectrum, 200 scans were accumulated in a mass range from *m/z* 147 to 1200. The Burker Data Analysis software was used for internal calibration and

also creating a mass peak list with signal-to-noise (S/N) above 12. Elemental formulae were assigned to the recalibrated *m/z* values with a maximal error of 0.5 ppm allowing up to 100 C, 200 H, 10 O, 4 N, and 4 S atoms.

4.5. Results and Discussion

Our previous studies using FT-ICR-MS with electrospray ionization in negative-ion mode and GC-MS and GC-IRMS revealed that solid bitumen and heavy oil samples in our sample set most likely come from the same source. Furthermore, changes in the distribution and concentration of aliphatic and aromatic hydrocarbons as well as acidic NSO compounds (e.g. carbazole-type compounds) are mainly controlled by thermal maturity (Hosseini *et al*., 2017; Hosseini *et al*., 2018). In the following, aromatic compounds in the Turkish solid bitumen and heavy crude oil samples are investigated using APPI-(+) FT-ICR-MS focusing on the characterisation of organosulphur compounds and their evolution with thermal maturation. The possible mechanism(s) by which sulphur has been incorporated into the petroleum fluids is addressed as well.

4.5.1. Elemental class distributions

APPI (+) broadband mass spectra of three selected samples of each petroleum type representing the whole assigned maturity range in terms of API Gravity and T_{max} value are displayed in Figure 4.1. Signal patterns in the mass spectra of the heavy oils do not reflect maturity related changes. Specifically the number of assigned monoisotopic (i.e. containing only the most abundant isotope of each atom) signals, the weight-average (M_w) and number-average (M_n) molecular weights shows no systematic variation. The mass spectra of the solid bitumen extracts shown in the same figure exhibit strong pattern differences which reflect the wide range of maturity covering early mature (Üçkardeşler vein: T_{max}: 433 ºC) to overmature (Roboski vein: T_{max} > 470 ºC). The number of assigned monoisotopic signals, M_w and M_n systematically decrease with ongoing maturation (Fig. 4.1).

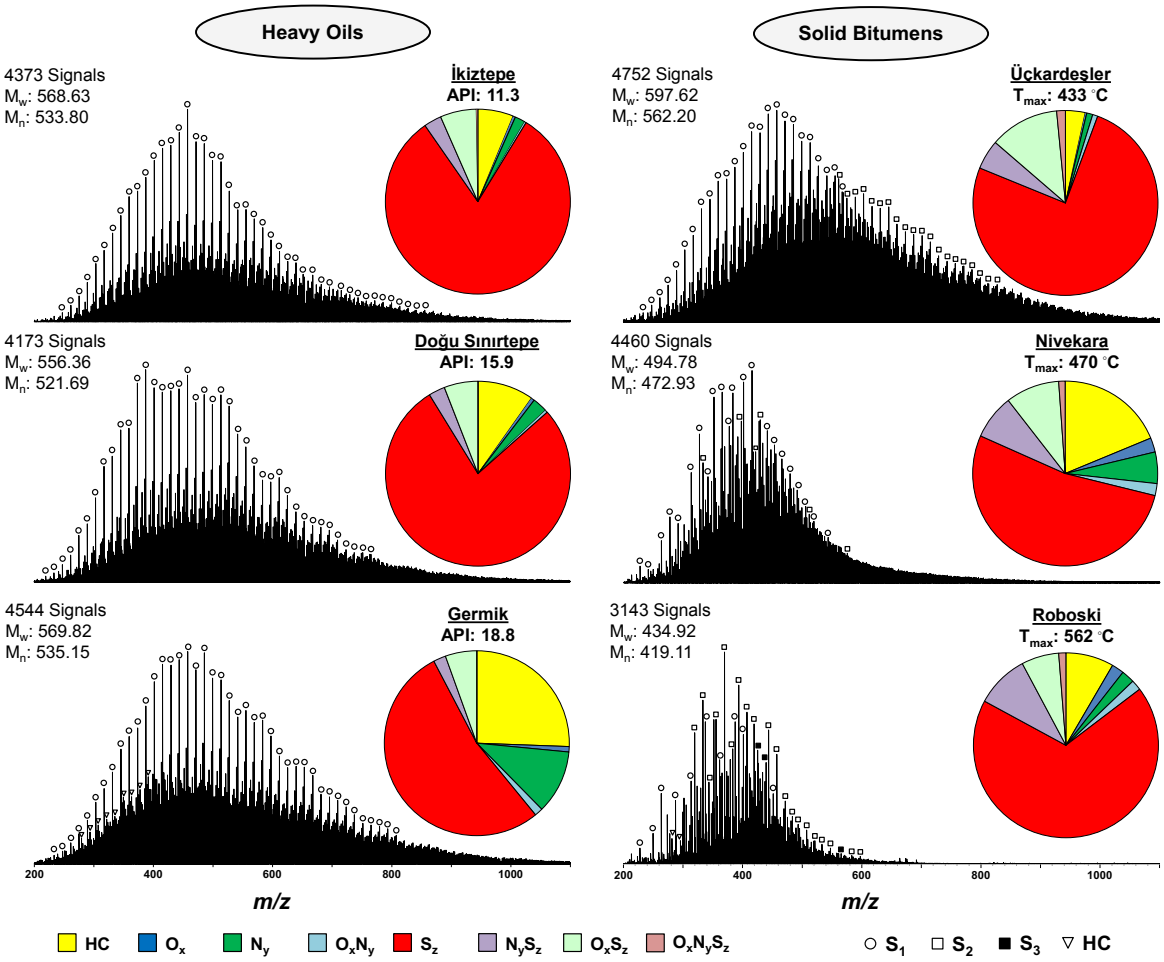

Fig. 4.1. Broadband positive-ion APPI FT-ICR mass spectra of selected samples of different maturation levels from heavy oils and solid bitumens as indicated by API gravities and T_{max} values, respectively. The embedded pie diagrams display the elemental class distribution.

The elemental class distributions, shown as pie charts, revealed that sulphur only (S_z) compounds are predominant in both sample types. In heavy crude oils, the relative abundance of the S_z class decreases systematically with increasing API gravities from 82 to 53%, whereas in solid bitumens S_z class abundance decreases from 76% in the low mature Üçkardeşler vein to 53% in the Nivekara vein (T_{max}: 470 ºC) and then rises again to 68% TMIA in the overmature Roboski vein sample. The relative abundance evolution

of condensed aromatic hydrocarbons (HC) and nitrogen only (N_y) classes are quite similar. In heavy oils, they increase with increasing API gravities from 6 to 26% and from 2 to 11%, respectively. In solid bitumens, firstly both the HC and N_y classes are relatively enriched from 3 to 19 and from 1 to 8% TMIA, respectively, followed by a relative depletion in late stages of maturity from 19 to 8% (HC) and from 8 to 2% TMIA (N_y), respectively. Other abundant components are oxygen and sulphur (O_xS_z) and nitrogen and sulphur (N_yS_z) elemental classes. In heavy oils, the relative intensity of both classes slightly decreases with increasing API gravity from 7 to 5% and from 3 to 2% TMIA, respectively. In solid bitumens, the relative abundance of the O_xS_z class decreases from 15% (Harbul vein) to 7% (Roboski vein) TMIA, whereas the N_yS_z class rises from 5% to 9% TMIA.

Elemental ratios for heavy oils and solid bitumens have been calculated from the positive-ion APPI FT-ICR mass spectral peak magnitudes given in Table 4.1. It is evident that the sulphur content in both petroleum types is quite high, from 5 to ~9%, forming the main heteroatom in the detected polar compounds, followed by oxygen and nitrogen. Despite the fact that the negative-ion ESI mode is insensitive to thiophenic sulphur compounds, the relative abundances of S atoms in combination with pyrrolic nitrogen are still significantly high, at 1.9 to 5.4 % (Tab. 4.1). Also, it should be taken

Tab. 4.1. Elemental composition and ratios of whole oils and crude extracts of solid bitumens, obtained from APPI (+) and ESI (-) FT-ICR MS.

	Sample info.	API	Res. Temp. (°C)	APPI (+), wt. %								ESI (-), wt. %				
				C	H	N	O	S	H/C	S_{org}/C	S_{org}/N	C	H	N	O	S
Heavy Oils	İkiztepe	11.3	46	80.7	9.7	0.5	0.8	8.3	0.12	0.10	17	-	-	-	-	-
	B. Kozluca	12.6	56	80.6	9.9	0.5	0.7	8.3	0.12	0.10	17	-	-	-	-	-
	B. Raman	13.0	66	81.1	10.0	0.5	0.8	7.7	0.12	0.09	15	-	-	-	-	-
	G. Dinçer	15.7	63	81.4	9.8	0.5	0.7	7.7	0.12	0.09	15	83.5	8.4	2.4	2.1	3.6
	D. Sınırtepe	15.9	50	81.7	9.7	0.5	0.8	7.3	0.12	0.09	15	-	-	-	-	-
	Raman	18.0	60	82.2	10.0	0.6	0.7	6.6	0.12	0.08	11	83.5	8.8	2.1	2.5	3.1
	Mağrip	18.5	88	82.4	9.8	0.8	1.3	5.6	0.12	0.07	7	-	-	-	-	-
	Germik	18.8	71	83.5	10.1	0.7	0.7	5.1	0.12	0.06	7	85.0	8.6	2.4	2.1	1.9
		T_{max} (°C)														
Solid Bitumens	Üçkardeşler	433		80.4	9.2	0.7	1.1	8.5	0.11	0.11	12	79.6	7.6	3.8	3.6	5.4
	Harbul	434		80.5	9.3	0.6	1.0	8.7	0.12	0.11	15	80.3	7.8	3.0	3.7	5.2
	Segürük	437		81.2	8.8	1.0	1.1	7.9	0.11	0.10	8	82.3	7.6	3.4	2.9	3.8
	Avgamasya	450		84.2	8.2	1.1	1.3	5.2	0.10	0.06	5	84.3	6.5	3.9	1.8	3.5
	Milli	453		83.6	8.5	1.2	1.7	5.0	0.10	0.06	4	79.9	8.2	1.7	7.6	2.6
	Nivekara	470		84.1	8.3	0.9	1.3	5.4	0.10	0.06	6	-	-	-	-	-
	Anılmış	519		84.2	6.9	0.8	1.5	6.7	0.08	0.08	8	-	-	-	-	-
	Roboski	562		83.5	6.0	1.0	2.4	7.2	0.07	0.09	7	77.1	6.6	1.8	11.8	2.7

into account that the APPI mode, is extensively insensitive to saturated components and therefore the reported abundances are relative quantifications (Walters *et al*., 2015) and belongs only to those fractions that are ionisable by the chosen ionisation mode. However, since the effect of composition on the response factor for APPI is considered to be much less significant than in other ionisation methods e.g. ESI, the overall ion count is believed to approximately proportional to actual abundance (Walters *et al*., 2015). Also the calculated elemental ratios are provided in Table 4.1 and will be discussed later in this report.

4.5.2. Sulphur-containing compound classes

The relative abundances of all major compound classes in the heavy oils and crude solid bitumen extracts are listed in Table 4.2. The variation in abundances of each S-containing compound class normalized to the sum of all sulphur-containing compound classes with ongoing maturation for both sample types is illustrated using two bar charts in Figure. 4.2. It is evident that the APPI-ionisable aromatic fractions of all samples are very rich in organic sulphur compounds and their relative abundances are quite sensitive to even very small thermal maturity variations. For instance, small differences in API gravities of the İkiztepe and Batı Kozluca heavy oils (1.3° API), and in T_{max} between the Harbul and Segürük solid bitumen veins (3 ºC) are clearly reflected by relative abundance changes in the S-containing compound classes (Fig. 4.2). In summary, total monoisotopic ion abundances of all S-containing compounds in the APPI-(+)-sensitive portion of heavy oils and solid bitumens decrease systematically from 91% to 61% in the immature to peak mature window. These thermally-induced variations are attributed to the dilution by further generation of non-sulphur compounds as well as by removal of sulphur most likely in part as H_2S and partly by retention in insoluble residue (pyrobitumen) formed by disproportionation of NSO compounds (Orr and Sinninghe Damsté, 1990). However, the peak to overmature solid bitumens show a subsequent relative enrichment of summed sulphur containing compounds from 67 to 83%. This reversal is most likely due to the reactions occurring during the highest transformation

Tab. 4.2. Total monoisotopic ion abundances of the major chemical species in heavy oils and solid bitumens of SE Turkey, detected by APPI-(+) FT-ICR MS.

	Sample info.	S_1	S_2	S_3	HC	S_1O_1	S_2O_1	N_1S_1	N_1	N_1S_2	S_4	O_1	N_1O_1	O_4
Heavy Oils	İkiztepe	46.1	27.1	7.7	6.2	3.7	2.6	2.3	1.8	0.7	0.6	0.3	0.2	0.1
	B. Kozluca	46.2	27.0	7.6	5.7	4.3	3.0	2.5	1.9	0.7	0.3	0.1	0.1	0.2
	B. Raman	48.0	24.6	6.3	6.6	5.0	2.8	2.0	2.9	0.4	0.2	0.7	0.2	0.1
	G. Dinçer	49.3	24.6	6.0	7.7	4.2	2.2	2.5	2.1	0.5	0.2	0.2	0.2	0.3
	D. Sınırtepe	49.7	22.9	5.2	9.8	4.0	1.8	2.4	2.6	0.4	0.1	0.4	0.2	0.1
	Raman	51.3	20.5	4.0	10.1	4.3	1.3	2.6	4.2	0.3	0.0	0.5	0.4	0.3
	Mağrip	47.5	14.7	2.5	18.3	4.7	0.9	2.1	4.7	0.2	0.0	1.0	0.5	0.1
	Germik	39.7	11.9	1.7	25.6	4.6	0.9	2.2	11.1	0.0	0.0	0.6	1.4	0.3
Solid Bitumens	Üçkardeşler	33.6	29.5	10.9	3.4	6.5	5.6	3.1	1.1	2.1	1.4	0.0	0.3	0.2
	Harbul	32.7	27.7	11.0	4.1	8.3	6.2	2.9	1.0	2.5	1.6	0.1	0.4	0.3
	Segürük	33.2	27.3	9.9	4.9	6.2	3.4	5.7	2.9	3.0	0.8	0.1	0.9	0.3
	Avgamasya	33.4	16.8	2.7	15.0	6.5	1.6	7.1	6.6	2.3	0.0	1.3	3.4	0.3
	Milli	35.1	15.4	2.1	17.3	5.5	1.1	6.4	7.3	1.5	0.0	1.2	3.1	0.1
	Nivekara	33.5	16.8	2.5	18.8	7.9	1.5	6.1	5.4	1.7	0.0	2.1	2.1	0.2
	Anılmış	34.1	24.2	4.8	12.3	5.8	2.4	5.3	2.6	2.4	0.1	2.1	1.1	0.3
	Roboski	32.3	29.0	6.7	8.4	3.5	2.3	6.1	2.2	3.1	0.2	1.0	1.1	0.8

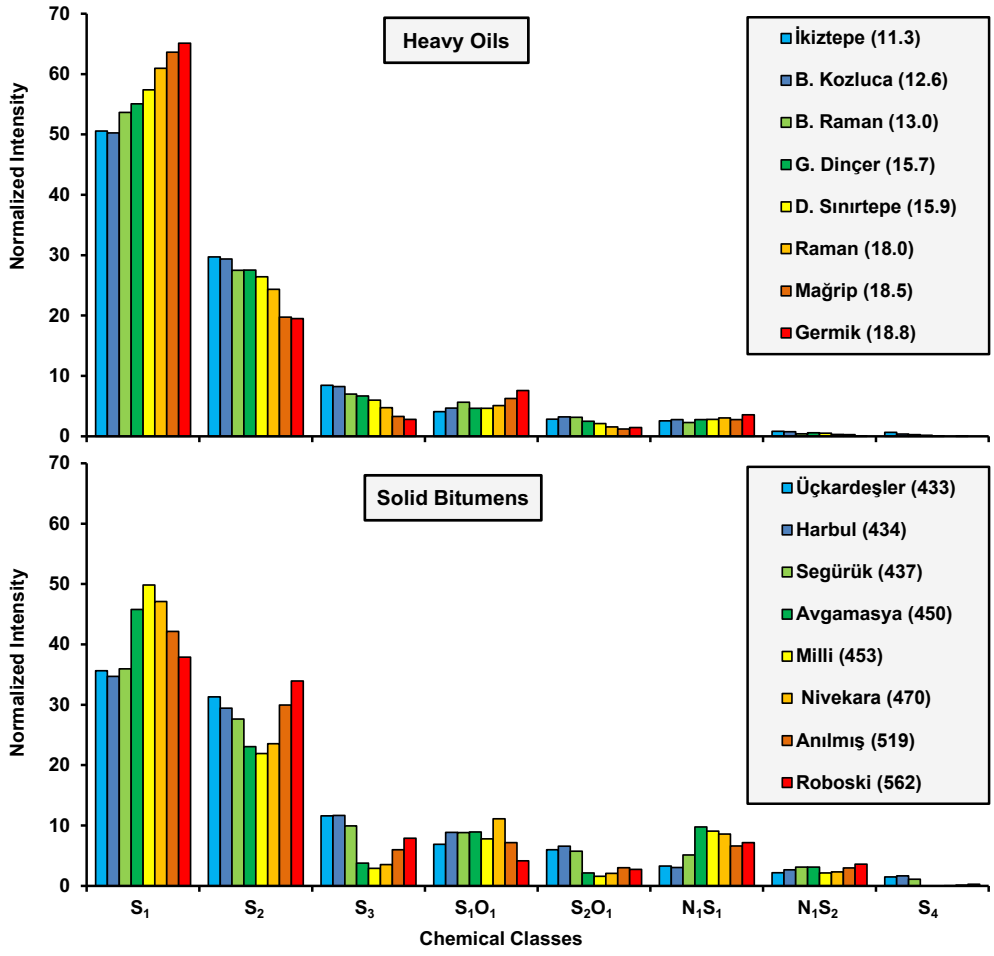

Fig. 4.2. Distribution of the major S-containing compound classes normalized to the sum of all S-containing compounds and their variations as a function of maturity in heavy oils and solid bitumens from SE Turkey.

levels, as discussed later in this paper. Looking at the individual sulphur-compound classes, a relative increase of those with one sulphur atom (S_1, S_1O_1, N_1S_1) and a relative decrease of those with more sulphur atoms (S_2, S_3, S_2O_1) in low to peak mature samples is observed. In late to overmature samples, compounds with one sulphur atom are again relatively depleted and those with more than one sulphur atom are relatively enriched.

4.5.3. Incorporation mechanism of organic sulphur

The organic sulphur in petroleum is always derived by reduction of inorganic sulphate. In general, there are two major mechanisms by which sulphur is incorporated into organic matter: BSR and TSR. While BSR occurs in low temperature regimes (60 - 80 °C) and needs small polar compounds like acids as electron acceptors for reduction, TSR is restricted to high temperatures (100 - 140 °C) and needs aliphatic compounds from the gasoline range for reduction. There are two main possible scenarios for BSR in a petroleum system: The first option is during early diagenesis in the source rock at low temperatures where the organic matter is immature to early mature. Sulphate is bacterially reduced to H_2S and elemental sulphur which both are then incorporated into (immature) macromolecules in the kerogen and asphaltene fractions, resulting in its becoming sulphur-rich; during early catagenesis sulphur-rich oils are generated from these precursors (di Primio and Horsfield, 1996). The second option would be a reservoired low sulphur petroleum, generated by a clastic source rock, that has been uplifted. At temperatures <80 °C, and as long as the reservoir has not be pasteurised (Wilhelms *et al*., 2001), biodegradation takes places including BSR resulting in sulphur incorporation into more mature compounds. TSR occurs in reservoirs at elevated depth and temperatures and becomes important only in the catagenesis zone where kerogen is in the late stages of oil generation and oil is cracking to gas (Vairavamurthy *et al*., 1995). TSR is promoted by H_2S. Consequently, oils in reservoirs that received a charge of migrated H_2S from a deeper reservoir can exhibit a higher extent of TSR alteration than expected from locally initiated TSR. Therefore, oils in low temperature reservoirs can contain compounds indicative of advanced TSR alteration while preserving sulphide

species that are less thermally stable (Walters *et al*., 2015). TSR produces sulphur-rich oils or condensates and solid bitumen. The oils or condensates have characteristically high amounts of thiadiamondoids (Wei *et al*., 2012). Using APPI and ESI FT-ICR MS analysis, they have been shown to be enriched in sulphur- and oxygen-containing compounds, with oxygen numbers up to 8 (Walters *et al*., 2015). According to our results it appears that the first pathway, bacterial sulphate reduction, is the main mechanism for incorporation of sulphur into the investigated petroleum samples. First of all, the present day temperature of the reservoirs hosting the heavy oils (Tab. 4.1) are clearly below the specified threshold for TSR mechanism (>100 ºC), but all studied oils are non-biodegraded (Hosseini *et al*., 2018) and heavy. This may indicate that they were produced from kerogens with high organic sulphur content, as they are believed to yield sulphur-rich heavy oils at early stage of generation due to relative weakness of S-S and C-S bonds compared to C-C bridges (Sinninghe Damsté *et al*., 1989; Werne *et al*., 2004). Moreover, in TSR altered oils total sulphur content remains at the same level with ongoing maturation because of competing sulphurisation and desulphurisation processes in the presence of sulphate, whereas a continual decrease in total sulphur in the investigated heavy oils and early to high mature solid bitumens (T_{max} range: 433 to 470 ºC) follows a different course resulting in the absence of sulphate (Orr, 1974; Orr and Sinninghe Damsté, 1990; Aizenshtat *et al*., 1995).

TSR altered oils and condensates are chemically distinct from unaltered ones, using ultrahigh resolution approaches such as APPI FT-ICR MS and it is possible to characterize the involved mechanism(s) by which sulphur is introduced into the organic matter (e.g. Kelemen *et al*., 2008; Kelemen *et al*., 2010; Walters *et al*., 2011). For instance, the relative abundance of aromatic hydrocarbons shows divergent trends for unaltered and TSR-altered oils (Walters *et al*., 2015). In our sample set, the relative concentration of aromatic hydrocarbons increase with maturation in both petroleum types except for overmature bitumens (T_{max} > 470 ºC), well in accordance with the previously reported trend for TSR-unaltered petroleum fluids (Tab. 4.2 and Fig. 4.1) (Walters *et al*., 2011; Walters *et al*., 2015). To our knowledge, solid bitumen samples have not been

investigated with APPI FT-ICR MS before in general but we would expect to find comparable compositional differences as observed for the crude oils.

The double bond equivalent (DBE) as a measure for the degree of aromatisation as well as cyclisation is defined by the number of double bonds and rings in a molecule. The color-coded carbon number versus DBE plots of the S_1, S_2 and S_3 compound classes for the selected samples of different maturation levels are displayed in Figure 4.3. The carbon number distribution of these species like other major components clearly shows a decrease in the degree of alkylation over a broad range of maturity. Also, the DBE value is shifted to higher values with maturation, entirely consistent with the variations of oils unaffected by TSR during maturation (Walters *et al*., 2015). In addition, it has been documented that concentration and distribution of the N_1 classes, measured by ESI (-) and APPI (+) modes, is influenced by TSR and thermal reactions in a different way. While in different types of unaltered petroleum occurrences i.e. crude oils, source rocks as well as solid bitumens, the relative abundance of the N_1 class increases with maturation, it shows a clear decrease with increasing TSR alteration (Walters *et al*., 2011; Oldenburg *et al*., 2014; Poetz *et al*., 2014; Walters *et al*., 2015; Hosseini *et al*., 2017). In the studied heavy oils and solid bitumens, again with the exception of the overmature bitumens, the relative abundance of the N_1 class climbs with increasing maturity, neglecting a TSR related mechanism for introducing organic sulphur into the investigated samples (Tab. 4.2 and pie charts in Fig. 4.1), and entirely consistent with the observed drop in the S_{org}/N ratios in Tab. 4.1 (Orr, 1974; Thompson, 1994).

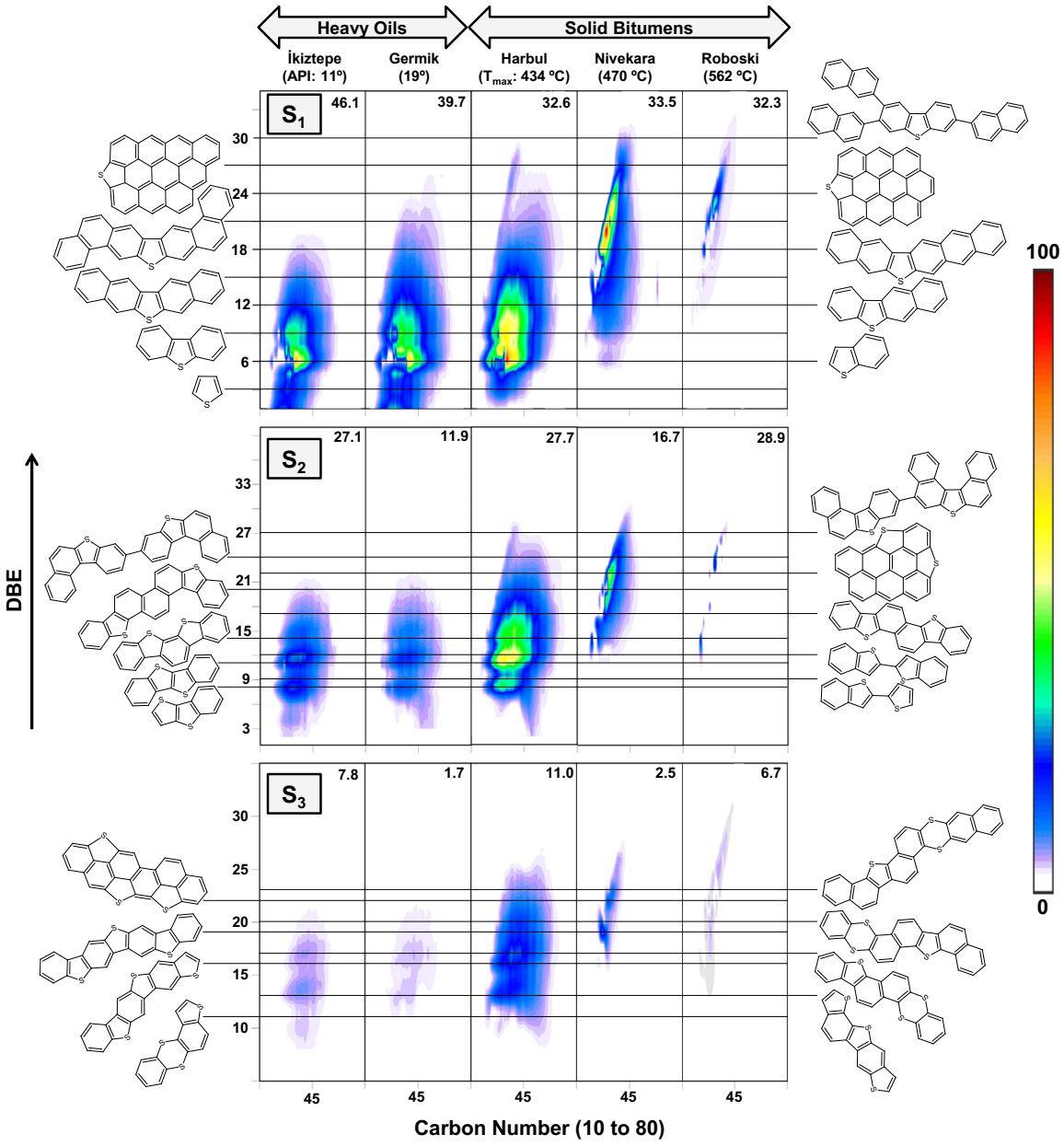

Fig. 4.3. Distribution of carbon number against DBE for the S_1, S_2 and S_3 compound classes measured by APPI(+)-FT-ICR MS. These plots are colour coded by their relative abundance normalized to the highest abundance measured for each sample. There is a scale change in the DBE axis for each compound class. Value in upper right corner of plots is the relative intensity of each compound class relative to total monoisotopic ion abundances (Tab. 4.2). Plausible core structures for selected DBE classes are provided as well.

4.5.4. Evolution of organic sulphur compounds

It is generally known that, in the absence of TSR, the occurrence of organically-bound sulphur is primarily dependent upon the source kerogen which is determined by environmental conditions; and secondarily is controlled by the maturity level (e.g. Ho *et al*., 1974; Hughes, 1984; Sinninghe Damste and De Leeuw, 1990; di Primio and Horsfield, 1996). Since, on the one hand, the investigated petroleums originated from the same or a similar source, as already documented in detail by the authors (Hosseini *et al*., 2018) and, on the other hand, they are different in phase i.e. liquid and solid, as well as in maturation level; they make an ideal natural laboratory in order to scrutinize the phase effect as well as thermal processes on the evolution of organic sulphur compounds.

4.5.4.1. Sulphur-containing compound classes

Considering only S-containing compounds (excluding the HC, N_y and O_x elemental classes), in all samples and at all maturation levels, the S_1 compound class is the most abundant organosulphur component followed by the S_2 class (Fig. 4.2). Interestingly, the distribution pattern of aromatic S-containing species is exactly the same in both low API gravity oils (API range: 11 to 13) and crude extracts from least mature solid bitumens (T_{max} range: 433 to 437 ºC), with $S_1 > S_2 > S_3 > S_1O_1 > S_2O_1 > N_1S_1 > N_1S_2 > S_4$. The observed similarity in distribution of OSCs strongly implies the same thermal evolutionary pathways in two different phases and we believe it has the potential to be considered in correlation studies; though more case studies need to be considered to support and develop the idea. Furthermore, with ongoing maturation the observed variations in the relative abundances of OSCs are comparable in different sample types. For example, in both of them the relative concentration of the S_3 class decreases. Simultaneously, the relative abundances of nitrogen and sulphur- as well as oxygen and sulphur-containing compounds are increased because of sulphur incorporation into N_1 and O_1 compounds (Fig. 4.2).

4.5.4.2. Aromaticity of sulphur-containing compounds

Hydrogen plays an important role during the maturation of sedimentary organic matter. This applies to organosulphur compounds during thermally induced cracking, cyclisation as well as aromatisation (Poetz *et al*., 2014). The DBE parameter also can be used as a convenient measure for the hydrogen saturation of a molecule. For example, the DBE class of a fully hydrogenated molecule is zero and every additional ring or double bond reduces the number of hydrogen atoms by two. The DBE distributions of the major sulphur-containing compound classes (S_1, S_2, S_3, S_1O_1 and N_1S_1) for both heavy oils and solid bitumens are shown in Figure 4.4. In heavy oils, by the stepwise increase in API gravity, those components with higher amounts of sulphur atoms are influenced by thermal processes. While the total DBE values of the S_1 as well as S_1O_1 classes remain constant, in the S_2 to S_4 classes they gradually decrease with advancing maturation. Also, the total DBE values in the N_1S_1 class in heavy oils is slightly shifted to higher DBEs. In mildly thermally degraded solid bitumens, the variation of DBE values of different compound classes resemble heavy oils, whereas at more advanced levels of maturity they are either significantly decreased (S_1 and S_1O_1) or depleted (S_2, S_3, S_4 and N_1S_1) in lower DBEs and shifted towards higher DBE classes (Fig. 4.4). These observations are pointing to an elevated degree of condensation and aromatisation of the organosulphur compounds with increasing maturity, entirely consistent with the observed decreases in the atomic H/C ratios (Tab. 4.1), Hydrogen Index values as well as their solvent extractability (Hosseini *et al*., 2017).

4.5.4.3. Modified van Krevelen diagrams

The variations mentioned above can be visualized by the modified van Krevelen diagram proposed by Kim *et al*. (2003). In Figure 4.5, the colour coded van Krevelen plots are shown for the major sulphur-containing compound classes i.e. the $S_{1\text{-}4}$, S_1O_1 and N_1S_1, in selected samples of different maturity from both sample types. Variations of hydrogen and sulphur content relative to C in the monoisotopic assigned peaks of selected classes are plotted as ratios S/C (abscissa) and H/C (ordinate) and their relative

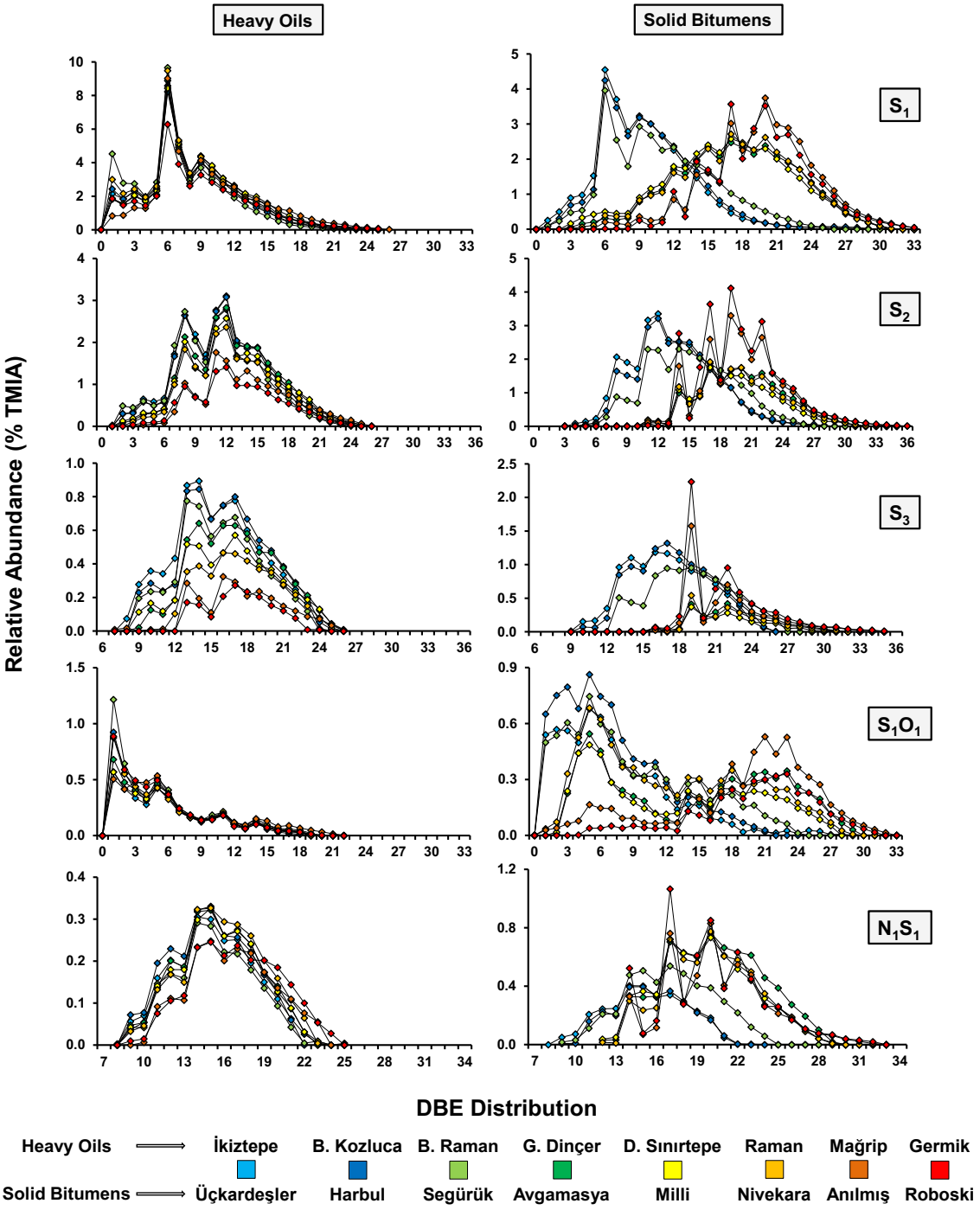

Fig. 4.4. DBE distribution of the S_1, S_2, S_3, S_1O_1 and N_1S_1 compound classes in heavy oils and solid bitumens from SE Turkey.

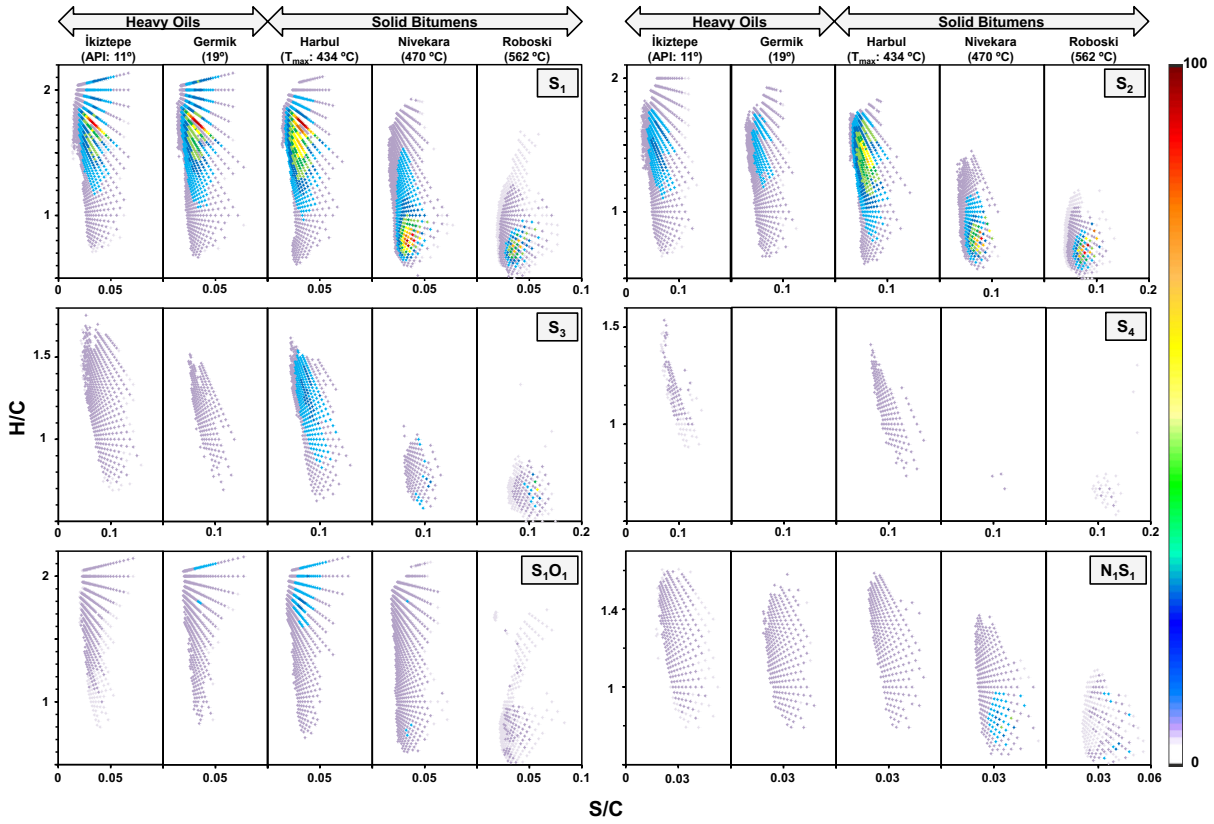

Fig. 4.5. The 3D Van-Krevelen plots for elemental data obtained from the positive-ion APPI FT-ICR MS for the major S-containing compounds of heavy oils and solid bitumens from SE Turkey.

intensity is reflected by the color-code. Conventional van Krevelen diagrams use the O/C ratio which can be replaced by S/C or N/C ratios depending on the sample types as well as the employed ionisation mode. As the number of sulphur atoms in each plot is constant, variations in the S/C ratio are attributed to the number of C atoms in the elemental composition.

Values of the *y*-axis (H/C ratio) are indicative of the degree of saturation as well as aromaticity. In both sample types, the aromaticity is increased with ongoing maturation due to lower atomic H/C ratios. Selected heavy oils are displaying the lowest (11) and highest (19) API gravities in our sample set. While the variation of aromaticity in the S_1,

S_1O_1 as well as N_1S_1 classes appears to be similar in both oils, it is more discernible in other classes by more than one sulphur atom i.e. the S_2, S_3 and S_4 species. In this regard, monitoring the S_4 class distribution in both sample types is of interest, and can be used to understand how the evolutionary pathway of the OSC changes at highest maturation levels. As it shown in Table 4.2 and graphically displayed in Figure 4.5, the S_4 class is only abundant in the lower API gravities (API < 18) and depleted in higher ones (API > 18), most likely due to thermal cracking. Similarly, the S_4 class is represented well in the low mature solid bitumens and becomes depleted with increasing thermal stress. Such behavior is expected, in accordance with the observed trends for different compound classes in the previous studies on both source rocks as well as crude oils (e.g. Oldenburg *et al*., 2014; Poetz *et al*., 2014; Walters *et al*., 2015). Surprisingly, at the highest maturation levels (T_{max} > 470 ºC) the S_4 class appears again and its relative concentration increases progressively with ongoing maturation. Also, the same increasing trend is observed for the S_2 and S_3 classes. Simultaneously, it is reversed in the monosulphur compounds (S_1) and their relative intensity is decreased at high maturation levels (Tab. 4.2, Fig. 4.2). The unusual observed trends at higher maturation levels is most likely attributed to reincorporation of the active sulphur species released from thermally decomposing polymers as described by Aizenshtat *et al*. (1995). While O, N and C atoms which are released as relatively non-active LMW compounds (e.g. CO_2 , H_2O, NH_3 , CH_4), S is released as highly active species in cross-linking reactions; thus, it is very likely that these species will be reincorporated into the organic matter by one of the many known high-temperature pathways (Aizenshtat *et al*., 1995; Yen and Chilingarian, 2000). This is entirely consistent with ESI (-) results on these samples where the intensity of the N_1 class is decreased due to neoformation of the N_1S_1 and N_1S_2 compounds at high maturation levels (Hosseini *et al*., 2017).

4.5.4.4. Alkylation degree

The carbon number distributions for a given compound class represent the degree of alkyl substitution (Hughey *et al*., 2002), and thermal maturity has a significant influence

on the carbon number distributions in an homologous series (e.g. Hughey *et al*., 2004). The carbon number distributions for the S_1 class in selected low and high DBE values are plotted in Figure 4.6. The respective possible core structure without any alkyl side chain is provided as well. Also the blue numbers represent the number of carbon atoms in the alkyl side chain(s). In low DBEs (Fig. 4.6, left), the number of alkyl carbons in the heavy oils as well as least mature bitumens range from 5 to 58 carbons maximize around 19-25. The high carbon numbers reflect extensive alkyl substitution. With increasing thermal stress, the intensity as well as the extent of alkylation degree is decreased systematically due to side chain cracking reactions. In contrast, at high DBE values (Fig. 4.6, right), the alkylation degree is reduced drastically in highly mature solid bitumen. For instance in the Roboski vein the number of alkyl carbons ranges from 0 to 17, maximizing at 2 to 3. Also at high DBEs, the intensity of alkylation for all heavy oils and least mature bitumens is reduced enormously. Similar evolutionary patterns are observed in other compound classes with different DBE values.

4.5.4.5. Venn Diagram analysis

A Venn Diagram, also called Set Diagram or Logic Diagram, displays the logical relationships between two or more sets of items pictorially, highlighting how the items are similar and different. Since the investigated samples have a common source, and because thermal maturation is known to be the main alteration process, the Venn Diagram analysis can be used to visualize the thermal evolution of organosulphur compounds described above. As displayed in Figure 4.7, four samples of different thermal maturation levels from both petroleum types were selected, named as set A, B, C and D. In both, set A and D has the lowest and highest maturation level, respectively. It should be noted that the respective maturity ranges are very different in both sample types. Set A is employed as "reference sample" in order to see how chemical compositions change with ongoing maturation. In each row, the intersections (i.e. $A \cap B$) of the reference sample (set A) and the next mature samples i.e. set B, C and D, are shown as AB, AC and AD, respectively.

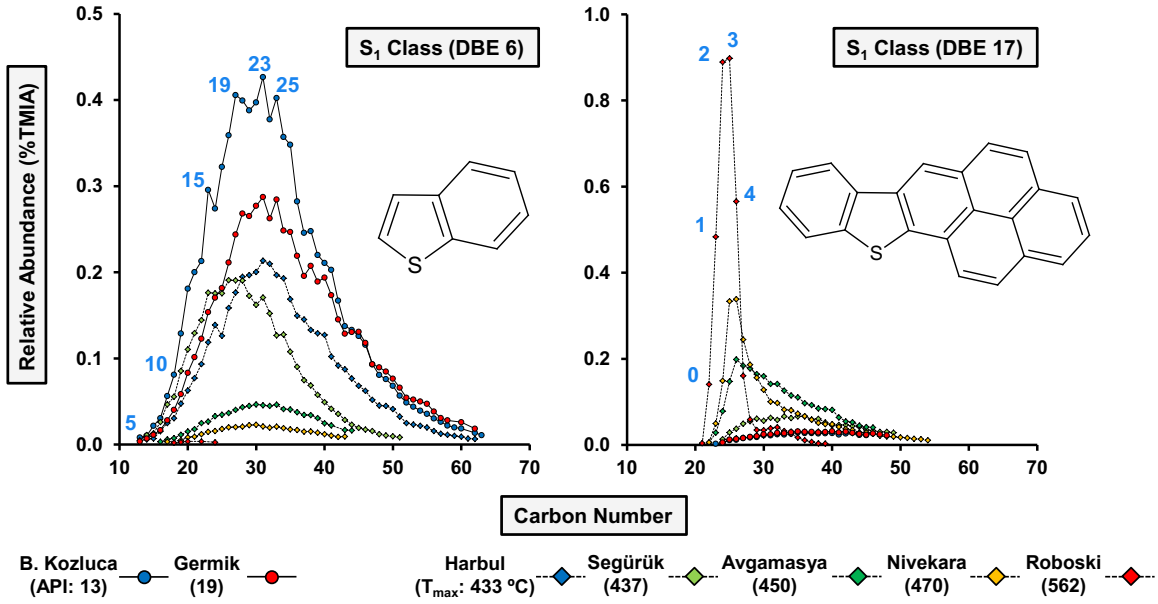

Fig. 4.6. Carbon number distribution at the low as well as high DBEs of the S_1 compound class in selected samples of both petroleum types. The chemical structures depict the respective possible core structures.

Furthermore for each union of two sets (e.g. A ∪ B), elemental class distribution of both complements of each set is provided by pie charts e.g. "A-AB" and "B-AB" meaning those elements which are exclusively in A and B sample, respectively. Similarly, the compound class distribution of organosulphur compounds in each complement is normalized and displayed separately, enabling to visualize the thermal evolution of individual OSC compound classes in the investigated samples.

In both crude oils and solid bitumens, the assigned monoisotopic elemental compositions in the intersections are decreasing as a function of maturation from 78% to 54% and from 64% to 13%, respectively. This reduction is more pronounced in solid bitumens because of significant maturity difference between the reference sample (set A) and set D.

In each raw, the reference sample (set A) is compared with a sample with higher maturity i.e. B, C and D. Thus the extent of maturity difference (ΔT) increases in the

order AB<AC<AD. With increasing ΔT, the unique compounds in the reference sample is becoming more and more enriched in OSCs (see pie charts named as "A-AB", "A-AC" and "A-AD"). In contrast, the unique elements in "B-AB", "C-AC" and "D-AD" is becoming more and more depleted in OSCs due to dilution processes by further generation of non-sulphur containing compounds, in particular the HC and N_y classes, and also by sulphur removal as discussed above (Orr and Sinninghe Damsté, 1990). Also the distribution of OSCs is changing systematically in both sides. According to the observed variations, it is clear the thermal processes preferentially cleave the C-S bond in compounds with higher sulphur atoms. For example, increase in the relative concentration of the S_1 class is associated with decreasing of the S_4 compounds. Moreover, the already discussed reversal trend at high-thermally degraded bitumens is clearly discernible in the unique compounds of the Roboski vein i.e. "D-AD".

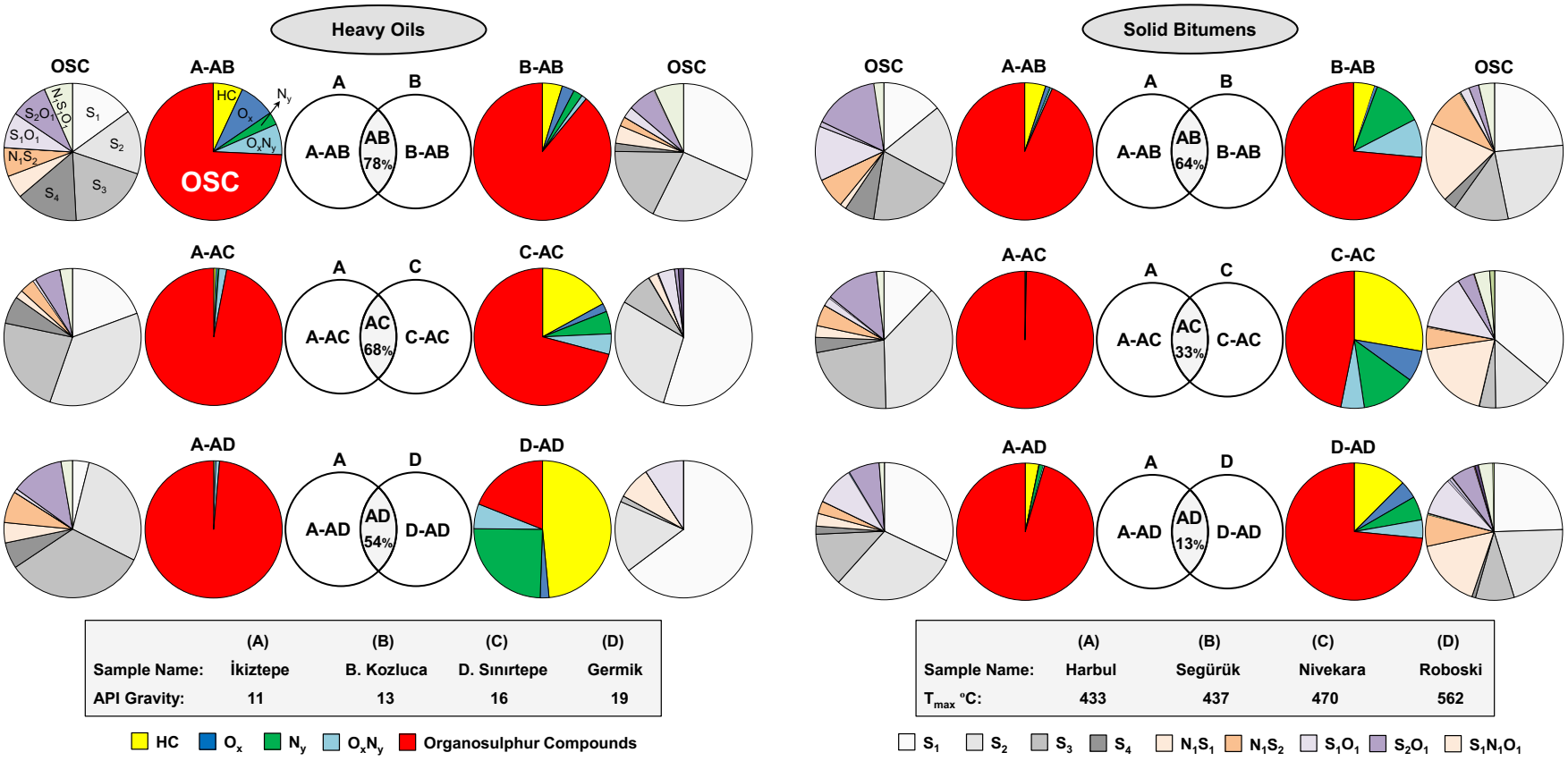

Fig. 4.7. Variations of elemental compositions, irrespective of their intensity values, in both heavy oils and solid bitumens as a function of maturity using two-set Venn Diagrams. Sample A in both sample types is used as low-maturity reference. The elemental class distributions of unique elements in each union as well as compound class distributions of only S-containing components are illustrated by pie charts.

4.6. Conclusions

Here, for the first time, organosulphur compounds in Turkish solid bitumen veins and heavy oils from proximal oilfields have been investigated using positive-ion APPI FT-ICR MS. These sulphur-rich petroleum occurrences are known to have originated from the same source, and thermal maturation is known to be the main alteration process. This makes the sample set an ideal natural laboratory for studying thermal evolution of OSC in the liquid as well as solid petroleums within a broad maturation window. It is here concluded that detected sulphur species are not derived from TSR processes, but have been incorporated into the source macromolecules via BSR during early diagenesis. The source generates sulphur-rich heavy oils in the early oil window. General parameters such as relatively low temperature reservoirs of heavy oils (< 88 ºC) and the nature of investigated oils i.e. non-biodegraded sulphur-rich heavy oils are pointing to a BSR mechanism. In addition, a continual decrease in relative abundances of OSC compounds detected with APPI FT-ICR-MS and a relative increase in the abundances of aromatic HC as well as N_1 compound classes with ongoing maturation are pointing towards a BSR pathway or exclude a TSR mechanism. the thermal evolution of organosulphur compounds reveals that in the low maturation levels, exactly the same distribution patterns exist for OSCs in both petroleum types, change in the order $S_1 > S_2 > S_3 > S_1O_1 > S_2O_1 > N_1S_1 > N_1S_2 > S_4$. The subsequent variations with increasing maturity are comparable in both sample types, implying the same evolutionary pathway in both solid and liquid petroleums. Most notably, for highly mature solid bitumens (T_{max} > 470 ºC), a reversal is observed in nearly all compound class abundances. At this level, released sulphur from thermally decomposing compounds are incorporated into other components such as $S_{2\text{-}4}$, N_1S_1, N_1S_2, etc. Finally, the Venn Diagram analysis nicely visualize thermally induced variations in selected samples of both heavy oils and solid bitumens.

5. SUMMARY AND OUTLOOK

5.1. Summary

Within the framework of this dissertation the following questions were addressed:

1) Why do Turkish solid bitumens, ostensibly generated from the same source, display a wide variety in physicochemical characteristics that is strongly related to geographic location?

In order to answer this question, various analytical tools from pyrolysis to ultrahigh resolution mass spectrometry were employed. T_{max} values indicate that there is a clear maturity trend across the region, increasing progressively from west to east. Also, the extractability of organic matter as well as hydrogen content decreases systematically with increasing T_{max} values, entirely consistent with the obtained data from maturity sensitive molecular parameters. The influence of biodegradation is excluded due to the presence of *n*-alkanes in nearly all samples. According to geochemical results, the investigated solid bitumens are in various thermal degradation levels from asphaltite to pyrobitumen, and thermal maturation is undoubtedly the major factor controlling their chemical composition. Also the intensity of thermal alteration is inferred to be strongly related to regional tectonic history, as the study area is located in an active collision zone and compressional pressure generating an overall increase in maturation from west to east. In addition, it appears that compressional forces are responsible for the formation of veins and vugs during the main phase of the Alpine Orogeny during the Miocene.

The macromolecular building blocks analysed by Py-GC have undergone a progressive shortening of *n*-alkyl chains take place which is accompanied by increasing proportion of gaseous pyrolysate as well as aromatic moieties. The ESI-(-) FT-ICR MS data reveal that the chemical composition of the acidic constituents is mainly controlled by maturity. With ongoing maturity from early mature to mature bitumens (T_{max} < 470

ºC), the variations of various compound classes in the investigated bitumens are comparable with those that have been reported previously by others. Interestingly, for highly mature bitumens (T_{max} > 470 ºC) a reversal trend is observed in the relative intensity of the N_1, N_2, N_1O_1, N_2O_1 as well as nearly all oxygen compound classes (O_1 to O_6). Moreover, at the same time this inversion is not observed in the nitrogen and sulphur containing compounds i.e. the N_1S_1 and N_1S_2, and their relative intensity are increased continuously. We believe that this is attributed to the role of hydrogen and sulphur elements at highest maturation levels as discussed in detail at the end of this chapter.

2) Are the surface and subsurface petroleum occurrences in the investigated area genetically related?

A comprehensive geochemical correlation was established in order to address this issue. Thirty solid bitumens along with ten heavy oils and thirteen oil seep samples from proximal areas were investigated using various geochemical tools. First of all, the geochemical characteristics of each petroleum types were evaluated in terms of source organofacies as well as alteration processes i.e. thermal maturation and biodegradation. A strong genetic relationship between the surface and subsurface petroleum occurrences was observed and this genetic affinity is even more pronounced by comparison of the low-thermally degraded solid bitumens and low-biodegraded seeps with heavy oils. The source-sensitive molecular parameters based on *n*-alkanes, isoprenoids, hopanes, steranes as well as aromatic hydrocarbons, demonstrate a marine carbonate source for all studied samples, except for the Dadaş and İşkar seeps (marine shale).

Furthermore, other correlation criteria were employed to display some of the compositional changes during solidification processes. Even though both surficial and subsurface hydrocarbon types, with no doubt, are originated from a geochemically similar source, they are different in homohopane distributions as well as isotopic values.

Considering the distribution of C_{31}-C_{35} 17α,21β(H)-homohopanes, it is clear that the low-thermally degraded solid bitumens are highly enriched in C_{31}- and depleted in higher homologs i.e. C_{33}-, C_{34}- and C_{35}-homohopanes relative to heavy oils and seeps. This is attributed to transformation processes that are active during and/or after solidification, particularly in sulphur-rich systems, led to cracking of high molecular weight homologs of homohopanes to lower ones.

Similarly, variations of the $\delta^{13}C$ values of individual *n*-alkanes demonstrate that solid bitumens are more enriched in ^{13}C than the heavy oils. Since both petroleum types are known to be originated from the same source, different variation of the $\delta^{13}C$ values is mainly due to the phase effect and preferential removal of light isotopes (^{12}C) during solidification. Furthermore, the influence of thermal alteration is clearly discernible in solid bitumens of different thermal transformation levels. While the least mature bitumens show the lightest $\delta^{13}C$ values relative to other veins, high-thermally degraded ones are remarkably enriched in ^{13}C especially for the lower molecular weight *n*-alkanes (<*n*-C_{20}).

To summarize, our results strongly confirm that surface and subsurface hydrocarbon occurrences in the investigated region are genetically related, thereby providing new insights on the petroleum system in this part of the southeast Turkey.

3) How does sulphur introduced into the investigated petroleum fluids and through which mechanism(s)? How do organosulphur compounds evolve in liquid and solid petroleum occurrences?

For this, the positive-ion APPI FT-ICR MS analysis as a powerful tool for characterization and ionizing nonpolar organosulphur compounds in complex organic mixtures was employed. According to the elemental ratios measured from ultrahigh resolution mass spectrometry, sulphur is the main heteroatom in the investigated samples and their content is strongly controlled by the maturation levels.

It is evident that sulphur has been introduced into the source organic matter via BSR mechanism at very early diagenesis, based on various observations: Low temperatures of the oil reservoirs exclude a TSR mechanism which is normally occurs at hot conditions. Furthermore, the nature of crude oils i.e. being extra-heavy without any signs of biodegradation, implies they have been originated from a sulphur-rich kerogen at early stages of oil generation because of weaker carbon-sulphur and sulphur-sulphur bonds. The progressively decrease of sulphur content with ongoing maturation is also suggest a BSR mechanism as in TSR altered oils it remains at the same level. In addition, the molecular-level information achieved from FT-ICR MS technique was confirmed the inferred mechanism mentioned above. For instance, variations of relative intensity of the aromatic hydrocarbon and N_1 compound classes, the S_{org}/N ratios, and decrease in the alkylation degree of the major compound classes with advancing maturation were authenticated a BSR- or excluded a TSR-related mechanism.

Considering the distribution patterns for the major organosulphur components, it is evident that the geochemical evolutionary pathway is the same in both petroleum types i.e. solid bitumens and liquid heavy oils.

The most interesting and exciting parts of this dissertation was finding a reasonable explanation for the unexpected behavior of nearly all compound classes at high-thermally degraded solid bitumens. For instance, according to literature, it is expected that the relative abundances of the S_1 class rises with ongoing thermal stress due to thermal cracking. Simultaneously and due to the same reason, a continual decrease is expected for high molecular weight S-containing compounds such as the S_2, S_3 and S_4. The relative intensity of these compound classes from early mature to mature bitumens (T_{max} < 470 ºC), were exactly as expected. Surprisingly, at higher maturation levels (T_{max} > 470 ºC) a reversal trend was observed in all of them. The S_1 class went through a maximum whereas other classes went through a minimum and their relative abundances were started to increase again. Also, the same reversal trends have been observed in the major compound classes in the ESI (-) data. This is interesting as no FT-ICR MS data have been published on petroleum fluids of this elevated maturity up to now. It appears that these unexpected observed trends at extremely degraded solid bitumens are firstly

attributed to the significant decrease of the hydrogen content and secondly to the highly active sulphur species released from thermally decomposing polymers. The former was terminated the cyclisation as well as aromatisation processes and the latter led to the reincorporation of thermally released sulphur elements into other major compound classes. While O, N and C atoms which are release as relatively non-active LMW compounds (e.g. CO_2 , H_2O, NH_3 , CH_4), S releases as highly active species in cross-linking reactions; thus, it is very likely that these species will be reincorporated into the organic matter by one of the many known high-temperature pathways. Therefore, at high-thermally degraded solid bitumens, when hydrogen content was not as high as enough for the cyclisation and aromatisation reactions, the thermally released heteroatoms were interacted together, forming high molecular weight components (e.g. the S_2, S_3, S_4, etc.). Thus, the relative intensity of the S_1 class was decreased but others were increased. The progressively increase in the relative intensity of the N_1S_1 as well as the N_1S_2 classes can be clarified in a same way.

5.2. Outlook

Although in this project some of the important questions about Turkish solid bitumens have been answered, there are still some enigmatic aspects that need to be addressed.

We did not have accesses to the potential source rocks in order to find the possible source of both solid bitumens and heavy oils. Therefore, an additional research could be conducted in order to establish a source-oil correlation.

The investigated area is an ideal natural laboratory to study the influences of phase effects as well as thermal stress on different chemical components in the organic matters and petroleum fluids, as surface and subsurface petroleum occurrences are proven to be originated from the same source and more importantly a wide variety of degradation levels are available.

In this study, acidic and non-acidic component of petroleum fluids have been documented making use of ultrahigh resolution mass spectrometry. To reveal changes of

other organic compounds in the investigated samples additional ionization methods can be used.

The organosulphur components in the given sample set is really interesting and have the potential to be investigated in more details using chemical degradation analyses in order to study the biomarkers released upon different desulphurization experiments.

REFERENCES

Abraham, H., 1960, Asphalts and Allied Substances: Historical review and natural raw materials, v. 1, 6th ed.: New York, Van Nostrand, 370 p.

Aizenshtat, Z., E. B. Krein, M. A. Vairavamurthy, and T. P. Goldstein, 1995, Role of Sulfur in the Transformations of Sedimentary Organic Matter: A Mechanistic Overview, Geochemical Transformations of Sedimentary Sulfur: ACS Symposium Series, v. 612, American Chemical Society, p. 16-37.

Ala, M. A., and B. Moss, 1979, Comparative petroleum geology of southeast Turkey and northeast Syria: J. Pet. Geology, v. 1, p. 3-27.

Alexander, R., R. I. Kagi, G. W. Woodhouse, and J. K. Volkman, 1983, The geochemistry of some biodegraded Australian oils: The APPEA Journal, v. 23, p. 53-63.

Attanasi, E. D., and R. F. Meyer, 2010, Natural bitumen and extra-heavy oil: Survey of energy resources, v. 22, p. 123-140.

Bartle, K. D., E. Ekinci, B. Frere, M. Mulligan, S. Sarac, and C. E. Snape, 1981, The nature and origin of Harbolite and a related asphaltite from southeastern Turkey: Chemical Geology, v. 34, p. 151-164.

Behar, F., V. Beaumont, and H. D. B. Penteado, 2001, Rock-Eval 6 technology: performances and developments: Oil & Gas Sci. Technol., v. 56, p. 111-134.

Bell, K. G., and J. M. Hunt, 1963, Native bitumens associated with oil shales: Organic Geochemistry.

Bost, F. D., R. Frontera-Suau, T. J. McDonald, K. E. Peters, and P. J. Morris, 2001, Aerobic biodegradation of hopanes and norhopanes in Venezuelan crude oils: Organic Geochemistry, v. 32, p. 105-114.

Bradley, W. H., 1931, Origin and microfossils of the oil shale of the Green River Formation of Colorado and Utah, v. 168, US Govt. Print. Off.

Cassani, F., and G. Eglinton, 1991, Organic geochemistry of Venezuelan extra-heavy crude oils 2. Molecular assessment of biodegradation: Chemical Geology, v. 91, p. 315-333.

Cater, J., and J. Gillcrist, 1994, KARSTIC RESERVOIRS OF THE MID-CRETACEOUS MARDIN GROUP, SE TURKEY: Tectonic and Eustatic Controls on their Genesis, Distribution and Preservation: Journal of Petroleum Geology, v. 17, p. 253-278.

Chakhmakhchev, A., M. Suzuki, and K. Takayama, 1997, Distribution of alkylated dibenzothiophenes in petroleum as a tool for maturity assessments: Organic Geochemistry, v. 26, p. 483-489.

Chakhmakhchev, A., and N. Suzuki, 1995, Aromatic sulfur compounds as maturity indicators for petroleums from the Buzuluk depression, Russia: Organic Geochemistry, v. 23, p. 617-625.

Chen, H., A. Hou, Y. E. Corilo, Q. Lin, J. Lu, I. A. Mendelssohn, R. Zhang, R. P. Rodgers, and A. M. McKenna, 2016, 4 Years after the Deepwater Horizon Spill: Molecular Transformation of Macondo Well Oil in Louisiana Salt Marsh Sediments Revealed by FT-ICR Mass Spectrometry: Environmental Science & Technology, v. 50, p. 9061-9069.

Chung, H., M. Rooney, M. Toon, and G. E. Claypool, 1992, Carbon Isotope Composition of Marine Crude Oils: AAPG Bulletin, v. 76, p. 1000-1007.

Clark, J., and R. Philp, 1989, Geochemical characterization of evaporite and carbonate depositional environments and correlation of associated crude oils in the Black Creek Basin, Alberta: Bulletin of Canadian Petroleum Geology, v. 37, p. 401-416.

Clayton, C. J., 1991, Effect of maturity on carbon isotope ratios of oils and condensates: Organic Geochemistry, v. 17, p. 887-899.

Clayton, C. J., and M. Bjorøy, 1994, Effect of maturity on 13C12C ratios of individual compounds in North Sea oils: Organic Geochemistry, v. 21, p. 737-750.

Cobbold, P. R., M. Diraison, and E. A. Rossello, 1999, Bitumen veins and Eocene transpression, Neuquén Basin, Argentina: Tectonophysics, v. 314, p. 423-442.

Cobbold, P. R., G. Ruffet, L. Leith, H. Loseth, N. Rodrigues, H. A. Leanza, and A. Zanella, 2014, Radial patterns of bitumen dykes around Quaternary volcanoes, provinces of northern Neuquén and southernmost Mendoza, Argentina: Journal of South American Earth Sciences, v. 56, p. 454-467.

Connan, J., 1984, Biodegradation of crude oils in reservoirs: Advances in petroleum geochemistry, v. 1, p. 299-335.

Connan, J., J. Bouroullec, D. Dessort, and P. Albrecht, 1986, The microbial input in carbonate-anhydrite facies of a sabkha palaeoenvironment from Guatemala: A molecular approach: Organic Geochemistry, v. 10, p. 29-50.

Connan, J., O. Kavak, E. Akin, M. N. Yalçin, K. Imbus, and J. Zumberge, 2006, Identification and origin of bitumen in Neolithic artefacts from Demirköy Höyük (8100 BC): Comparison with oil seeps and crude oils from southeastern Turkey: Organic Geochemistry, v. 37, p. 1752-1767.

Connan, J., G. Kozbe, O. Kavak, J. Zumberge, and K. Imbus, 2013, The bituminous mixtures of Kavuşan Höyük (SE Turkey) from the end of the 3rd millennium (2000BC) to the Medieval period (AD 14th century): Composition and origin: Organic Geochemistry, v. 54, p. 2-18.

Connan, J., G. Lacrampe-Couloume, and M. Magot, 1995, Origin of gases in reservoirs: INTERNATIONAL GAS RESEARCH CONFERENCE, p. 21-61.

Connan, J., A. Restle, and P. Albrecht, 1980, Biodegradation of crude oil in the Aquitaine basin: Physics and Chemistry of the Earth, v. 12, p. 1-17.

Connan, J., and B. M. Van Der Weide, 1978, Chapter 3 Thermal Evolution of Natural Asphalts, *in* G. V. Chilingarian, and T. F. Yen, eds., Developments in Petroleum Science, v. 7, Elsevier, p. 27-55.

Çorbacıoğlu, H., 2015, GDA Ağır Petrollerinin (I. Grup Petrollerinin Kökeni ve Kuzey Irak Petrol Sistemi ile Korelasyonu, proceeding of 20th international petroleum and natural gas congress and exhibition of Turkey, Ankara, Turkey, p. 159-160.

Cornelius, C., 1984, Geochemical aspects of heavy oil/bitumen exploration: The future of heavy crude and tar sands, 2nd International Conference: New York, McGraw-Hill, p. 318-335.

Cornelius, C., 1987, Classification of natural bitumen: a physical and chemical approach: Exploration for heavy crude oil and natural bitumen: AAPG Studies in Geology, v. 25, p. 165-174.

Curiale, J. A., 1986, Origin of solid bitumens, with emphasis on biological marker results: Organic Geochemistry, v. 10, p. 559-580.

Curiale, J. A., 2008, Oil–source rock correlations – Limitations and recommendations: Organic Geochemistry, v. 39, p. 1150-1161.

Dahl, B., and G. Speers, 1986, Geochemical characterization of a tar mat in the Oseberg Field Norwegian Sector, North Sea: Organic Geochemistry, v. 10, p. 547-558.

Dawson, D., K. Grice, R. Alexander, and D. Edwards, 2007, The effect of source and maturity on the stable isotopic compositions of individual hydrocarbons in sediments and crude oils from the Vulcan Sub-basin, Timor Sea, Northern Australia: Organic Geochemistry, v. 38, p. 1015-1038.

Demaison, G., 1977, Tar sands and supergiant oil fields: AAPG Bulletin, v. 61, p. 1950-1961.

Demirel, I. H., T. S. Yurtsever, and S. Guneri, 2001, Petroleum systems of the Adiyaman region, Southeastern Anatolia, Turkey: Marine and Petroleum Geology, v. 18, p. 391-410.

di Primio, R., and B. Horsfield, 1996, Predicting the generation of heavy oils in carbonate/evaporitic environments using pyrolysis methods: Organic Geochemistry, v. 24, p. 999-1016.

Didyk, B., B. R. T. Simoneit, S. C. Brassell, and G. Eglinton, 1978, Organic geochemical indicators of palaeoenvnonmental conditions of sedimentation: Nature, v. 272, p. 216-222.

Dow, W. G., 1974, Application of oil-correlation and source-rock data to exploration in Williston Basin: AAPG bulletin, v. 58, p. 1253-1262.

Dzou, L. I. P., R. A. Noble, and J. T. Senftle, 1995, Maturation effects on absolute biomarker concentration in a suite of coals and associated vitrinite concentrates: Organic Geochemistry, v. 23, p. 681-697.

Egeran, E. N., 1951, On the oil fields Iocated in south-eastern Turkey: Maden Tetkik ve Arama Dergisi, v. 41.

Erdem-Senatalar, A., E. Ekinci, K. Bartle, and B. Frere, 1991, Hydrocarbon minerals from south-eastern Turkey: a comparison of the chemical natures of the neighbouring Raman-Dincer crude oile and Avgamasya asphaltite: Erdöl und Kohle, Erdgas, Petrochemie vereinigt mit Brennstoff-Chemie, v. 44, p. 298-300.

Espitalie, J., M. Madec, B. Tissot, J. J. Mennig, and P. Leplat, 1977, Source Rock Characterization Method for Petroleum Exploration, Offshore Technology Conference.

Evans, C. R., M. A. Rogers, and N. J. L. Bailey, 1971, Evolution and alteration of petroleum in western Canada: Chemical Geology, v. 8, p. 147-170.

Fisher, S., R. Alexander, R. Kagi, and G. Oliver, 1998, Aromatic hydrocarbons as indicators of biodegradation in North Western Australian reservoirs: The sedimentary basins of Western Australia, v. 2, p. 185-194.

George, S. C., S. M. Llorca, and P. J. Hamilton, 1994, An integrated analytical approach for determining the origin of solid bitumens in the McArthur Basin, northern Australia: Organic Geochemistry, v. 21, p. 235-248.

Goodarzi, F., and P. F. Williams, 1986, Composition of natural bitumens and asphalts from Iran: 2. Bitumens from the Posteh Ghear valley, south-west Iran: Fuel, v. 65, p. 17-27.

Gorur, N., and O. Tuysuz, 2001, Cretaceous to Miocene palaeogeographic evolution of Turkey: implications for hydrocarbon potential: J. Pet. Geology, v. 24, p. 119-146.

Grantham, P. J., and L. L. Wakefield, 1988, Variations in the sterane carbon number distributions of marine source rock derived crude oils through geological time: Organic Geochemistry, v. 12, p. 61-73.

Gu, X. X., Y. M. Zhang, B. H. Li, S. Y. Dong, C. J. Xue, and S. H. Fu, 2012, Hydrocarbon- and ore-bearing basinal fluids: a possible link between gold mineralization and hydrocarbon accumulation in the Youjiang basin, South China: Mineralium Deposita, v. 47, p. 663-682.

Harput, O. B., F. Goodarzi, and O. Erturk, 1992, Thermal Maturation and Source Rock Potential of Sedimentary Succession in Southeast Anatolia, Turkey: Energy Sources, v. 14, p. 317-329.

Head, I. M., D. M. Jones, and S. R. Larter, 2003, Biological activity in the deep subsurface and the origin of heavy oil: Nature, v. 426, p. 344.

Hellmuth, K., 1989, Natural analogues of bitumen and bituminized radioactive waste.

Helms, J. R., X. Kong, E. Salmon, P. G. Hatcher, K. Schmidt-Rohr, and J. Mao, 2012, Structural characterization of gilsonite bitumen by advanced nuclear magnetic resonance spectroscopy and ultrahigh resolution mass spectrometry revealing pyrrolic and aromatic rings substituted with aliphatic chains: Organic Geochemistry, v. 44, p. 21-36.

Hempton, M. R., 1985, Structure and deformation history of the Bitlis suture near Lake Hazar, southeastern Turkey: Geological Society of America Bulletin, v. 96, p. 233-243.

Hiçyılmaz, C., and N. E. Altun, 2006, Improvements on combustion properties of asphaltite and correlation of activation energies with combustion results: Fuel Processing Technology, v. 87, p. 563-570.

Hirschberg, A., L. DeJong, B. Schipper, and J. Meijer, 1984, Influence of temperature and pressure on asphaltene flocculation: Society of Petroleum Engineers Journal, v. 24, p. 283-293.

Ho, T. Y., M. A. Rogers, H. V. Drushel, and C. B. Koons, 1974, Evolution of sulfur compounds in crude oils: AAPG bulletin, v. 58, p. 2338-2348.

Horsfield, B., 1989, Practical criteria for classifying kerogens: some observations from pyrolysis-gas chromatography: Geochimica et Cosmochimica Acta, v. 53, p. 891-901.

Horsfield, B., J. Heckers, D. Leythaeuser, R. Littke, and U. Mann, 1991, A study of the Holzener Asphaltkalk, northern Germany: observations regarding the distribution, composition and origin of organic matter in an exhumed petroleum reservoir: Marine and Petroleum Geology, v. 8, p. 198-211.

Hosseini, S. H., B. Horsfield, S. Poetz, H. Wilkes, M. N. Yalçın, and O. Kavak, 2017, Role of Maturity in Controlling the Composition of Solid Bitumens in Veins and Vugs from SE Turkey as Revealed by Conventional and Advanced Geochemical Tools: Energy & Fuels, v. 31, p. 2398-2413.

Hosseini, S. H., B. Horsfield, H. Wilkes, A. Vieth-Hillebrand, M. N. Yalçın, and O. Kavak, 2018, Comprehensive geochemical correlation between surface and subsurface hydrocarbon occurrences in the Batman-Mardin-Şırnak area (SE Turkey): Marine and Petroleum Geology, v. 93, p. 95-112.

Huc, A. Y., P. Nederlof, R. Debarre, B. Carpentier, M. Boussafir, F. Laggoun-Défarge, A. Lenail-Chouteau, and N. Bordas-Le Floch, 2000, Pyrobitumen occurrence and formation in a Cambro–Ordovician sandstone reservoir, Fahud Salt Basin, North Oman: Chemical Geology, v. 168, p. 99-112.

Hughes, W. B., 1984, Use of thiophenic organosulfur compounds in characterizing crude oils derived from carbonate versus siliciclastic sources, Petroleum Geochemistry and Source Rock Potential of Carbonate Rocks (J. G. Palacas, ed.), American Association of Petroleum Geologists, Tulsa, OK, p. 181–196.

Hughes, W. B., A. G. Holba, and L. I. P. Dzou, 1995, The ratios of dibenzothiophene to phenanthrene and pristane to phytane as indicators of depositional environment and lithology of petroleum source rocks: Geochimica et Cosmochimica Acta, v. 59, p. 3581-3598.

Hughey, C. A., S. A. Galasso, and J. E. Zumberge, 2007, Detailed compositional comparison of acidic NSO compounds in biodegraded reservoir and surface crude oils by negative ion electrospray Fourier transform ion cyclotron resonance mass spectrometry: Fuel, v. 86, p. 758-768.

Hughey, C. A., R. P. Rodgers, A. G. Marshall, K. Qian, and W. K. Robbins, 2002, Identification of acidic NSO compounds in crude oils of different geochemical origins by negative ion electrospray Fourier transform ion cyclotron resonance mass spectrometry: Organic Geochemistry, v. 33, p. 743-759.

Hughey, C. A., R. P. Rodgers, A. G. Marshall, C. C. Walters, K. Qian, and P. Mankiewicz, 2004, Acidic and neutral polar NSO compounds in Smackover oils of different thermal maturity revealed by electrospray high field Fourier transform ion cyclotron resonance mass spectrometry: Organic Geochemistry, v. 35, p. 863-880.

Hunt, J. M., 1963, Composition and origin of the Uinta Basin bitumens.

Hunt, J. M., F. Stewart, and P. A. Dickey, 1954, Origin of hydrocarbons of Uinta basin, Utah: AAPG Bulletin, v. 38, p. 1671-1698.

Hunt, M., 1979, Petroleum geochemistry and geology, WH Freeman and company.

Hur, M., I. Yeo, E. Kim, M.-h. No, J. Koh, Y. J. Cho, J. W. Lee, and S. Kim, 2010, Correlation of FT-ICR Mass Spectra with the Chemical and Physical Properties of Associated Crude Oils: Energy & Fuels, v. 24, p. 5524-5532.

Hwang, R. J., S. C. Teerman, and R. M. Carlson, 1998, Geochemical comparison of reservoir solid bitumens with diverse origins: Organic Geochemistry, v. 29, p. 505-517.

Jacob, H., 1989, Classification, structure, genesis and practical importance of natural solid oil bitumen ("migrabitumen"): Int. J. Coal Geology, v. 11, p. 65-79.

Jacob, H., 1993, Nomenclature, Classification, Characterization, and Genesis of Natural Solid Bitumen (Migrabitumen), *in* J. Parnell, H. Kucha, and P. Landais, eds., Bitumens in Ore Deposits: Berlin, Heidelberg, Springer Berlin Heidelberg, p. 11-27.

Jinggui, L., P. Philp, M. Zifang, L. Wenhui, Z. Jianjing, C. Guojun, L. Mei, and W. Zhaoyun, 2005, Aromatic compounds in crude oils and source rocks and their application to oil–source rock correlations in the Tarim basin, NW China: Journal of Asian Earth Sciences, v. 25, p. 251-268.

Kar, Y., 2006, Importance of asphaltite deposits in southeastern Anatolia: Energy Sources, Part A, v. 28, p. 1343-1352.

Kara-Gülbay, R., and S. Korkmaz, 2012, Occurrences and origin of oils and asphaltites from South East Anatolia (Turkey): Implications from organic geochemistry: J. Pet. Sci. Eng., v. 90-91, p. 145-158.

Kara-Gülbay, R., and S. Korkmaz, 2013, Organic geochemistry of the asphaltite occurrences in the Gümüşhacıköy (Amasya) Area, Northern Turkey: Fuel, v. 107, p. 74-83.

Kavak, O., 2011, Organic geochemical comparison of asphaltites of Şırnak area with the oils of the Raman and Dinçer fields in Southeastern Turkey: Fuel, v. 90, p. 1575-1583.

Kavak, O., J. Connan, N. Erik, and M. Yalcin, 2010, Organic geochemical characteristics of Sirnak asphaltites in Southeast Anatolia, Turkey: Oil shale, v. 27, p. 58-84.

Kelemen, S. R., C. C. Walters, P. J. Kwiatek, M. Afeworki, M. Sansone, H. Freund, R. J. Pottorf, H. G. Machel, T. Zhang, G. S. Ellis, Y. Tang, and K. E. Peters, 2008, Distinguishing solid bitumens formed by thermochemical sulfate reduction and thermal chemical alteration: Organic Geochemistry, v. 39, p. 1137-1143.

Kelemen, S. R., C. C. Walters, P. J. Kwiatek, H. Freund, M. Afeworki, M. Sansone, W. A. Lamberti, R. J. Pottorf, H. G. Machel, K. E. Peters, and T. Bolin, 2010, Characterization of solid bitumens originating from thermal chemical alteration and thermochemical sulfate reduction: Geochimica et Cosmochimica Acta, v. 74, p. 5305-5332.

Kim, S., R. W. Kramer, and P. G. Hatcher, 2003, Graphical Method for Analysis of Ultrahigh-Resolution Broadband Mass Spectra of Natural Organic Matter, the Van Krevelen Diagram: Analytical Chemistry, v. 75, p. 5336-5344.

Kim, S., L. A. Stanford, R. P. Rodgers, A. G. Marshall, C. C. Walters, K. Qian, L. M. Wenger, and P. Mankiewicz, 2005, Microbial alteration of the acidic and neutral polar NSO compounds revealed by Fourier transform ion cyclotron resonance mass spectrometry: Organic Geochemistry, v. 36, p. 1117-1134.

Kohnen, M. E. l., J. S. Sinninghe Damsté, A. c. Kock-van Dalen, and W. D. L. Jan, 1991, Di- or polysulphide-bound biomarkers in sulphur-rich geomacromolecules as revealed by selective chemolysis: Geochimica et Cosmochimica Acta, v. 55, p. 1375-1394.

Kotarba, M. J., D. Więcław, Y. V. Koltun, L. Marynowski, J. Kuśmierek, and I. V. Dudok, 2007, Organic geochemical study and genetic correlation of natural gas, oil and Menilite source rocks in the area between San and Stryi rivers (Polish and Ukrainian Carpathians): Organic Geochemistry, v. 38, p. 1431-1456.

Larter, S., 1984, Application of analytical pyrolysis techniques to kerogen characterization and fossil fuel exploration/exploitation, Analytical pyrolysis, Elsevier, p. 212-275.

Larter, S., K. Bjørlykke, D. Karlsen, T. Nedkvitne, T. Eglinton, P. Johansen, D. Leythaeuser, P. Mason, A. Mitchell, and G. Newcombe, 1990, Determination of petroleum accumulation histories: examples from the Ula field, Central Graben, Norwegian North Sea, North Sea Oil and Gas Reservoirs—II, Springer, p. 319-330.

Larter, S., H. Huang, J. Adams, B. Bennett, O. Jokanola, T. Oldenburg, M. Jones, I. Head, C. Riediger, and M. Fowler, 2006, The controls on the composition of biodegraded oils in the deep subsurface: Part II—Geological controls on subsurface biodegradation fluxes and constraints on reservoir-fluid property prediction1: AAPG bulletin, v. 90, p. 921-938.

Larter, S., A. Wilhelms, I. Head, M. Koopmans, A. Aplin, R. Di Primio, C. Zwach, M. Erdmann, and N. Telnaes, 2003, The controls on the composition of biodegraded oils in the deep subsurface—part 1: biodegradation rates in petroleum reservoirs: Organic Geochemistry, v. 34, p. 601-613.

Lebküchner, R., 1969, Occurrences of the asphaltic substances in Southeastern Turkey and their genesis: Miner. Res. Explor. Bulletin, v. 72, p. 74-96.

Lebküchner, R. F., F. Orhun, and M. Wolf, 1972, Asphaltic substances in southeastern Turkey: AAPG Bulletin, v. 56, p. 1939-1964.

Levandowski, D., M. Kaley, S. Silverman, and R. Smalley, 1973, Cementation in Lyons Sandstone and its role in oil accumulation, Denver Basin, Colorado: AAPG Bulletin, v. 57, p. 2217-2244.

Li, M., D. Cheng, X. Pan, L. Dou, D. Hou, Q. Shi, Z. Wen, Y. Tang, S. Achal, M. Milovic, and L. Tremblay, 2010, Characterization of petroleum acids using combined FT-IR, FT-ICR–MS and GC–MS: Implications for the origin of high acidity oils in the Muglad Basin, Sudan: Organic Geochemistry, v. 41, p. 959-965.

Li, Y., Y. Xiong, W. Yang, Y. Xie, S. Li, and Y. Sun, 2009, Compound-specific stable carbon isotopic composition of petroleum hydrocarbons as a tool for tracing the source of oil spills: Marine Pollution Bulletin, v. 58, p. 114-117.

Liao, Y., Q. Shi, C. S. Hsu, Y. Pan, and Y. Zhang, 2012, Distribution of acids and nitrogen-containing compounds in biodegraded oils of the Liaohe Basin by negative ion ESI FT-ICR MS: Organic Geochemistry, v. 47, p. 51-65.

Lo, H. B., and B. J. Cardott, 1995, Detection of natural weathering of Upper McAlester coal and Woodford Shale, Oklahoma, U.S.A: Organic Geochemistry, v. 22, p. 73-83.

Love, G. D., C. E. Snape, A. D. Carr, and R. C. Houghton, 1995, Release of covalently-bound alkane biomarkers in high yields from kerogen via catalytic hydropyrolysis: Organic Geochemistry, v. 23, p. 981-986.

M. A. Ala, B. J. M., 1979, Comparative petroleum geology of southeast Turkey and northeast Syria: Journal of Petroleum Geology, v. 1, p. 3-27.

Machel, H. G., H. R. Krouse, and R. Sassen, 1995, Products and distinguishing criteria of bacterial and thermochemical sulfate reduction: Applied Geochemistry, v. 10, p. 373-389.

Mackenzie, A., and J. Maxwell, 1981, Assessment of thermal maturation in sedimentary rocks by molecular measurements, Organic maturation studies and fossil fuel exploration, Academic Press London, p. 239-254.

Mahlstedt, N., B. Horsfield, H. Wilkes, and S. Poetz, 2016, Tracing the Impact of Fluid Retention on Bulk Petroleum Properties Using Nitrogen-Containing Compounds: Energy & Fuels, v. 30, p. 6290-6305.

Mahon, K. I., H. Dembicki, A. Chaouche, J. Meredith, H. J. White, N. Kalyanaraman, D. Kennedy, and D. Carruthers, 2009, Intergranular Tar in a Deepwater Reservoir: Part I – Mechanisms of Asphaltene Deposition, AAPG HEDBERG CONFERENCE: "Basin and Petroleum System Modeling: New Horizons in Research and Applications", NAPA, CALIFORNIA, USA

McCarthy, K., K. Rojas, M. Niemann, D. Palmowski, K. Peters, and A. Stankiewicz, 2011, Basic petroleum geochemistry for source rock evaluation: Oilfield Review, v. 23, p. 32-43.

Meyer, R. F., E. D. Attanasi, and P. A. Freeman, 2007, Heavy oil and natural bitumen resources in geological basins of the world, Open File-Report 2007-1084, U.S. Geological Survey.

Meyer, R. F., and W. De Witt, 1990, Definition and world resources of natural bitumens, Citeseer.

Milner, C. W. D., M. A. Rogers, and C. R. Evans, 1977, Petroleum transformations in reservoirs: Journal of Geochemical Exploration, v. 7, p. 101-153.

Moldowan, J. M., W. K. Seifert, and E. J. Gallegos, 1985, Relationship between petroleum composition and depositional environment of petroleum source rocks: AAPG bulletin, v. 69, p. 1255-1268.

Monger, T., and J. Fu, 1987, The nature of CO2-induced organic deposition: SPE Annual Technical Conference and Exhibition.

Monson, B., and J. Parnell, 1992, The origin of gilsonite vein deposits in the Uinta Basin, Utah.

Mossman, D. J., and B. Nagy, 1996, Solid bitumens: an assessment of their characteristics, genesis, and role in geological processes: Terra Nova, v. 8, p. 114-128.

Mueller, E., R. P. P. Philp, and J. Allen, 1995, Geochemical characterization and relationship of oils and solid bitumens from SE Turkey: J. Pet. Geology, v. 18, p. 289-307.

Murillo, W. A., A. Vieth-Hillebrand, B. Horsfield, and H. Wilkes, 2016, Petroleum source, maturity, alteration and mixing in the southwestern Barents Sea: New insights from geochemical and isotope data: Marine and Petroleum Geology, v. 70, p. 119-143.

Muscio, G., B. Horsfield, and D. Welte, 1991, Compositional changes in the macromolecular organic matter (kerogens, asphaltenes and resins) of a naturally matured source rock sequence from Northern Germany as revealed by pyrolysis methods: Org. Geochem.: Advances and Applications in the Natural Environment, v. 15, p. 447-449.

Nagy, B., and G. C. Gagnon, 1961, The geochemistry of the Athabasca petroleum deposit. I. Elution and spectroscopic analysis of the petroleum from the vicinity of McMurray, Alberta: Geochimica et Cosmochimica Acta, v. 23, p. 155-185.

Nairn, A., and A. Alsharhan, 1997, Sedimentary basins and petroleum geology of the Middle East, Elsevier.

Nciri, N., S. Song, N. Kim, and N. Cho, 2014, Chemical characterization of gilsonite bitumen: Journal of Petroleum & Environmental Biotechnology, v. 5, p. 1.

Noah, M., S. Poetz, A. Vieth-Hillebrand, and H. Wilkes, 2015, Detection of Residual Oil-Sand-Derived Organic Material in Developing Soils of Reclamation Sites by Ultra-High-Resolution Mass Spectrometry: Environ. Sci. Technol., v. 49, p. 6466-6473.

Odden, W., T. Barth, and M. Talbot, 2002, Compound-specific carbon isotope analysis of natural and artificially generated hydrocarbons in source rocks and petroleum fluids from offshore Mid-Norway: Organic Geochemistry, v. 33, p. 47-65.

Okay, A. I., 2008, Geology of Turkey: a synopsis: Anschnitt, v. 21, p. 19-42.

Oldenburg, T. B. P., M. Brown, B. Bennett, and S. R. Larter, 2014, The impact of thermal maturity level on the composition of crude oils, assessed using ultra-high resolution mass spectrometry: Organic Geochemistry, v. 75, p. 151-168.

Orhun, F., 1969, Characteristic properties of the asphaltic substances in Southeastern Turkey, their degrees of metamorphosis and their classification problems: Miner. Res. Explor. Bulletin, v. 72, p. 97-109.

Orr, W. L., 1974, Changes in sulfur content and isotopic ratios of sulfur during petroleum maturation-study of Big Horn Basin Paleozoic oils: AAPG Bulletin, v. 58, p. 2295-2318.

Orr, W. L., 1978, Sulphur in heavy oils, oil sands and oil shales, *in* O. P. Strausz, and E. M. Lown, eds., Oil Sand and Oil Shale Chemistry: Berlin, Verlag Chemie International, p. 223-243.

Orr, W. L., and J. S. Sinninghe Damsté, 1990, Geochemistry of sulfur in petroleum systems, ACS Publications.

Orr, W. L., and C. M. White, 1990, Geochemistry of Sulfur in Fossil Fuels: ACS Symposium Series, v. 429, American Chemical Society, 724 p.

Palmer, S. E., 1984, Effect of water washing on C15+ hydrocarbon fraction of crude oils from northwest Palawan, Philippines: AAPG Bulletin, v. 68, p. 137-149.

Palmer, S. E., 1993, Effect of biodegradation and water washing on crude oil composition: Organic Geochemistry. Plenum Press, New York, p. 511-533.

Parker, C. A., 1974, Geopressures and secondary porosity in the deep Jurassic of Mississippi.

Parnell, J., 2004, Mineral Radioactivity in Sands as a Mechanism for Fixation of Organic Carbon on the Early Earth: Origins of life and evolution of the biosphere, v. 34, p. 533-547.

Parnell, J., H. Kucha, and P. Landais, 1993, Bitumens in ore deposits, Heidelberg, Springer-Verlag, p. 520.

Peters, K., C. Walters, and J. Moldowan, 2005, The Biomarker guide, biomarkers and isotopes in petroleum exploration and earth history, vol 1–2, Cambridge University Press New York.

Peters, K. E., and M. G. Fowler, 2002, Applications of petroleum geochemistry to exploration and reservoir management: Organic Geochemistry, v. 33, p. 5-36.

Peters, K. E., F. D. Hostettler, T. D. Lorenson, and R. J. Rosenbauer, 2008, Families of Miocene Monterey crude oil, seep, and tarball samples, coastal California: AAPG Bulletin, v. 92, p. 1131-1152.

Peters, K. E., and J. M. Moldowan, 1991, Effects of source, thermal maturity, and biodegradation on the distribution and isomerization of homohopanes in petroleum: Organic Geochemistry, v. 17, p. 47-61.

Peters, K. E., and J. M. Moldowan, 1993, The biomarker guide: interpreting molecular fossils in petroleum and ancient sediments.

Peters, K. E., J. M. Moldowan, M. Schoell, and W. B. Hempkins, 1986, Petroleum isotopic and biomarker composition related to source rock organic matter and depositional environment: Organic Geochemistry, v. 10, p. 17-27.

Poetz, S., B. Horsfield, and H. Wilkes, 2014, Maturity-Driven Generation and Transformation of Acidic Compounds in the Organic-Rich Posidonia Shale as Revealed by Electrospray Ionization Fourier Transform Ion Cyclotron Resonance Mass Spectrometry: Energy & Fuels, v. 28, p. 4877-4888.

Powell, T. G., and R. W. Maqueen, 1984, Precipitation of Sulfide Ores and Organic Matter: Sulfate Reactions at Pine Point, Canada: Science, v. 224, p. 63-66.

Powell, T. G., and D. M. Mokirdy, 1973, The effect of source material, rock type and diagenesis on the n-alkane content of sediments: Geochimica et Cosmochimica Acta, v. 37, p. 623-633.

Pu, F., R. P. Philip, L. Zhenxi, and Y. Guangguo, 1990, Geochemical characteristics of aromatic hydrocarbons of crude oils and source rocks from different sedimentary environments: Organic Geochemistry, v. 16, p. 427-435.

Purcell, J. M., C. L. Hendrickson, R. P. Rodgers, and A. G. Marshall, 2006, Atmospheric Pressure Photoionization Fourier Transform Ion Cyclotron Resonance Mass Spectrometry for Complex Mixture Analysis: Analytical Chemistry, v. 78, p. 5906-5912.

Purcell, J. M., P. Juyal, D.-G. Kim, R. P. Rodgers, C. L. Hendrickson, and A. G. Marshall, 2007, Sulfur speciation in petroleum: Atmospheric pressure photoionization or chemical derivatization and electrospray ionization Fourier transform ion cyclotron resonance mass spectrometry: Energy & Fuels, v. 21, p. 2869-2874.

Radke, M., 1987, Organic geochemistry of aromatic hydrocarbons: Advances in petroleum geochemistry, v. 2, p. 141-207.

Radke, M., 1988, Application of aromatic compounds as maturity indicators in source rocks and crude oils: Marine and Petroleum Geology, v. 5, p. 224-236.

Radke, M., and D. Welte, 1981, The methylphenanthrene index (MPI): a maturity parameter based on aromatic hydrocarbons: Advances in organic geochemistry, v. 1983, p. 504-512.

Radke, M., D. H. Welte, and H. Willsch, 1982, Geochemical study on a well in the Western Canada Basin: relation of the aromatic distribution pattern to maturity of organic matter: Geochimica et Cosmochimica Acta, v. 46, p. 1-10.

Radke, M., D. H. Welte, and H. Willsch, 1986, Maturity parameters based on aromatic hydrocarbons: Influence of the organic matter type: Organic Geochemistry, v. 10, p. 51-63.

Radke, M., H. Willsch, and D. H. Welte, 1980, Preparative hydrocarbon group type determination by automated medium pressure liquid chromatography: Analytical Chemistry, v. 52, p. 406-411.

Rigali, M. J., and B. Nagy, 1997, Organic free radicals and micropores in solid graphitic carbonaceous matter at the Oklo natural fission reactors, Gabon: Geochimica Et Cosmochimica Acta, v. 61, p. 357-368.

Rigby, D., B. D. Batts, and J. W. Smith, 1981, The effect of maturation on the isotopic composition of fossil fuels: Organic Geochemistry, v. 3, p. 29-36.

Rogers, M., J. McAlary, and N. Bailey, 1974, Significance of reservoir bitumens to thermal-maturation studies, Western Canada Basin: AAPG Bulletin, v. 58, p. 1806-1824.

Rowland, S. J., R. Alexander, R. I. Kagi, and D. M. Jones, 1986, Microbial degradation of aromatic components of crude oils: A comparison of laboratory and field observations: Organic Geochemistry, v. 9, p. 153-161.

Ruble, T. E., A. N. Bishop, and R. P. Philp, 1994, Identification and characterization of a liquid precursor to gilsonite: The American Chemicak Society, p. 148.

Rullkötter, J., and W. Michaelis, 1990, The structure of kerogen and related materials. A review of recent progress and future trends: Organic Geochemistry, v. 16, p. 829-852.

Sachsenhofer, R. F., R. Gratzer, W. Tschelaut, and A. Bechtel, 2006, Characterisation of non-producible oil in Eocene reservoir sandstones (Bad Hall Nord field, Alpine Foreland Basin, Austria): Marine and Petroleum Geology, v. 23, p. 1-15.

Santamarıa-Orozco, D., B. Horsfield, R. Di Primio, and D. Welte, 1998, Influence of maturity on distributions of benzo-and dibenzothiophenes in Tithonian source rocks and crude oils, Sonda de Campeche, Mexico: Organic Geochemistry, v. 28, p. 423-439.

Sassen, R., 1988, Geochemical and carbon isotopic studies of crude oil destruction, bitumen precipitation, and sulfate reduction in the deep Smackover Formation: Organic Geochemistry, v. 12, p. 351-361.

Schaeffer-Reiss, C., P. Schaeffer, A. Putschew, and J. R. Maxwell, 1998, Stepwise chemical degradation of immature S-rich kerogens from Vena del Gesso (Italy): Organic Geochemistry, v. 29, p. 1857-1873.

Schoell, M., 1984, Recent advances in petroleum isotope geochemistry: Organic Geochemistry, v. 6, p. 645-663.

Schou, L., and M. B. Myhr, 1988, Proceedings of the 13th International Meeting on Organic Geochemistry Sulfur aromatic compounds as maturity parameters: Organic Geochemistry, v. 13, p. 61-66.

Schulte, A., 1980, Compositional variations within a hydrocarbon column due to gravity: SPE annual technical conference and exhibition.

Scott, A. C., 1989, Observations on the nature and origin of fusain: International Journal of Coal Geology, v. 12, p. 443-475.

Şengör, A. M. C., and Y. Yilmaz, 1981, Tethyan evolution of Turkey: a plate tectonic approach: Tectonophysics, v. 75, p. 181-241.

Sert, M., L. Ballice, M. Yüksel, and M. Sağlam, 2011, Effect of mineral matter on the isothermal pyrolysis product of Şırnak asphaltite (Turkey): Fuel, v. 90, p. 2767-2772.

Shalaby, M. R., M. H. Hakimi, and W. H. Abdullah, 2012, Geochemical characterization of solid bitumen (migrabitumen) in the Jurassic sandstone reservoir of the Tut Field, Shushan Basin, northern Western Desert of Egypt: International Journal of Coal Geology, v. 100, p. 26-39.

Sinninghe Damste, J. S., and J. W. De Leeuw, 1990, Analysis, structure and geochemical significance of organically-bound sulphur in the geosphere: State of the art and future research: Organic Geochemistry, v. 16, p. 1077-1101.

Sinninghe Damsté, J. S., T. I. Eglinton, J. W. De Leeuw, and P. A. Schenck, 1989, Organic sulphur in macromolecular sedimentary organic matter: I. Structure and origin of sulphur-containing moieties in kerogen, asphaltenes and coal as revealed by flash pyrolysis: Geochimica et Cosmochimica Acta, v. 53, p. 873-889.

Sivan, P., G. C. Datta, and R. R. Singh, 2008, Aromatic biomarkers as indicators of source, depositional environment, maturity and secondary migration in the oils of Cambay Basin, India: Organic Geochemistry, v. 39, p. 1620-1630.

Smith, D. F., T. M. Schaub, S. Kim, R. P. Rodgers, P. Rahimi, A. Teclemariam, and A. G. Marshall, 2008, Characterization of acidic species in Athabasca bitumen and bitumen heavy vacuum gas oil by negative-ion ESI FT− ICR MS with and without acid− Ion exchange resin prefractionation: Energy & Fuels, v. 22, p. 2372-2378.

Sofer, Z., 1988, Biomarkers and carbon isotopes of oils in the Jurassic Smackover Trend of the Gulf Coast States, U.S.A: Organic Geochemistry, v. 12, p. 421-432.

Soylu, C., 1987, Source rock potential of Dadas Formation (southeast Turkey): Petroleum Geochemistry and Exploration in the Afro-Asian Region. Balkema, Rotterdam, p. 509-517.

Stahl, W. J., 1980, Compositional changes and 13C12C fractionations during the degradation of hydrocarbons by bacteria: Geochimica et Cosmochimica Acta, v. 44, p. 1903-1907.

Stasiuk, E., L. Schramm, and C. Morrison, 1999, Some effects of surfactant and other chemical additions to nascent primary froth during the hot water flotation of bitumen: ABSTRACTS OF PAPERS OF THE AMERICAN CHEMICAL SOCIETY, p. U605-U605.

Stasiuk, L. D., 1997, The origin of pyrobitumens in upper Devonian Leduc formation gas reservoirs, Alberta, Canada: an optical and EDS study of oil to gas transformation: Marine and Petroleum Geology, v. 14, p. 915-929.

Stevenson, J., J. Mancuso, J. Frizado, P. Truskoski, and W. Kneller, 1990, Solid pyrobitumen in veins, Panel Mine, Elliot Lake District, Ontario: Canadian Mineralogist, v. 28, p. 161-169.

Sun, Y., Z. Chen, S. Xu, and P. Cai, 2005, Stable carbon and hydrogen isotopic fractionation of individual n-alkanes accompanying biodegradation: evidence from a group of progressively biodegraded oils: Organic Geochemistry, v. 36, p. 225-238.

Taylor, K. C., and B. F. Hawkins, 1992, Emulsions in Enhanced Oil Recovery, Emulsions: Advances in Chemistry, v. 231, American Chemical Society, p. 263-293.

Ten Haven, H., J. De Leeuw, J. S. Damsté, P. Schenck, S. Palmer, and J. Zumberge, 1988, Application of biological markers in the recognition of palaeohypersaline environments: Geological Society, London, Special Publications, v. 40, p. 123-130.

Theuerkorn, K., B. Horsfield, H. Wilkes, R. di Primio, and E. Lehne, 2008, A reproducible and linear method for separating asphaltenes from crude oil: Organic Geochemistry, v. 39, p. 929-934.

Thompson, K. F. M., 1987, Fractionated aromatic petroleums and the generation of gas-condensates: Organic Geochemistry, v. 11, p. 573-590.

Thompson, K. F. M., 1994, A classification of petroleum on the basis of the ratio of sulfur to nitrogen: Organic Geochemistry, v. 21, p. 877-890.

Tissot, B., and D. Welte, 1984, Petroleum Formation and Occurrence: Berlin (Sprin gcr-Verlag).

Vairavamurthy, M. A., W. L. Orr, and B. Manowitz, 1995, Geochemical Transformations of Sedimentary Sulfur: An Introduction, Geochemical Transformations of Sedimentary Sulfur: ACS Symposium Series, v. 612, American Chemical Society, p. 1-14.

van Aarssen, B. G., T. P. Bastow, R. Alexander, and R. I. Kagi, 1999, Distributions of methylated naphthalenes in crude oils: indicators of maturity, biodegradation and mixing: Organic Geochemistry, v. 30, p. 1213-1227.

van Graas, G. W., 1990, Biomarker maturity parameters for high maturities: calibration of the working range up to the oil/condensate threshold: Organic Geochemistry, v. 16, p. 1025-1032.

Verbeek, E. R., and M. A. Grout, 1992, Structural evolution of gilsonite dikes, eastern Uinta Basin, Utah.

Verbeek, E. R., and M. A. Grout, 1993, Geometry and structural evolution of gilsonite dikes in the eastern Uinta basin, Utah.

Vieth, A., and H. Wilkes, 2006, Deciphering biodegradation effects on light hydrocarbons in crude oils using their stable carbon isotopic composition: A case study from the Gullfaks oil field, offshore Norway: Geochimica Et Cosmochimica Acta, v. 70, p. 651-665.

Volk, H., U. Mann, O. Burde, B. Horsfield, and V. Suchý, 2000, Petroleum inclusions and residual oils: constraints for deciphering petroleum migration: Journal of Geochemical Exploration, v. 71, p. 307-311.

Volkman, J. K., R. Alexander, R. I. Kagi, S. J. Rowland, and P. N. Sheppard, 1984, Biodegradation of aromatic hydrocarbons in crude oils from the Barrow Sub-basin of Western Australia: Organic Geochemistry, v. 6, p. 619-632.

Walters, C. C., S. R. Kelemen, P. J. Kwiatek, R. J. Pottorf, P. J. Mankiewicz, D. J. Curry, and K. Putney, 2006, Reactive polar precipitation via ether cross-linkage: A new mechanism for solid bitumen formation: Organic Geochemistry, v. 37, p. 408-427.

Walters, C. C., K. Qian, C. Wu, A. S. Mennito, and Z. Wei, 2011, Proto-solid bitumen in petroleum altered by thermochemical sulfate reduction: Organic Geochemistry, v. 42, p. 999-1006.

Walters, C. C., F. C. Wang, K. Qian, C. Wu, A. S. Mennito, and Z. Wei, 2015, Petroleum alteration by thermochemical sulfate reduction – A comprehensive molecular study of aromatic hydrocarbons and polar compounds: Geochimica et Cosmochimica Acta, v. 153, p. 37-71.

Waples, D., and T. Machihara, 1991, AAPG Methods in Exploration Series, No. 9: Biomarkers for geologists—A Practical Guide to the Application of Steranes and Triterpanes in Petroleum Geology: American Association of Petroleum Geologists, Tulsa.

Wei, Z., C. C. Walters, J. Michael Moldowan, P. J. Mankiewicz, R. J. Pottorf, Y. Xiao, W. Maze, P. T. H. Nguyen, M. E. Madincea, N. T. Phan, and K. E. Peters, 2012, Thiadiamondoids as proxies for the extent of thermochemical sulfate reduction: Organic Geochemistry, v. 44, p. 53-70.

Weiss, H., A. Wilhelms, N. Mills, J. Scotchmer, P. Hall, K. Lind, and T. Brekke, 2000, NIGOGA—The Norwegian industry guide to organic geochemical analyses: Norsk Hydro, Statoil, Geolab Nor, SINTEF Petroleum Research and the Norwegian Petroleum Directorate.

Wen, C. S., G. V. Chilingarian, and T. Fu Yen, 1978, Chapter 7 Properties and Structure of Bitumens, *in* G. V. Chilingarian, and T. F. Yen, eds., Developments in Petroleum Science, v. 7, Elsevier, p. 155-190.

Wenger, L. M., C. L. Davis, and G. H. Isaksen, 2001, Multiple Controls on Petroleum Biodegradation and Impact on Oil Quality.

Werne, J. P., D. J. Hollander, T. W. Lyons, and J. S. Sinninghe Damsté, 2004, Organic sulfur biogeochemistry: Recent advances and future research directions, *in* J. P. Amend, K. J. Edwards, and T. W. Lyons, eds., Sulfur Biogeochemistry - Past and Present, Geological Society of America.

Werner, A., F. Behar, J. C. De Hemptinne, and E. Behar, 1996, Thermodynamic properties of petroleum fluids during expulsion and migration from source rocks: Organic Geochemistry, v. 24, p. 1079-1095.

Werner, A., F. Behar, J. C. de Hemptinne, and E. Behar, 1998, Viscosity and phase behaviour of petroleum fluids with high asphaltene contents: Fluid Phase Equilibria, v. 147, p. 343-356.

Widdel, F., and R. Rabus, 2001, Anaerobic biodegradation of saturated and aromatic hydrocarbons: Current Opinion in Biotechnology, v. 12, p. 259-276.

Wilhelms, A., S. Larter, I. Head, P. Farrimond, R. Di-Primio, and C. Zwach, 2001, Biodegradation of oil in uplifted basins prevented by deep-burial sterilization: Nature, v. 411, p. 1034-1037.

Wilhelms, A., and S. R. Larter, 1994, Origin of tar mats in petroleum reservoirs. Part II: formation mechanisms for tar mats: Marine and Petroleum Geology, v. 11, p. 442-456.

Wilkes, H., C. Boreham, G. Harms, K. Zengler, and R. Rabus, 2000, Anaerobic degradation and carbon isotopic fractionation of alkylbenzenes in crude oil by sulphate-reducing bacteria: Organic Geochemistry, v. 31, p. 101-115.

Wilkes, H., S. Kühner, C. Bolm, T. Fischer, A. Classen, F. Widdel, and R. Rabus, 2003, Formation of n-alkane- and cycloalkane-derived organic acids during anaerobic growth of a denitrifying bacterium with crude oil: Organic Geochemistry, v. 34, p. 1313-1323.

Williams, J., 1974, Characterization of oil types in Williston Basin: AAPG Bulletin, v. 58, p. 1243-1252.

Williams, P., and F. Goodarzi, 1981, Iranian bitumens; late-stage alteration products of crude oils: Organic Maturation Studies of Fossil Fuel Exploration. Academic Press, London, p. 319-336.

Yalçın Erik, N., and O. Özcelik, 2007, Organic facies variation from well data on the Cudi Group, the Eastern part of SE Turkey: Geochemistry International, v. 45, p. 1152-1163.

Yalçin Erik, N., O. Özçelik, M. Altunsoy, and H. I. Illeez, 2005, Source-Rock Hydrocarbon Potential of the Middle Triassic—Lower Jurassic Cudi Group Units, Eastern Southeast Turkey: International Geology Review, v. 47, p. 398-419.

Yalçın, M. N., 2012, Asphaltite occurences in southeastern Anatolia (Turkey)-How are they formed?, proceeding of 2nd International Conference “Alpine-Petrol 2012”, Krakow, Poland, p. 35-36.

Yen, T. F., and G. V. Chilingarian, 2000, Asphaltene and Asphalts, 2, Developments in Petroleum Science, Elsevier, 621 p.

Yilmaz, Y., 1993, New evidence and model on the evolution of the southeast Anatolian orogen: Geological Society of America Bulletin, v. 105, p. 251-271.

Yilmaz, Y., E. Yiğitbaş, and Ş. C. Genç, 1993, Ophiolitic and metamorphic assemblages of southeast Anatolia and their significance in the geological evolution of the orogenic belt: Tectonics, v. 12, p. 1280-1297.

Zhang, S., and H. Huang, 2005, Geochemistry of Palaeozoic marine petroleum from the Tarim Basin, NW China: Part 1. Oil family classification: Organic Geochemistry, v. 36, p. 1204-1214.

Zumberge, J., F. Johanson, and S. Brown, 1992, Petroleum Geochemistry and Correlation of Crude Oils from the Arabian Plate. GeoMark Research: Inc., Houston, USA (non-proprietary report).